CHFR EXPRESSION IN BREAST CANCER CELLS: ITS RELEVANCE TO TUMORIGENESIS AND GENOMIC STABILITY

by

Lisa Marie Privette

A dissertation submitted in partial fulfillment
of the requirements for the degree of
Doctor of Philosophy
(Human Genetics)
in The University of Michigan
2008

Doctoral Committee:

Professor Elizabeth M. Petty, Chair
Professor Thomas W. Glover
Professor Diane M. Robins
Associate Professor Celina G. Kleer
Associate Professor Mats E.D. Ljungman

DEDICATION

Dedicated to:
my parents, Bonnie and Kenneth Privette
my grandmother, Jewell Couch
and
my fiancé, John Vinnedge II

ACKNOWLEDGEMENTS

First and foremost, I am sincerely grateful for the outstanding mentorship I received from Dr. Elizabeth Petty. Her professional and personal guidance and support has allowed me to become an independent scientist and a better, stronger person. By giving me the freedom to ask my own questions, she let me explore my interests and scientific passions as I became an independent thinker, but she never let me stray too far off course and for that, I am extremely thankful. I deeply admire her dedication to both teaching and biomedical research and I hope that I can match that same level of enthusiasm and dedication in my own career. After nearly six years, she is not only a mentor but a friend and a role model as well.

I would like to thank my thesis committee for their guidance and enthusiastic support. They provided a great amount of intellectual insight and direction. They never let me get lost in the details and always seemed to know when to "cut bait" when a project was not working out well.

Thank you to past and present members of the Petty lab (Ken, Elif, Lezlie, Roma, Maria, Esther, Amy, Janice, Ming, Olga, Linda, and Lesley) for making the lab a fun and interesting place to be every day. Thank you for your support and your help. I especially want to thank Elif and Maria for teaching me so much in the lab.

I will never be able to express how grateful I am for my incredible friends, Sarah Weigel, Nicole (Holmes) Clarkson, and Esther Peterson. Though they were states away, Sarah and Nicole were always there for emotional support and guidance.

Graduate school would have been much harder were it not for Esther. Although she was always sitting right behind me, she was always by my side. Thank you all for the fun times we had together and for always listening.

Most importantly, I am sincerely grateful for my family and my fiancé for their love and never-ending support and encouragement. I am especially indebted to my mom, Bonnie, and my grandmother, Jewell, who are simply inspirational women and taught me how to be strong and independent. Finally, I want to thank my fiancé John. He always knows exactly when and how to make me laugh to make the daily stresses disappear and he has been a constant source of love and support. God truly knew what I needed when He sent him to me and I cannot wait to spend the rest of our lives together. Spending nearly six years of my life so far away from my family and my fiancé was probably the hardest part of graduate school but even though they were miles apart, I always felt that they were standing right next to me.

TABLE OF CONTENTS

LIST OF FIGURES

Figure

LIST OF TABLES

Table

ABSTRACT

CHFR EXPRESSION IN BREAST CANCER CELLS: ITS RELEVANCE TO TUMORIGENESIS AND GENOMIC STABILITY

by

Lisa Marie Privette

Chair: Elizabeth M. Petty

Breast cancer can develop when genes that control the cell cycle and genomic stability are aberrantly expressed or non-functional. *CHFR* encodes an E3 ubiquitin ligase that reportedly delays mitosis in response to microtubule-targeting drugs (i.e. nocodazole and taxanes). Loss of *CHFR* mRNA expression has been reported in many cancers, including breast cancer, but the relevance of this to tumorigenesis remains unknown.

To test if CHFR was relevant for mammary tumorigenesis, we analyzed the effects of altered expression in breast cancers. Nearly 40% of cultured and primary breast cancers had low or no CHFR, which was associated with large tumor size in patient samples. Decreased CHFR expression by RNAi in immortalized human mammary epithelial cell (IHMEC) lines resulted in taxane sensitivity and the acquisition of tumorigenic phenotypes including faster growth rates, higher mitotic indices, enhanced invasiveness and motility, epithelial-to-mesenchymal transitions, increased aneuploidy, and colony formation in soft agar. Conversely, over-expressing CHFR in breast cancer cells caused slower growth and decreased invasiveness and motility.

To determine if CHFR was critical for genomic stability, cells transfected with CHFR siRNA were analyzed for chromosome segregation defects. Transient CHFR loss led to increased aneuploidy, misaligned metaphase chromosomes, anaphase bridges, multi-polar condensed spindles, multi-nucleated cells, and mislocalization of the mitotic checkpoint proteins MAD2 and BUBR1. CHFR was found to interact with three proteins required for mitotic spindle formation and chromosome segregation, including MAD2 and Aurora A where CHFR loss led to elevated Aurora A oncoprotein levels, but no change in MAD2 expression. Alpha-tubulin was identified as a novel target for CHFR-mediated ubiquitination and degradation after treatment with nocodazole. Decreased CHFR increased acetylated α-tubulin, a mitotic spindle protein implicated in cellular response to taxane treatment.

These findings indicate that CHFR has tumor suppressive qualities and may be a biomarker for chemotherapeutic response to taxanes. CHFR has a previously unrecognized role as a regulator of genomic stability via its functional impact on BUBR1, MAD2, Aurora A, and α-tubulin. CHFR may be one of the few proteins that can control the cell cycle, chemotherapeutic response, and genomic stability - processes that go awry in breast cancer.

CHAPTER 1

CHFR IS A MITOTIC CHECKPOINT PROTEIN

Introduction

Breast cancer is a relatively common malignancy and is the most frequently diagnosed cancer in women in the United States. According to the American Cancer Society, one in eight women will be diagnosed in their lifetime. It is estimated to account for 26% of all new cancer cases and will likely be the second leading cause of cancer-related death in American women in the year 2007 [1].

The American Society of Clinical Oncology (ASCO) currently recommends testing for four breast cancer biomarkers, combined with traditional characterization of tumor grade and stage, in order to predict prognosis, recurrence, and course of treatment. ASCO recommends that every primary invasive breast cancer should be analyzed for estrogen and progesterone receptor (ER and PR, respectively) expression status in order to identify cancers that will be responsive to endocrine therapies such as anti-estrogens and aromatase inhibitors. Though the prognosis of ER and PR positive tumors used to be poor because they were non-responsive to traditional chemotherapy such as paclitaxel, they now have a favorable prognosis due to these targeted therapies. Testing for HER2 expression and/or amplification is also recommended in order to determine if patient treatment should include trastuzumab. Her2 is a member of the epidermal growth factor

receptor (EGFR) family and its expression has been associated with aggressive tumors and poor prognosis. ASCO also recommends that newly diagnosed, early stage non-metastatic breast cancers should be tested for the expression of urokinase plasminogen activator (uPA) and plasminogen activator inhibitor-1 (PAI-1) as low levels of these two proteins indicate a low risk of cancer recurrence. High expression of these biomarkers has also been associated with increased invasion, metastasis, and angiogenesis. Finally, ASCO suggests that newly diagnosed, early stage ER-positive breast cancers should be subjected to gene expression profiling, particularly with the RT-PCR based Onco*type* DX assay, which measures the expression of 21 genes. This assay can be used to predict the risk of recurrence in patients treated with tamoxifen. Other gene expression profiling methods, including microarrays, have been considered for diagnosis, treatment indications, and the prediction of prognosis, but they have not been adequately tested in order to be recommended by ASCO [2]. Other biomarkers for breast cancer prognosis and disease progression also have been considered, such as ploidy status, p53 expression, and cyclin E expression, but none have demonstrated sufficient evidence to support their use in clinical practice [2].

There are several ways to treat breast cancer, including surgery, radiation therapy, endocrine therapy such as anti-estrogens, and chemotherapy. The most common drugs recommended to be used in combination in early breast cancer are cyclophosphamide, methotrexate, fluorouracil, doxorubicin (adriamycin), epirubicin, and the microtubule-targeting drugs, paclitaxel (Taxol), and docetaxel (Taxotere) [1]. However, the tumor response to the chosen therapy is highly dependent on the molecular and genetic changes that have occurred in order for the cancer to arise. For instance, anti-estrogen therapy

will be ineffective if the cancer does not express the estrogen receptor (ER). Therefore, researchers and clinicians must identify the molecular and genetic characteristics of the tumor in order to determine the best course of treatment. Paclitaxel and docetaxel belong to the class of drugs called taxanes, which destabilize the microtubules of actively dividing cells, such as cancer cells, resulting in their death by apoptosis. Other microtubule-targeting drugs including nocodazole and colcemid, which over-stabilize microtubules, can induce an apoptotic response similar to the taxanes but they are not used for chemotherapy. One potential biomarker for chemotherapeutic response to taxanes is the expression of CHFR, though very little is known about this protein, its role in tumorigenesis, and its cellular functions.

CHFR Protein Structure and Homologs

Checkpoint with FHA and Ring Finger (CHFR) was initially identified in a screen to find novel mitotic checkpoint proteins containing a forkhead-associated (FHA) domain [3]. In addition to the N-terminal FHA domain, CHFR also has a central RING finger domain and a C-terminal cysteine-rich region (Figure 1.1) [3]. The functional relevance of the FHA domain in CHFR remains largely unknown, except that its deletion creates a dominant-negative form of the protein, suggesting that it is critical to its normal cellular function [3, 4]. The zinc-binding RING finger domain has proven essential for the early prophase checkpoint function of CHFR. It confers CHFR's E3 ubiquitin ligase activity, which creates ubiquitin chains on target proteins either via the amino acid residue lysine-48, thereby targeting proteins to the proteasome for degradation, or via lysine-63 linkages that may alter target proteins' function [5, 6]. The RING finger domain is also necessary for CHFR auto-ubiquitination [7]. Recently, the cysteine-rich region was identified as

the interacting region between CHFR and one of its target proteins, Aurora A [8]. Recently, a putative C2H2 zinc-finger motif, which was renamed a PAR-Binding Zinc-finger (PBZ) motif, was identified in the C-terminal cysteine-rich region of CHFR. This region was found to be poly(ADP-ribosyl)ated by PARP1. Although mutating the PBZ domain did not inhibit CHFR's ubiquitinating activity, it did impair the dominant-negative function of the FHA-domain deletion mutant. There was also inconclusive evidence that the PBZ motif may be required for CHFR's early mitotic checkpoint function [9]. Of interest, the targeting of proteins to portions of the mitotic apparatus is dependent on the recognition of poly(ADP-ribose) (PAR) by PAR-binding motifs.

According to the domain architecture and organization, there are evolutionarily conserved protein orthologs of CHFR even in yeast, both *Saccharomyces cerevisae* and *Schizosaccharomyces pombe* (Figure 1.1) [3, 10]. These minimally described orthologs, Defective in Mitotic Arrest 1 and 2 (Dma1 and Dma2), were important for regulating the mitotic spindle checkpoint, mitotic spindle position, and cytokinesis through the septation-initiation network [10-12]. As will be described later, two studies indicated that human and mouse CHFR may have similar functions as the yeast orthologs.

Interestingly, a human paralog of CHFR was described recently. Ring finger protein 8 (RNF8), shares the FHA and RING domains architecture of CHFR, though it appears to have diverged a bit in terms of cellular function (Figure 1.1). Initially, RNF8 was described as a mitotic protein important for spindle formation, cytokinesis, and mitotic exit, much like the yeast orthologs [13]. However, unlike CHFR, it also was characterized recently as an important DNA damage response protein to double-strand breaks. RNF8 interacts with phosphorylated MDC1, an interaction that is dependent on

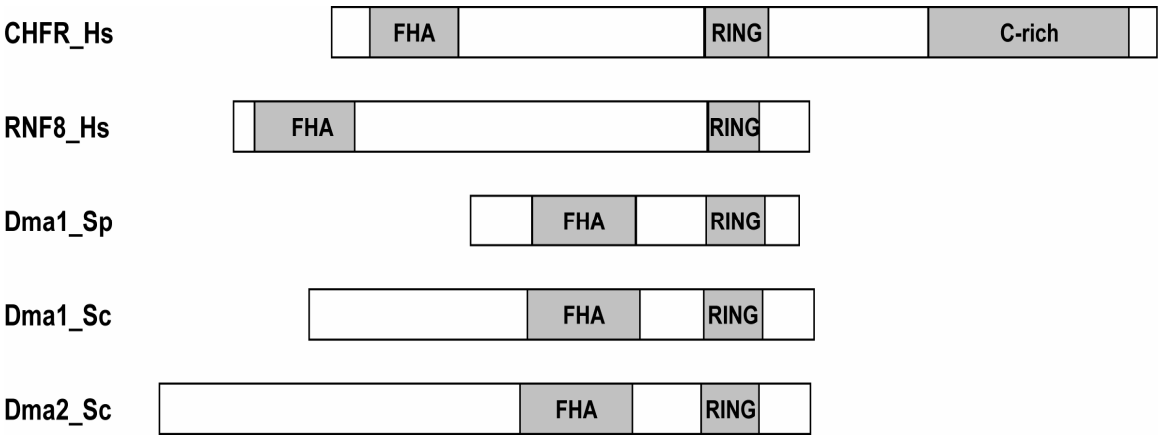

Figure 1.1: The protein structures of CHFR and CHFR homologs

CHFR and CHFR homologs have variable length N-termini followed by phospho-protein binding FHA domain and a RING domain, which is required for E3 ubiquitin ligase activity. The human CHFR protein also has a C-terminal cysteine-rich region though its paralog, Ring Finger protein 8 (RNF8), does not have this region. CHFR is evolutionarily conserved and yeast orthologs, Dma1 and Dma2, have been characterized in both *Schizosaccharomyces pombe* (Sp) and *Saccharomyces cerevisiae* (Sc).

RNF8's FHA domain, in order to mediate double-strand break associated ubiquitinations and facilitate the accumulation of 53BP1 and BRCA1 at DNA double-strand breaks [14, 15]. Both groups noted that RNF8 ubiquitinates histones H2A and H2AX and that loss of RNF8 expression by RNAi abrogated double-strand break retention of the ubiquitin-binding protein RAP80 and increased cellular sensitivity to ionizing radiation [14, 15].

There is a growing amount of evidence that CHFR, unlike RNF8, does not mediate a classical cellular response to DNA damage based on results from commonly used assays to assess DNA damage response. While the role of CHFR in the cellular response to ionizing radiation has been inconclusive [16, 17], it does not seem to have a role in the DNA damage response induced by cisplatin (CDDP), UV radiation, or the topoisomerase inhibitors etoposide (VP16) and Topotecan [7, 18, 19].

Since its initial publication, studies on CHFR have primarily focused on its expression in cancer cells and potential role in oncogenesis, but some progress also has been made in identifying its biochemical function and target proteins. This chapter will address the discoveries that have been published to date for CHFR, including its mitotic checkpoint functions, reported protein targets for its ubiquitin ligase activity, and evidence supporting its role as a tumor suppressor protein and biomarker for chemotherapeutic response to taxanes.

CHFR Checkpoint Functions

The Microtubule-Stress Prophase Checkpoint

As mentioned above, CHFR does not seem to participate in the DNA damage checkpoint or DNA repair pathways. On the contrary, CHFR regulates an early mitotic

checkpoint, during prophase, in response to the disruption of normal microtubule formation or stabilization as assessed after treatment with microtubule poisons such as nocodazole, colcemid, and taxanes [3]. During mitotic stress, CHFR temporarily delays the cell cycle by about three hours, during which chromosome condensation and nuclear envelope breakdown is inhibited, and Cyclin B1/Cdc2 is restricted to the cytoplasm where it is inactive [3, 17, 18]. CHFR also regulates the coordination of chromosome condensation and centrosome separation during prophase [3]. Together, these results identified CHFR as the first key member of a novel early mitotic checkpoint in prophase, referred to here as the CHFR-mediated prophase checkpoint (Figure 1.2).

The ability of CHFR to delay chromosome condensation has been confirmed both by visually identifying a lack of condensed chromosomes and by the absence of phosphorylation of histone H3 on residues Ser10 and Ser28 when CHFR is over-expressed in several cell lines [3, 17, 18, 20]. In addition, the CHFR-mediated prophase checkpoint is typically monitored by calculating the mitotic index of cells treated with microtubule poisons; CHFR expressing cells will have fewer mitotic cells, as evidenced by condensed chromosomes and no nuclear envelope, compared to non-expressing cells [3, 18, 20, 21].

Elegant studies performed by Kang et al. in *Xenopus laevis* egg extracts have begun to elucidate how CHFR regulates entry into mitosis. As previously mentioned, CHFR delayed the onset of mitosis by retaining inactive Cyclin B1/Cdc2 in the cytoplasm in human cells. In *X. laevis* extracts the addition of full-length CHFR, but not RING finger mutants, resulted in prolonged inhibitory phosphorylation of Cdc2 on residue Tyr15. In addition, CHFR delayed the phosphorylation of the Cdc2-regulatory

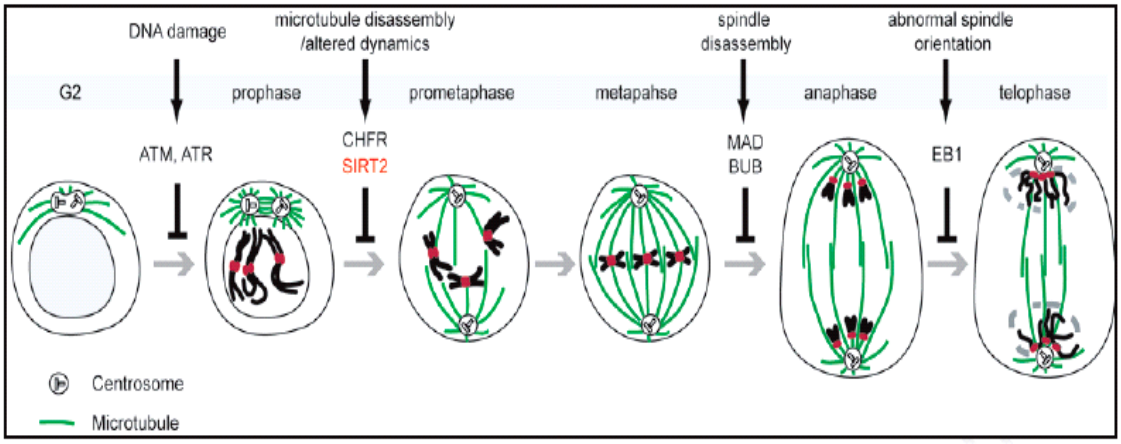

Figure 1.2: Four cell cycle checkpoints regulate the entry and completion of mitosis.

The CHFR-mediated prophase checkpoint occurs after the DNA damage checkpoint, during prophase, in response to altered microtubule dynamics. The mitotic spindle checkpoint regulates the metaphase-anaphase transition later in mitosis. The "abnormal spindle orientation" checkpoint associated with the EB1 protein has only been identified in yeast [22].

proteins Wee1 and Cdc25C at the G2 to M transition. However, the steady-state level of expression for these proteins, and the Cdc25C regulatory protein Chk1, remained unchanged in the presence of CHFR, indicating that they were not probable ubiquitination targets. Therefore, it is likely that the prolonged inhibitory phosphorylation of Cdc2 at Tyr15 is due to the over-activation of Wee1 kinase, which phosphorylates Cdc2 at Tyr15, and the inhibition of Cdc25C phosphatase that is normally responsible for activating Cyclin B1/Cdc2 by removing the inhibitory phosphorylation on Tyr15 of Cdc2 (Figure 1.3).

One of the proteins that can regulate both Cdc25C and Wee1 via phosphorylation is polo-like kinase 1 (PLK1). Kang et al. determined that CHFR could, in fact, ubiquitinate PLK1 in *X. laevis* extracts [6]. In support of this model, the E3 ubiquitin ligase activity of CHFR via its RING finger domain is required for proper checkpoint function, suggesting that CHFR must ubiquitinate a target protein for the cell cycle delay to occur. However, though the pathway described above is a likely explanation for the series of events that occurs downstream of CHFR in response to mitotic stress, these results have not been easily replicated in mammalian cells. The ability of CHFR to ubiquitinate and/or regulate PLK1 has not been consistently reproduced, raising questions as to the legitimacy of this pathway in mammalian cells, as discussed further below.

Another potential pathway for the CHFR-regulated mitotic stress checkpoint during prophase is through the p38 stress-activated kinases in which CHFR acts upstream of p38 through an as-of-yet unknown mechanism [23]. There is also evidence that Sirtuin 2 (SIRT2), a tubulin and histone deacetylase, may also participate in the same microtubule stress-induced prophase checkpoint as CHFR. Like CHFR, SIRT2 over-

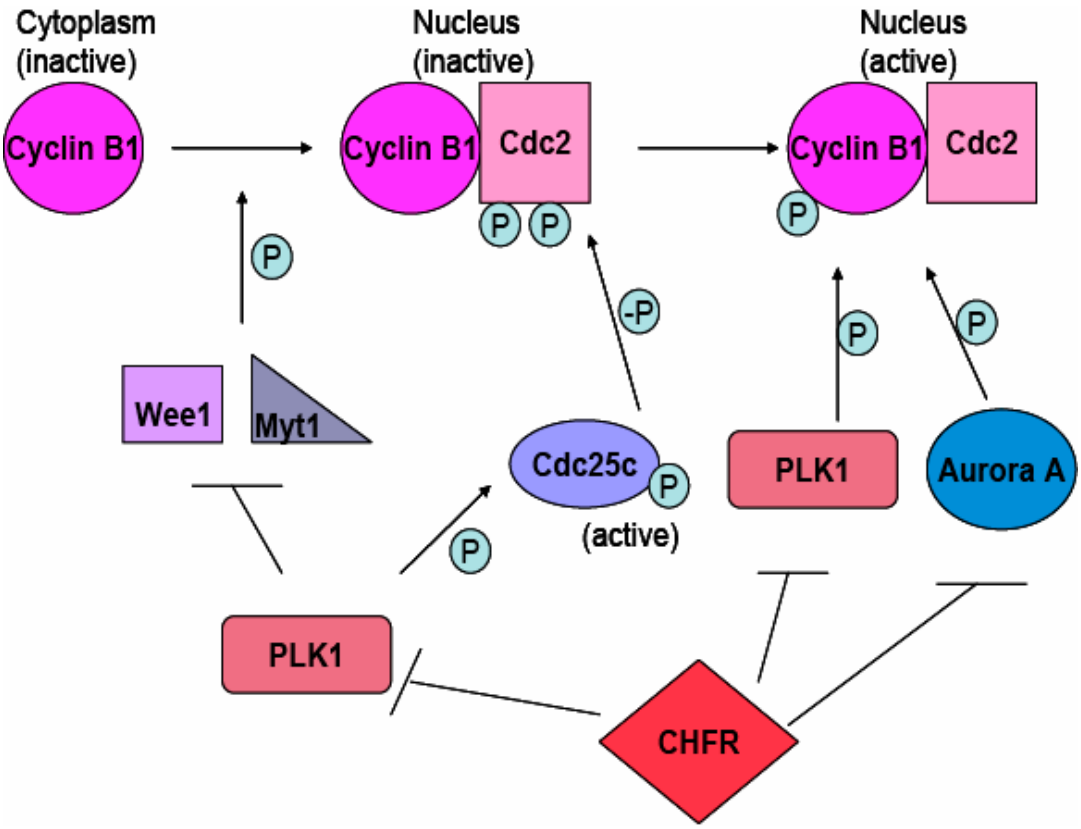

Figure 1.3: CHFR may coordinate mitotic entry by controlling Cyclin B1 translocation to the nucleus via negatively regulating PLK1 and Aurora A activity.

CHFR negatively regulates Aurora A, and possibly PLK1, by ubiquitinating these proteins and targeting them for degradation by the proteasome. When CHFR inactivates PLK1 and Aurora A, the Wee1 and Myt1 kinases inhibit the Cyclin B1/Cdc2 complex by inhibitory phosphorylation on residue Tyr15 and prevent its translocation to the nucleus in order to initiate mitosis. In addition, the Cdc25c phosphatase is never activated by PLK1 to remove this inhibitory phosphorylation.

expression results in a decreased mitotic index and inhibited chromosome condensation in response to nocodazole or paclitaxel treatment. The NAD-dependent tubulin deacetylase activity of SIRT2 was required for this response [24]. Finally, another potential player in the mitotic stress-induced prophase checkpoint is Sensitivity to Nitrogen Mustard 1 (SNM1). Akhter et al. found that mouse embryonic fibroblasts from *Snm1* knockout mice behaved like human cells that had lost CHFR expression. *Snm1* null cells arrested during the spindle checkpoint with condensed chromosomes and separated (and duplicated) centrosomes following nocodazole exposure whereas wild-type cells from littermates arrested with decondensed chromosomes and unseparated centrosomes [25]. Furthermore, *Snm1* wild-type cells delayed mitotic entry by about four hours and maintained cyclin A expression longer, indicating an arrest in prophase, when compared to null fibroblasts [25]. Much like *CHFR* null human cells, *Snm1*$^{-/-}$ mouse embryonic fibroblasts were less likely to survive nocodazole treatment when compared to wild-type cells [25]. Of interest because the CHFR homolog RNF8 can regulate 53BP1, Akhter el al. also found that Snm1 could interact with 53bp1 and the APC/cyclosome complex [13, 25]. Together these observations suggest that a currently unrecognized pathway of protein interactions involving CHFR is critical for normal progression through the recently described prophase checkpoint.

The Mitotic Spindle Assembly Checkpoint

In addition to participating in an early mitotic checkpoint during prophase, one report indicated that CHFR might be required for later events in mitosis, such as chromosome segregation, to maintain genomic stability. Embryonic fibroblasts from *Chfr* knockout mice not only showed a prolonged time in prophase, but also an extended

amount of time in anaphase. The *Chfr* null mouse embryonic fibroblasts, which became aneuploid in culture, also displayed lagging chromosomes during anaphase, failed nuclear segregation, and multi-nucleated cells indicating failed cytokinesis [8]. In support of these findings, recently published bioinformatics evidence indicated that CHFR may contain a KEN box motif, indicating that CHFR may be targeted for proteasome-mediated degradation by the anaphase-promoting APC/C complex, which is a critical component of the mitotic spindle assembly checkpoint and the regulatory complex that controls mitotic exit [26]. Therefore, CHFR may have multiple mitotic checkpoint functions and, contrary to initial thought, does not function only in response to mitotic stress due to microtubule-targeting drugs.

CHFR Interacting Proteins

Polo-like Kinase 1 (PLK1)

As mentioned previously, there is evidence that CHFR can ubiquitinate PLK1 in *Xenopus* extracts, but tests to assess the ability of CHFR to regulate PLK1 activity or protein levels in mammalian cells have been inconclusive. Findings in support of CHFR controlling PLK1 include results indicating that over-expressed CHFR mutants, which mimic unphosphorylated CHFR, can decrease PLK1 expression and kinase activity in HeLa cells [16]. Of interest, mouse embryonic fibroblasts from *Chfr* knockout mice were found to over-express PLK1 compared to cells from wild-type and heterozygous littermates, suggesting that CHFR can ubiquitinate PLK1 to target it for degradation [8].

To the contrary, there are other reports that have not been able to find a correlation between CHFR expression and PLK1 expression or activity. For example,

Matsusaka and Pines were unable to find an association between PLK1 expression and induction of the CHFR-mediated prophase checkpoint due to colcemid treatment [23]. In addition, other studies have not been able to find a relationship between CHFR expression and the amount of PLK1 protein, either as a trend among breast cell lines or following CHFR over-expression in HCT116 cells [17, 21]. It is apparent that more work is required to determine if PLK1 is a target for CHFR-mediated ubiquitination and regulation. Perhaps the interaction is specific for a particular species, tissue, or treatment.

Aurora A kinase

Another protein that regulates the activity and translocation of cyclin B1 to the nucleus to initiate mitosis is Aurora A kinase [27]. Therefore, Aurora A has also been speculated to be a target for ubiquitination by CHFR. Summers et al. analyzed Aurora A expression and activation in HCT116 cells over-expressing CHFR and found that even though there was no change in Aurora A expression or localization to the centrosomes, they did discover that the nocodazole-induced CHFR-mediated mitotic delay was associated with inactive Aurora A that was unphosphorylated at residue Thr288 at the centrosomes [17]. Compelling evidence that CHFR ubiquitinates Aurora A was provided by Yu et al. in which they found that Aurora A was over-expressed in *Chfr* null mouse embryonic fibroblasts and tissues [8]. Additionally, using human cell lines they determined that the C-terminal cysteine-rich region of CHFR interacts with the N-terminus of Aurora A by immunoprecipitation and that this interaction led to the ubiquitination of Aurora A [8].

Proteins Regulating Ubiquitination Activity

Since CHFR has been described as an E3 ubiquitin ligase due to the presence of its RING domain, there must be E2 enzymes that it interacts with in order to function. CHFR has been shown to utilize the E2 ubiquitin-conjugating (Ubc) proteins Ubc4, Ubc5A, and Ubc5B in order to form Lys48-based polyubiquitin chains, but not E2 enzymes UbcH7, UbcH8, or UbcH10 [5, 6]. CHFR has also been found to interact with the E2 enzyme complex Ubc13-MMS2 hetero-dimer to form lysine-63 linked polyubiquitin chains, which are associated with modifying protein function, not targeting them for degradation by the proteasome [5]. Both of these findings were recently confirmed in *S. cerevisiae* for the yeast orthologs of CHFR [28]. In addition to ubiquitin-conjugating E2 enzymes, CHFR has been shown to interact with the deubiquitinating protein ubiquitin-specific protease 7 (USP7) by immunoprecipitation [29]. USP7 was found to deubiquitinate CHFR and inhibit its auto-ubiquitinating activity, thereby preventing the degradation of CHFR [29]. Interestingly, USP7 and CHFR both localize to PML bodies in the nucleus; in particular, CHFR has been shown to be in PML bodies in interphase cells [4, 29].

Additional Interacting Proteins

Another potential interacting protein for CHFR is protein kinase B (PKB). It was determined that PKB could phosphorylate CHFR on residues Thr39 and Ser208, potentially inhibiting the ubiquitin ligase activity of CHFR. However, phosphorylation-defective mutants of CHFR did not alter the checkpoint response to paclitaxel [16]. Bothos et al. also found that CHFR was phosphorylated during mitosis, though they did not determine which kinase was responsible [5].

CHFR and Cancer

Mutations, Alternative Transcripts, and Chromosomal Aberrations

CHFR has been implicated as a tumor suppressor in multiple cancers despite the fact that no heritable mutations in germline cells associated with a predisposition to cancer phenotypes have been identified and few mutations in somatic cancer cells have been described. Though many groups have not been able to identify coding mutations in the *CHFR* gene, particularly in breast and colon cancers, several single-nucleotide polymorphisms (SNPs) have been identified [21, 30, 31]. However, three missense mutations in *CHFR* were found in primary non-small cell lung cancers, two mutations between the FHA and RING domains, and one in the cysteine-rich region, all three of which were unable to rescue the CHFR checkpoint in DLD-1 cells during nocodazole treatment [31]. However, even these mutations were rare events as they were only found in three patients, all of whom were smokers, out of 53 different patient samples tested [31]. Recently published data has indicated that one of these coding single nucleotide polymorphisms (SNPs), V539M (Accession No. NM_018223; V580M for Accession No. AF_170724) found within the C-terminal cysteine-rich region, was significantly associated with a lower risk of colorectoral cancer if the patient had the methionine amino acid instead of the valine [32]. This SNP was also strongly associated with the absence of metastases, TNM stage, and microsatellite instability, all of which indicate a favorable prognosis. This variant was within the hap 10 (TGACTA) haplotype block that also contained the P138L SNP, which had correlated with the microsatellite instability phenotype [32]. Two additional deletion mutations have also been identified in which

either residues 135-146 were deleted between the FHA and RING domains or residue Ala470 was deleted in the C-terminal cysteine-rich region [31].

Though they have not been studied extensively, alternative mRNA transcripts have been identified for *CHFR*. Toyota et al. identified transcripts that were missing exons two, five, and/or six and the transcript missing exon two is believed to result in an isoform lacking the FHA domain (Figure 1.4) [3, 33]. This isoform was also found to be highly expressed in cancer cells when compared to matched normal tissues [33]. Though full-length CHFR was found to suppress cell growth when over-expressed, the FHA domain deletion mutant of CHFR was less effective in suppressing cell growth and had been previously identified as a dominant negative form of CHFR [3, 33].

CHFR is located at human chromosome 12q24.33, which is a site of allelic imbalance in many cancers. Deletion of 12q24 was described in adenoid cystic carcinoma and as a prognostic indicator of recurrence in Wilm's tumor and pituitary adenomas [34-36]. Band 12q24 also was associated with the presence of a metastasis suppressor gene, as amplification of 12q24 correlated with metastasis-free survival in breast cancer patients and decreased metastatic potential of prostate cancer cells [37-39]. Further characterization of 12q24 would be required to determine if *CHFR* is the gene responsible for predicting cancer recurrence and metastasis in these association studies.

CHFR Expression and Correlations with Clinico-Pathological Variables

Many studies have focused on studying the loss of *CHFR* mRNA expression due to promoter hyper-methylation in cancers compared to normal cells and tissues, and they are summarized in Table 1.1 [18, 19, 21, 30, 33, 40-64]. Although *CHFR* mRNA expression was decreased or lost in many cancers, sometimes up to 50% of samples,

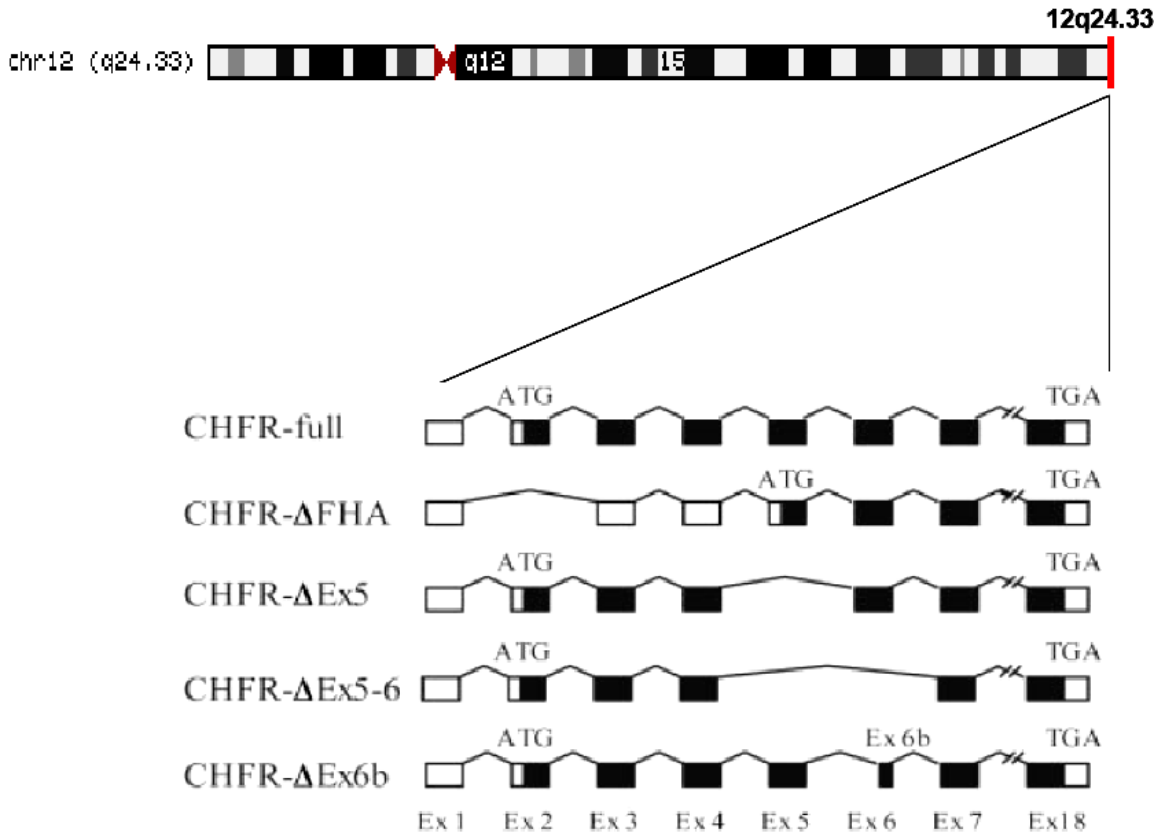

Figure 1.4: The chromosomal location and genomic structure of *CHFR* and its splice variants.

CHFR is located at the distal end of human chromosome 12 at 12q24.33. Full length CHFR consists of 18 exons and the start codon for translation is in exon two. Splice variants of *CHFR* include one in which exon two is skipped, causing translation to begin in exon five and the deletion of the FHA domain (ΔFHA). The other three splice variants either result in the deletion of exons five, or five and six, or an alternative exon six (6b).

promoter hyper-methylation only accounts for a percentage of these instances and is often tissue-dependent. In particular, 16-53% of cancers of the gastro-intestinal tract have hyper-methylated promoters of the *CHFR* gene; however, this is extremely rare in gynecological cancers with the exception of HPV-positive cervical carcinomas [33, 47, 59, 60, 63]. For example, 50% of breast cancer cell lines have decreased or lost *CHFR* expression compared to immortalized human mammary epithelial cells, but only 8% of the lines had a methylated promoter [21].

Altered mRNA expression of *CHFR* has been correlated with clinical and pathological variables (Table 1.1). In particular, low or lost *CHFR* was associated with a high mitotic index in colorectal and breast cancers [21, 33]. A hyper-methylated *CHFR* promoter was also associated with advanced patient age, high tumor grade, advanced stage, poor differentiation, female gender, and taxane sensitivity [40, 42, 47, 48, 53, 56, 58, 63]. Of these correlations, high mitotic index, advanced tumor stage, and taxane sensitivity have been replicated among different research groups [21, 33, 40, 42, 53, 58]. Only a few studies recently have reported on the frequency of altered CHFR protein expression in cancers versus normal tissue. Milne et al. found that 33% of gastric cancers were negative for CHFR expression by immunohistochemistry, which correlated with a diffuse histology [65]. Importantly, using immunohistochemistry CHFR localization to the nucleus was altered in 66% of malignant peripheral nerve sheath tumors. In the same samples, decreased CHFR expression was associated with a multitude of clinical and pathological variables including young age, site of tumor to the trunk, head or neck, presentation of recurrent tumors, increased mitotic index, increased Ki67 staining for proliferation, abnormal karyotype, and poor patient prognosis [66].

Table 1.1: The frequency of CHFR promoter hyper-methylation and correlations with clinico-pathological variables.

Cancer Tissue	Percent Hyper-Methylated	Correlations and Findings	Reference
Lung cancer	19% (7/37) of primary cancers 19% (3/16) of cell lines	infrequent SNPs in coding region	(Mizuno et al, 2002)[a]
Esophageal cancer	16.3% (7/43) of primary cancers 26.7% (4/15) of cell lines	None found	(Shibata et al, 2002)[a]
Colon adenocarcinomas Non-small cell lung	37% (11/30) of primary cancers 10% (2/20) of primary cancers	some methylation in normal colon	(Corn et al, 2003)[a]
Colorectal cancer Colorectal adenomas Head and neck cancer Hepatocellular cancer	40% (25/63) of primary cancers 53% (27/51) of primary cancers 30% (16/54) of primary cancers 0% (0/20) of primary cancers	Associated with increased mitotic index	(Toyota et al, 2003)[a]
Colon cancer Colon cancer Breast cancer	36% (8/22) of primary cancers 43% (9/21) of cell lines 0% (0/19) of cell lines	None tested	(Bertholon et al, 2003)[a]
Breast cancer	8% (2/24) of cell lines	Low expression associated with high mitotic index	(Erson and Petty, 2004)[b]
Gastric cancer Gastric cancer	39% (24/61) of primary cancers 20% (4/20) of cell lines	None tested	(Satoh et al, 2003)[c,d]
Gastric cancer Gastric cancer	35% (25/71) of primary cancers 20% (2/10 cell lines)	None found	(Honda et al, 2004)[a]
Gastric cancer Gastric cancer	44% (19/43) of primary cancers 67% (8/12) of cell lines	None tested	(Kang, H. C. et al, 2004)[a,d]
Biliary tract carcinomas	16% (6/37) of primary cancers	None found	(Tozawa et al, 2004)[a]
Low-grade noninvasive gastric neoplasia High-grade noninvasive gastric carcinoma Submucosal invasive gastric adenocarcinomas	10% (1/10) of primary cancers 45% (10/22) of primary cancers 35% (7/20) of primary cancers	Methylation correlated with advanced patient age and high tumor grade	(Homma et al, 2005)[a]
Colorectal cancer	31% (19/62) of primary cancers	Associated with MLH1 promoter hyper-methylation, microsatellite instability	(Brandes et al, 2005)[a]
Cutaneous T-cell lymphoma	19% (5/28) of primary cancers	None tested	(van Doorn et al, 2005)[e,d]
Nasopharyngeal carcinomas	61% (22/36) of primary cancers 88% (7/8) of cell lines	None found	(Cheung et al, 2005)[a,d]
Oral squamous cell carcinoma	31% (4/13) of primary cancers 22% (2/9) of cell lines	Low expression associated with high mitotic index and taxane sensitivity	(Ogi et al, 2005) [c]
Acute myelocytic and lymphocytic leukemia	39% (16/41) of primary cancers	None tested	(Gong et al, 2005)[a]
Hepatocellular cancer	35% (22/62) of primary cancers	Correlated with infiltrative growth pattern and advanced stage	(Sakai et al, 2005)
Gastric cancer	37% (15/41) of primary cancers	No correlation with response to Taxol treatment	(Yoshida et al, 2006)[c]
Breast cancer	0.9% (1/110) of primary cancers	None tested	(Tokunaga et al, 2006)[a]
Gastric cancer	52% (24/46) of primary cancers	Correlated with clinical response to Taxol treatment	(Koga et al, 2006)[a]
Esophageal cancer Gastric cancer	24% (9/38) of primary cancers 30% (16/53) of primary cancers	Correlated with female gender, but not with tumor stage	(Morioka et al, 2006)[a]
Colorectal cancer	26% (25/98) of primary cancers	None tested	(Morioka et al, 2006)
Endometrial cancer	12% (6/50) of primary cancers	Correlated with poorly differentiated adenocarcinomas	(Yanokura et al, 2007)[a]
Ovarian cancer	0% (0/48) of primary cancers	None tested	(Ludwig et al, 2007)[a]
Cervical adenocarcinomas Cervical carcinoma	12% (2/14) of primary cancers 33% (2/6) of cell lines	Correlated with taxane sensitivity	(Banno et al, 2007)[a]
HPV+ cervical squamous cell carcinoma HPV+ cervical adenocarcinoma HPV+ cervical carcinoma	31% (5/16) of primary cancers 50% (4/8) of primary cancers 56% (5/9) of cell lines	Methylation designated as a late event	(Henken et al, 2007)[f]
Head and neck squamous cell carcinoma	25% (7/28) of primary cancers	Correlated with stage IV cancer	(Chen et al, 2007)[f]
Colorectal cancer	41% (29/71) of primary cancers	hMLH1 promoter methylation, gain of chromosome 8q, *BRAF* mutations	(Derks et al, 2007)[a]
Gastric Cancer	48% (12/25) of primary cancers	None tested	(Kang, G. H. et al, 2007)[g]
Colorectal Cancer	24% (217/888) of primary cancers	None tested	(Kawasaki et al, 2008)[g]

[a] methylation-specific PCR (MS-PCR), [b] 5-aza-dC treatment, [c] combined bisulfite restriction analysis (COBRA), [d] bisulfite sequencing, [e] CpG island microarray, [f] methylation-specific multi-plex ligation-dependent probe amplification (MS-MLPA), [g] MethyLight quantitative methylation-specific PCR

CHFR is a Tumor Suppressor and Regulator of Genomic Stability

The first indication that CHFR was a potent tumor suppressor was the creation of the *Chfr* knockout mouse, which was viable with no developmental defects [8]. A small percentage (9%) of these mice developed lymphomas by 40 weeks of age and later they were prone to developing spontaneous cancers of epithelial origin, primarily lung, liver and gastro-intestinal tumors. Fifty percent of the knockout mice also developed skin tumors following treatment with the chemical carcinogen dimethylbenz(a)anthracene (DMBA) at four months of age compared to none of their wild-type littermates [8]. There was also indication that the loss of *Chfr* led to cellular transformation because embryonic fibroblasts from the mice were able to form colonies in culture [8]. Interestingly, Chfr was found to be important for maintaining genomic stability in the embryonic fibroblasts from the *Chfr* null mice. About 30% of the cells became aneuploid after four passages likely due to several mitotic defects that were observed, which included lagging anaphase chromosomes, failed nuclear segregation and failed cytokinesis, resulting in 17% of the cells becoming multi-nucleated [8]. Of interest, they discovered that down-regulating Aurora A by RNAi rescued the genomic instability phenotype in *Chfr* null mouse embryonic fibroblasts [8].

CHFR as a Potential Biomarker for Chemotherapeutic Response to Taxanes

As indicated above and in Table 1.1, *CHFR* promoter hyper-methylation was previously shown to correlate with taxane sensitivity in gastric cancers and cervical carcinomas [40, 53]. In support of these findings, cultured cells that were transfected to over-express *CHFR* showed a decrease in apoptotic response to taxanes and enhanced

cell survival, whereas decreasing *CHFR* by RNAi resulted in enhanced sensitivity (ie: increased apoptotic response) to taxanes [3, 18-20]. These reports have indicated that the CHFR expression status of cancers might be an excellent biomarker for tumor response to taxane treatment. However, this poses a very interesting dichotomy for CHFR expression. On one hand, losing the potential tumor suppressive functions of CHFR may lead to cancer, whereas on the other hand, an absence of CHFR expression might actually be favorable as it would be a positive indicator of chemotherapeutic response to taxane treatment. Future work studying the potential role of CHFR as a biomarker for chemotherapeutic response to taxanes in diverse tissues, and the mechanism of this response, would definitely be valuable both at the bench and at the clinic.

CHFR is a novel mitotic checkpoint protein and potential biomarker for chemotherapeutic response to taxanes. Its expression also is frequently altered in many types of cancer and the null mouse is cancer-prone. These facts led to the hypothesis that CHFR is biologically relevant to the pathogenesis of human breast cancer and functions in the maintenance of genomic stability. To test this hypothesis, the first aim of this work was to define the relevance of CHFR expression to breast cancer pathogenesis in cell lines and primary tissues from mammary epithelium and the findings from these experiments are presented in Chapter 2. The second aim, which is described in Chapter 3, was to characterize the phenotypic effects of altering CHFR expression in cell culture models of breast cancer. Chapter 4 describes the findings from the third aim, which was to determine if CHFR has a role in maintaining genomic stability. Chapter 5 is a concluding chapter that discusses the significant findings of this thesis and potential future directions for this project.

CHAPTER 2

CHFR EXPRESSION IS FREQUENTLY LOW OR LOST IN BREAST CANCER

Summary

In recent years, there has been increasing evidence supporting the role of CHFR as a tumor suppressor, most of which report loss of mRNA expression in cancers compared to patient-matched normal tissues. This altered *CHFR* expression is occasionally due to promoter hyper-methylation, but other modes of lost expression have not been identified. However, mRNA expression does not always correlate with the functional protein expression due to post-transcriptional and post-translational regulation and modifications. Therefore, we studied both a panel of breast cancer cell lines as well as primary tissue samples from breast cancer patients for CHFR protein expression, using Western blotting and immunohistochemistry, respectively, to determine if expression was altered in breast cancers compared to normal mammary tissue. CHFR protein expression was low or lost in approximately 40% of both primary and cultured breast cancers, though when Western blotting was compared with quantitative RT-PCR to detect mRNA from cultured cells, fewer cell lines showed lost expression at the mRNA level. This discrepancy between mRNA and protein expression suggested that post-transcriptional or post-translational modification might occur to regulate CHFR protein expression.

Introduction

Frequently, genes that are relevant to tumorigenesis are not properly expressed in cancer cells when compared with normal tissues or immortalized, non-tumorigenic cell lines, an example of which is *CHFR*. In particular, a previous report from our lab showed that decreased *CHFR* mRNA expression occurred in 50% (12 of 24) of the cultured breast cancers tested by Northern blot analysis (Figure 2.1) [21].

Although many studies have focused on examining *CHFR* mRNA expression, typically with non-quantitative methods, this is not always a good indicator of functional protein expression and for studying correlations between gene expression and cellular phenotypes or clinico-pathological variables. This is because many expressed genes undergo post-transcriptional regulation to control protein expression [67]. For example, cells can adjust mRNA translation via phosphorylation of eukaryotic initiation factor-2α or by regulating other components of the translation machinery [68]. Many known growth signal transduction pathways that are deregulated in cancer cells, such as Ras, MAPK, and m-Tor, activate components of the translational machinery whereas, on the contrary, tumor suppressor proteins such as p53 and pRb are normally required to limit ribosomal and tRNA synthesis to inhibit translation [69].

Another mechanism of post-transcriptional regulation is through the RNAi pathway. In particular, micro RNAs (miRNAs) can quickly change protein expression in response to the environment by causing transcript degradation or by inhibiting the ribosome and additional proteins of the translational machinery from binding to the transcript [70]. There is abundant evidence that this mechanism of post-transcriptional regulation can be disrupted in cancers. These small RNAs, if over-abundant, could cause

excessive down-regulation of important tumor suppressors whereas the lack of miRNA production could allow the over-expression of oncogenes [71]. In addition, a group of miRNAs were recently found to be transcriptional targets of the key tumor suppressor protein p53; therefore, if p53 is mutated or nonfunctional in cancers, the downstream set of regulatory miRNAs, miR-34, that can control apoptosis and cell cycle arrest would also be lost [72]. Therefore, post-transcriptional regulation is a target for alteration during tumorigenesis. This evidence clearly indicates that the regulation of mRNA translation may frequently be altered in cancer cells compared to normal cells, making it unlikely that measures of mRNA expression would agree with protein production.

Although many studies have focused on *CHFR* mRNA expression, a more informative analysis would be to study protein expression. Therefore, this work focused on assessing CHFR protein expression in cultured and primary breast cancers. We hypothesized that CHFR protein expression would be altered in breast cancers compared to normal tissue or non-tumorigenic immortalized cell lines. To test this, CHFR expression was analyzed by quantitative RT-PCR and Western blotting in cultured breast cancer cells and immortalized human mammary epithelial cells (IHMECs) and by immunohistochemistry in primary breast tissue. CHFR expression was frequently lost or low in breast cancers, which correlated with a high mitotic index. There was a discrepancy between mRNA and protein levels in some cell lines, suggesting that post-transcriptional or post-translational regulation of CHFR protein expression may occur.

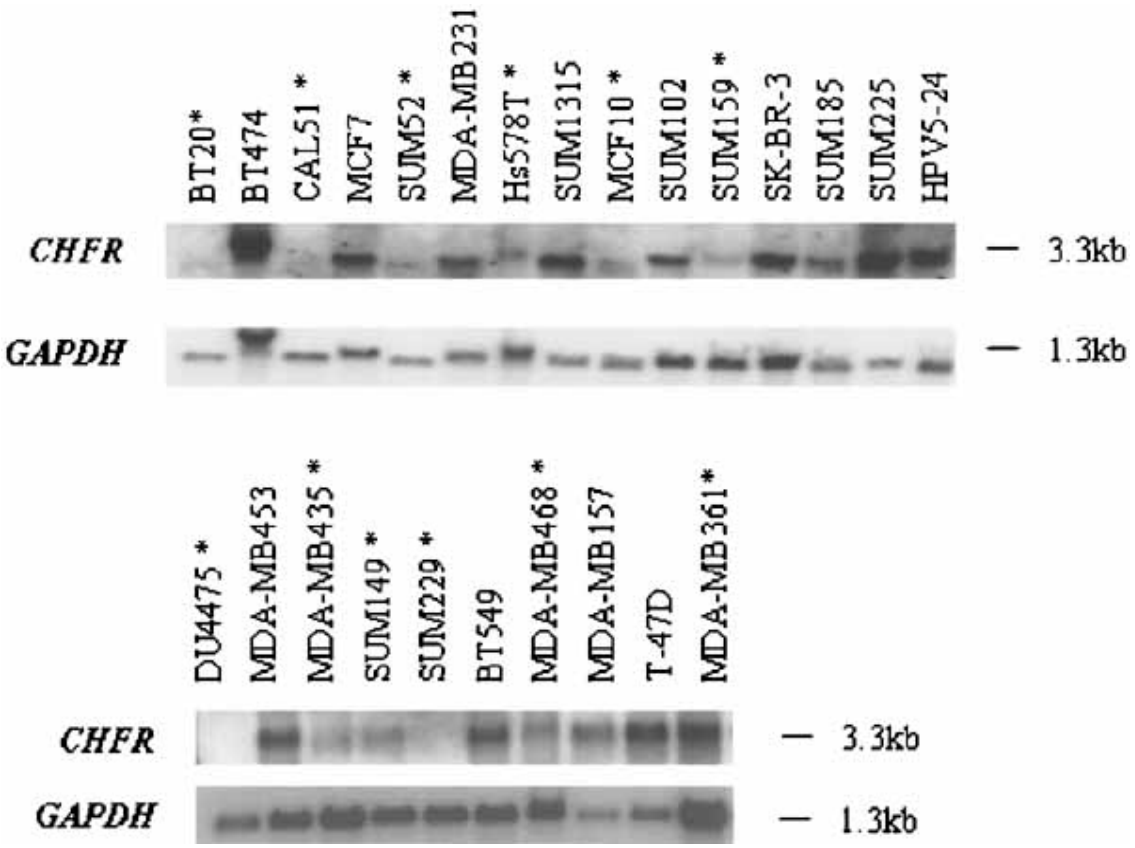

Figure 2.1: *CHFR* expression is low or lost in 50% of breast cell lines by Northern blot analysis.

Northern blotting using a probe for the central region of CHFR indicated that 50% (12 of 24) breast cell lines, not including the IHMEC line HPV5-24 used as a positive control, had low CHFR expression as indicated by an asterisk (*). MCF10A is another non-tumorigenic IHMEC line whereas the remaining samples are breast cancer cell lines. A probe for GAPDH was used as a loading control [21].

Materials and Methods

Cell Culture

Most cell lines were obtained from the American Type Culture Collection (AATC, Manassas, VA) and grown under recommended conditions. SUM1315, SUM102, SUM190, SUM159, SUM149, SUM52, SUM185, SUM225, SUM229, and the human papilloma virus (HPV)-immortalized series of non-tumorigenic immortalized human mammary epithelial cell (IHMEC) lines were developed and provided by S.P. Ethier (now available from Asterand) and cultured according to specified conditions [73]. A detailed description of relevant cell line information, including origins and hormone receptor status, has been compiled by Neve, R.M. *et al* [74]. For cell synchronization, $1x10^6$ cells were plated in a 100 mm dish and exposed to 2 mM thymidine for 12 hours, released into fresh media for 10 hours, then treated with another round of 2 mM thymidine for an additional 12 hours. Cells were then collected at the point of synchronization or released into fresh media for 4-10 hours to allow continuation into the S and G2/M phases of the cell cycle.

RT-PCR

For semi-quantitative duplex RT-PCR, reaction conditions were optimized as previously described [75]. Briefly, primer concentrations were optimized to create equal band intensity between *CHFR* and the internal *GAPDH* loading control, and the cycle number that resulted in the logarithmic phase of product generation was determined. Total RNA was isolated from cultured cell lines via the Qiagen RNeasy RNA isolation kit. cDNA was then generated from 1.0 μg of total RNA using the Qiagen Omniscipt

Reverse Transcription kit (Qiagen Inc.) and random hexamer primers. CHFR cDNA was amplified with the primers (forward/reverse, 5'-3'): CAGCAGTCCAGGATTACGTGTG/AGCAGTCAGGACGGGATGTTAC (500 bp) and GAPDH cDNA was amplified with the following primers (forward/reverse, 5'-3'): AGTCCATGCCATCACTGCCA/GGTGTCGCTGTTGAAGTCAG (340 bp). PCR products were separated on a 1.0% agarose gel in 1x TBE and stained with ethidium bromide. Band intensity was assessed using the IS-1000 Digital Imaging System (Alpha Innotech Corp).

For quantitative RT-PCR, cDNA samples from IHMECs and breast cancer cell lines were amplified in triplicate from the same total RNA sample following the manufacturer's instructions. Samples were amplified using TaqMan MGB FAM dye-labeled in an ABI7900HT model Real-Time PCR machine (Applied Biosystems). To amplify CHFR cDNA, probe set Hs00217191_m1 was utilized while the control, GAPDH, was amplified with probe set Hs99999905_m1 (Applied Biosystems). *CHFR* expression was considered low if it was less than the range of expression observed in immortalized epithelial cells.

Western Blotting

Whole cell lysates were collected according to manufacturer's instructions with the M-Per Mammalian Protein Extraction Buffer and HALT protease inhibitor cocktail with EDTA (Pierce) and the concentrations were quantified using the Bradford assay. To assess CHFR protein levels, 60.0 μg of total protein from 70-80% confluent cell cultures was separated on 10% SDS-PAGE gels using the Criterion or Ready gel systems (Bio-

Rad Laboratories) and immunoblotted to Hybond-P PVDF membrane (Amersham Biosciences). Following one hour of incubation in a blocking solution of 2.5% non-fat dry milk and 0.1% TBS-Tween20, a monoclonal antibody against CHFR (Abnova) was used at a 1:500 dilution in 2.5% non-fat dry milk and 0.05% TBS-Tween20 and incubated overnight at 4°C. CHFR was detected by hybridization with a goat anti-mouse:HRP secondary antibody (Cell Signaling Technology) at a 1:2000 dilution in 2.5% non-fat dry milk and 0.05% TBS-Tween20. For a loading control, blots were blocked in 5% non-fat dry milk and 0.1% TBS-Tween20 for one hour. The blots were then stripped and immunoblotted again with an antibody against GAPDH as a control. The anti-GAPDH antibody (Abcam) was used at a 1:10,000 dilution and detected with a goat anti-mouse:HRP antibody at a 1:15,000 dilution, both in 5% non-fat dry milk and 0.05% TBS-Tween20. The Super Signal West Pico Chemiluminescent kit (Pierce) was used for detection and blots were exposed to Kodak Biomax XAR film. Relative expression of CHFR was assessed by using the IS-1000 Digital Imaging System (Alpha Innotech Corp) for densitometry to determine signal intensity, then a ratio of CHFR:GAPDH or CHFR:β-Actin was calculated. CHFR expression was considered low if the ratio of relative expression was less than the range of expression observed within the immortalized epithelial cell lines.

Mitotic Index

Cells were collected at 70% confluence by trypsinization and resuspended in 0.075 M KCl on ice for 30 minutes. Cells were fixed in a 3:1 mixture of methanol and glacial acetic acid with mild vortexing, dropped onto glass slides, and stained with 544

μg/ml Giemsa solution. The mitotic index was calculated as the percentage of cells with condensed chromosomes. Nine hundred cells were counted on average for each cell line. Mitotic indices were calculated based on the percentage of cells that were in any stage of mitosis with visibly condensed chromosomes as analyzed by light microscopy. Mitotic indices less than 50% were considered "low," whereas indices more than 50% were considered "high."

Flow Cytometry

Cells were collected by trypsinization and pelleted, then washed in 1x PBS. Pelleted cells were fixed by the dropwise addition of ice-cold 100% ethanol and resuspended with mild vortexing. The ethanol was then aspirated off following centrifugation, and the cells were resuspended in 500 μl of 50 μg/ml propidium iodide and 100 μg/ml RNase in 1x PBS and analyzed by flow cytometry.

Tissue Samples and Immunohistochemistry

The monoclonal anti-CHFR antibody was used at a 1:50 dilution for hybridization to paraffin-embedded sections of human breast tissue using standard methods. Primary antibody was detected following protocols described by the manufacturer (DAKOCytomation,), using diaminobenzidine as a chromogen and with Harris Hematoxylin counterstain (Surgipath Medical Industries). Optimization and validation of the immunostaining conditions was performed on multi-organ tissue microarrays using a DAKO Autostainer.

To study CHFR expression in primary breast cancers, 160 paraffin-embedded patient samples arrayed on a single high density tissue microarray (TMA) were used for the analysis [76]. Details on this TMA have been previously described [77]. Tissue cores from 98 patients with invasive breast carcinoma were available to evaluate CHFR staining. The staining was scored using a 4 tiered scoring system (1=negative, 2=weak, 3=moderate, 4=strong) by two independent trained investigators in the Department of Pathology (Celina Kleer, MD and Lei Ding.) and ChromaVision computerized scoring (Clarient Inc.). To determine CHFR staining in normal mammary epithelia, paraffin-embedded tissues from patients were prepared as above. Digital images were obtained with an Olympus BX-51 microscope and SPOT camera system at either a 40x or 60x objective magnification. Images of normal breast samples were recoded at a 20x objective magnification.

Statistical Analysis

The Wilcoxon rank test was used to determine if there was an association between CHFR staining and clinico-pathological variables including patient age, tumor size, tumor grade, lymph node status, estrogen receptor (ER), progesterone receptor (PR), HER2/neu status, and patient survival. The Chi-square test, using a 2 x 2 contingency table, was used to test for statistical significance when comparing CHFR expression by Western blotting with mitotic indices.

Results

CHFR mRNA Expression in Breast Cancer Cell Lines

Previous reports indicated that CHFR mRNA was low in 50% of breast cancer cell lines as assessed by Northern blot analysis [21]. In this study, quantitative RT-PCR was employed to better define the levels of CHFR mRNA from asynchronous breast cancer cell lines compared to IHMECs. mRNA was collected from cells at 70-80% confluency, the same confluency previously used for Northern blot analysis. Quantitative RT-PCR was performed using a probe that hybridized to exons 12 and 13, which is near the middle of the probe previously used for Northern blot analysis. Quantitative RT-PCR revealed that only 18% (four of 22) of breast cancer cell lines showed CHFR expression levels lower than the range of expression observed in HPV-immortalized IHMECs (Figure 2.2). These four cell lines, CAL51, DU4475, Hs578T, and SUM229, were also found to have low or lost CHFR expression by Northern blot analysis [21]. In addition, a spontaneously immortalized IHMEC line, MCF10A, was also found to have low *CHFR* mRNA expression by both Northern blotting and quantitative RT-PCR.

Low CHFR Expression in Breast Cancer Cell Lines Correlates with a High Mitotic Index

Western blotting was performed to assess CHFR expression in breast cancer cell (BCC) lines and immortalized human mammary epithelial cell (IHMEC) lines. Variable expression was noted among the breast cancer cell lines. Densitometry analysis revealed that 41% (9 of 22) of asynchronous breast cancer cell lines appeared to have low or no CHFR expression compared to the lowest amount of expression observed among four

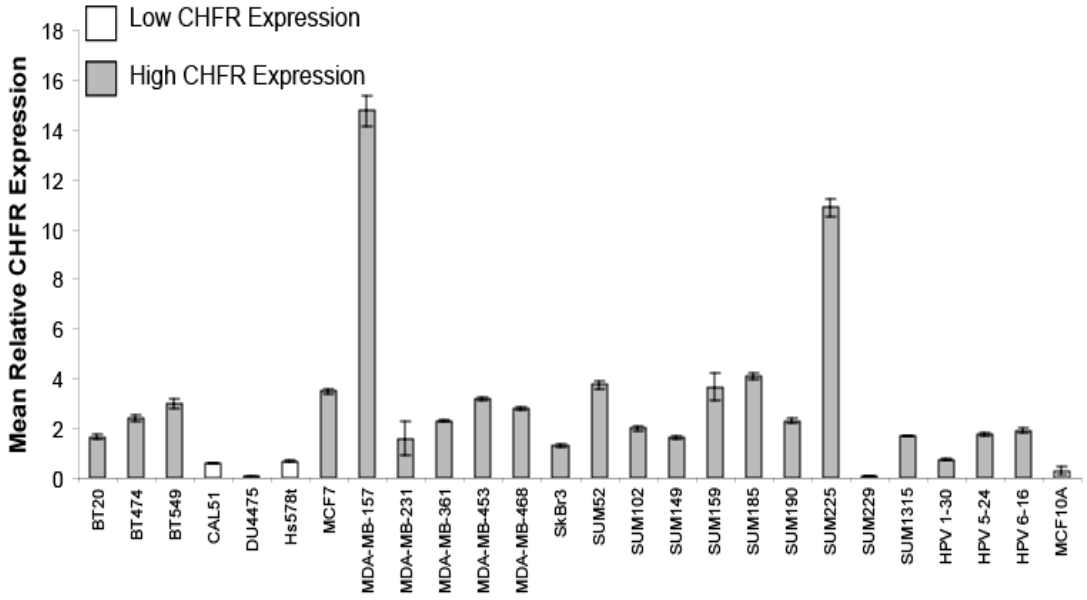

Figure 2.2: *CHFR* mRNA expression is low in 18% of breast cancer cell lines by quantitative RT-PCR.

Quantitative RT-PCR, using a probe that spanned exons 12 and 13 of the *CHFR* gene, indicated that 18% (four out of 22) breast cancer cell lines and the MCF10A IHMEC line (white bars) had low *CHFR* expression. Low expression was characterized as a ratio of *CHFR* to *GAPDH* lower than that observed in the range of HPV-immortalized IHMEC cells (< 0.7). The remaining cell lines (black bars) either had *CHFR* expression within the range of HPV-immortalized IHMECs (in bold) or were found to have high *CHFR* expression.

IHMEC cell lines, whereas only one cell line, MDA-MB-157, had expression higher than the range observed in IHMEC cells (Figure 2.3). This cell line also had highly upregulated mRNA expression as determined by quantitative RT-PCR (Figure 2.2). The remaining lines had expression levels that fell within the range of IHMEC cells.

The previously published mitotic indices of the breast cancer cell lines and two IHMEC lines, MCF10A and HPV4-12, were graphed and organized according to CHFR protein expression (Figure 2.4) [21]. There was a statistically significant correlation between CHFR protein expression and mitotic index following nocodazole treatment ($p<0.001$, Chi-square test). It became apparent that all of the cell lines that were determined to have low or no CHFR protein expression had high (>50%) mitotic indices. Of the remaining breast cancer cell lines, 62% had CHFR expression similar to the IHMEC lines and low mitotic indices and the two IHMEC lines had low mitotic indices. Only five breast cancer cell lines with "high" CHFR expression (i.e.: similar to the expression observed in IHMECs) had an uncharacteristically high mitotic index, which may be due to any number of mutations or alterations that could impair the poorly characterized CHFR-mediated prophase checkpoint pathway or other pathways.

CHFR Protein is Present During the S and G2/M Phases of the Cell Cycle

In order to test if CHFR protein expression was cell cycle regulated a series of breast cancer and IHMEC lines were synchronized with a double-thymidine block and released into fresh media. Cells were collected periodically for both whole cell lysates and for analysis by flow cytometry to determine their cell cycle profile. CHFR expression may have been noticeable in the G1 sample of some of the lines due to

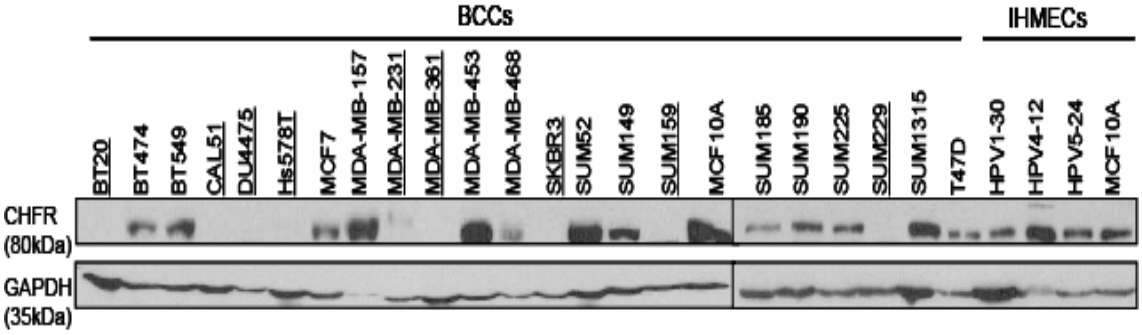

Figure 2.3: CHFR protein expression is low or lost in 41% of breast cancer cell lines by Western blotting.

Western blot analysis using a monoclonal CHFR antibody reveals that 9 of 22 (41%, underlined) asynchronous breast cancer cell lines, or BCCs, at 70-80% confluence have low CHFR expression compared to the lowest level of expression observed among four asynchronous immortalized human mammary epithelial cells (IHMECs). To control for loading, an antibody against GAPDH was used (bottom). This figure is a composite image of two separate Western blots. Whole cell lysate from the MCF10A IHMEC line was used as a control on both blots in the composite image.

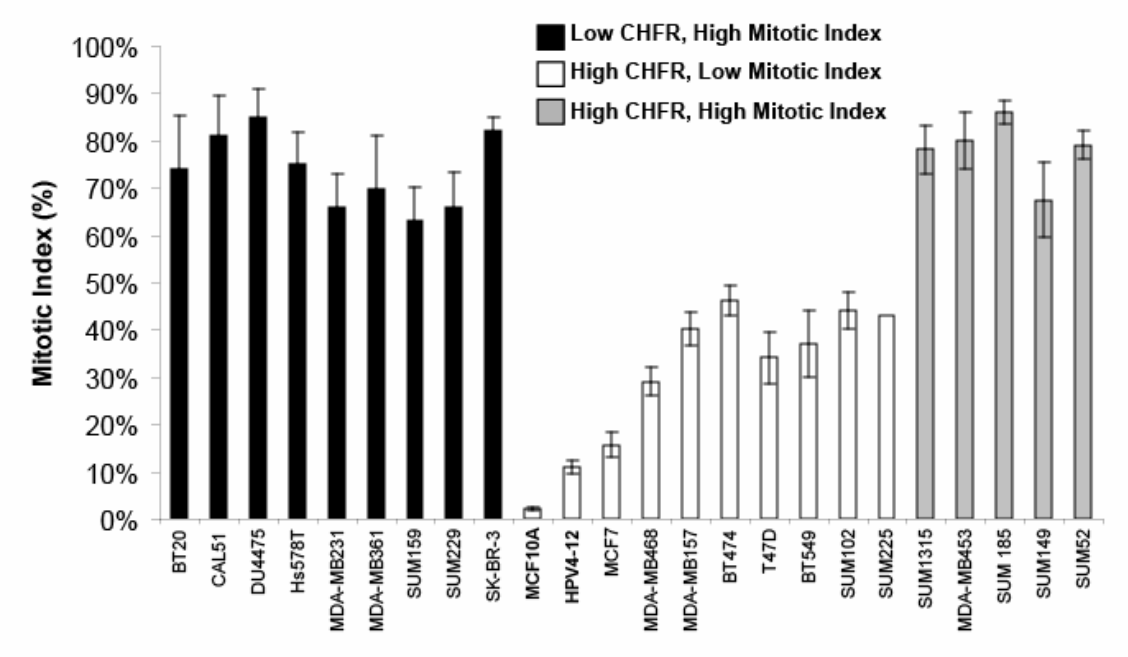

Figure 2.4: Low CHFR protein expression correlates with a high mitotic index in breast cancer cell lines.

The mitotic index of breast cancer cell lines and two IHMEC lines (bold) were plotted and arranged according to whether they were "low" or "high" CHFR expressing lines. High expressing cell lines are those in which CHFR expression was determined to be within the range observed in IHMEC lines by Western blotting. The mitotic index was considered high if it was greater than 50%. Cells were treated with nocodazole and mitotic indices were determined, following Giemsa staining of dropped slides, based on the percentage of cells with condensed chromosomes. There was a statistically significant correlation between CHFR expression and mitotic index ($p<0.001$, Chi-square test).

contamination with S phase cells. The synchronization process was inefficient for G1 phase enrichment as some lines had nearly equal percentages of G1 and S cells following the double-thymidine block. There was better enrichment for cells in the later stages of the cell cycle following release into fresh medium. CHFR was expressed at least during the S and G2/M phases of the cell cycle in the IHMEC cell lines HPV4-12 and MCF10A, supporting its role as a mitotic checkpoint protein (Figure 2.5). Of note, two of the four breast cancer cell lines, CAL51 and Hs578T, either did not express CHFR at all or actually had lower CHFR expression during the G2/M phases than the G1 and S phases. Both of these cell lines were characterized as having low or no CHFR expression by Western blotting, as indicated above, and a high mitotic index that signified an impaired CHFR-mediated prophase checkpoint.

CHFR Expression in Primary Breast Cancers

As expected, CHFR staining by immunohistochemistry was prominent in the cytoplasm of mammary gland epithelial cells from normal primary breast tissue (Figure 2.6). We also found prominent nuclear staining of CHFR in some cells of the epidermis near the edge of the biopsy sample, indicating that CHFR may translocate to the nucleus in rapidly dividing cells and tissues, which was supported by the fact that this was also observed in primary intestinal and testicular tissue (Figure 2.7, and data not shown). We next wanted to determine if CHFR expression was altered in primary breast cancers. From 160 patient samples of invasive breast carcinoma present on a tissue microarray (TMA), 142 were available to score for CHFR staining. Of the 142 patient samples of invasive breast cancer scored for CHFR staining, 36% were negative, but only 5.6%

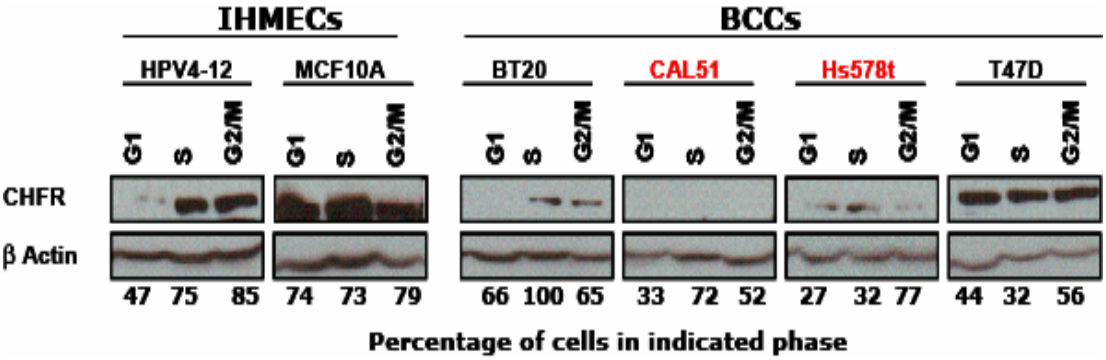

Figure 2.5: CHFR expression is present at least during the S and G2/M phases of the cell cycle in most breast cell lines studied.

Cell lines were synchronized at the G1/S transition with a double-thymidine block (G1) and then released in to fresh medium for 4-10 hours to enrich for S and G2/M phase cells. Cells were analyzed following propidium iodide staining by flow cytometry to determine the DNA content, which indicated cell cycle stage. The percentage of cells in each phase of the cell cycle is indicated below the sample. Western blotting was performed to indicate CHFR expression (top band) and GAPDH (bottom band) was used as a loading control.

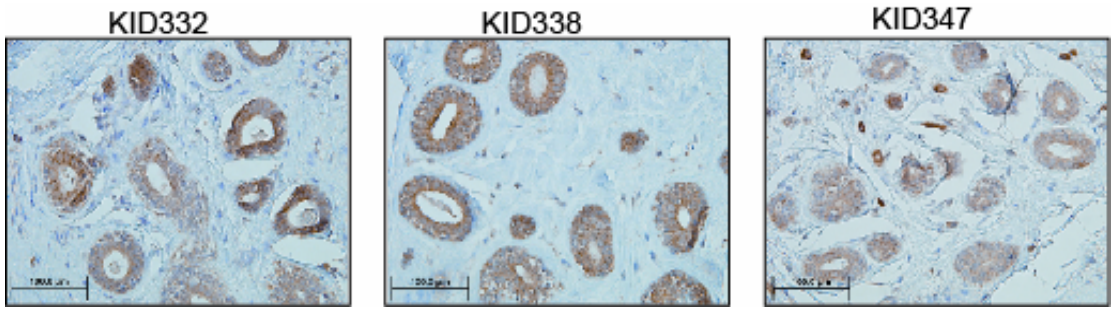

Figure 2.6: CHFR is expressed in the mammary gland epithelial cells from normal breast tissue.

Immunohistochemistry for CHFR protein expression showed prominent staining in the cytoplasm of the mammary gland epithelia in normal primary breast tissue samples. Representative examples are indicated by three separate patient tissues: KID332, KID338, and KID347. The bars indicate a size of 100 microns.

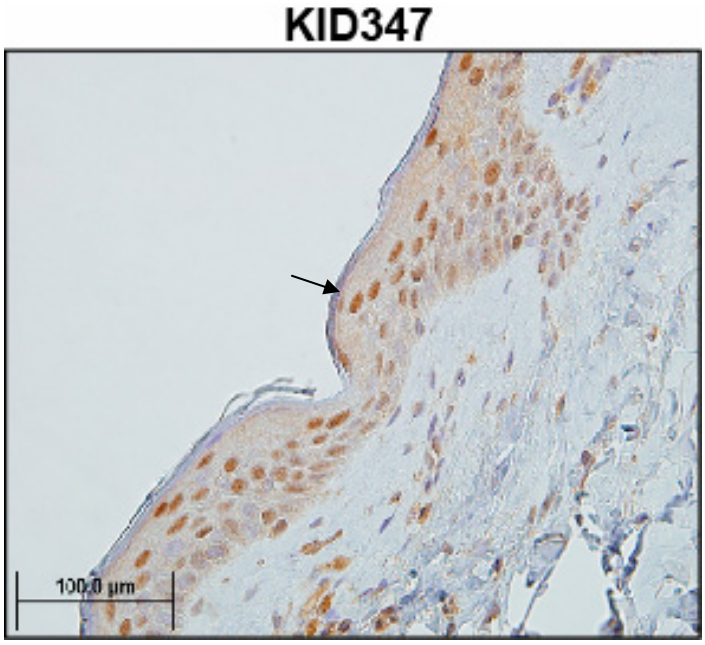

Figure 2.7: Immunohistochemistry for CHFR shows prominent nuclear and cytoplasmic staining in skin cells and stromal cells.

Immunohistochemistry for CHFR protein expression showed prominent staining in the nuclei and lighter staining in the cytoplasm of epidermal skin cells at the edge of the biopsy sample. This example is from patient KID347. The bar indicates a size of 100 microns.

showed strong CHFR staining. The number of patient samples per staining score are as follows: negative (1), 51; weak (2), 35; moderate (3), 48; and strong (4), 8 (Figure 2.8).

CHFR Expression Correlates with Clinical and Pathological Variables

Immunohistochemistry was performed on a tissue microarray that consisted of 160 tissue samples of primary invasive breast cancers. Of the 160 samples, 98 had complete clinico-pathological data for statistical analysis. The staining for CHFR expression was scored using a 4-tiered scoring system (1=negative, 2=weak, 3=moderate, 4=strong). Patient samples were annotated for several clinico-pathological variables including: tumor size, estrogen receptor (ER) status, progesterone receptor (PR) status, HER2/neu expression, lymph node status, patient age, and tumor grade. Primary samples were classified as positive for CHFR staining and expression if they scored between two and four in staining intensity. Since there is no published evidence as to a threshold of expression that is required for proper CHFR function, we included all positively stained samples in our analysis. Interestingly, there was a trend towards positive CHFR staining being correlated with ER-positive tumors ($p=0.0903$ by Wilcoxon rank test, $p=0.0653$ by t-test; Table 2.1). There was a striking significant correlation between positive CHFR staining and small (< 2cm) tumor size ($p=0.0179$, Wilcoxon rank test).

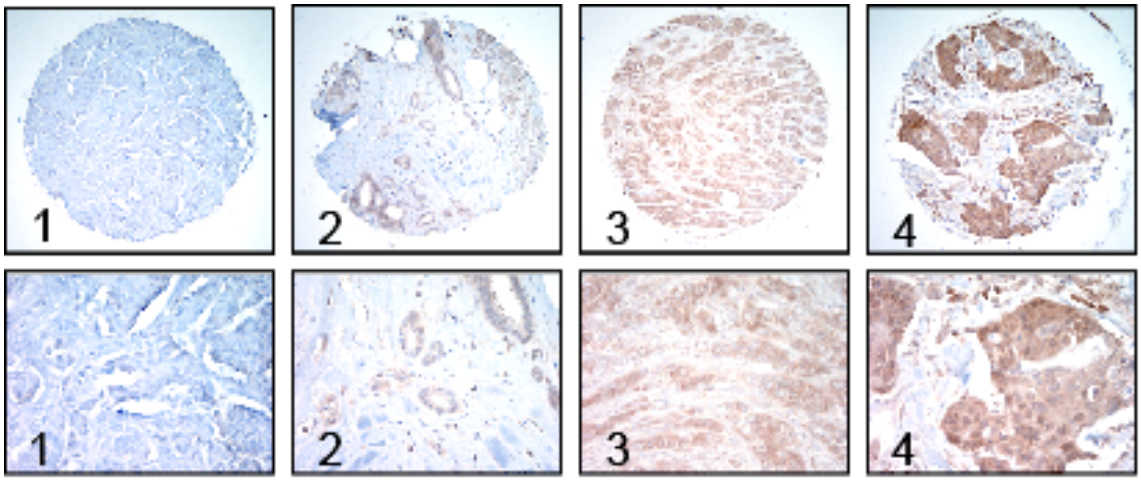

CHFR score	no. of patients
1 (negative)	51
2	35
3	48
4 (strong)	8

Figure 2.8: CHFR staining is negative in 36% (51 of 142) of primary invasive breast cancers as determined by immunohistochemistry.

Immunohistochemistry using a monoclonal antibody against CHFR on primary invasive breast cancers from a tissue microarray shows a range of CHFR expression. Intensity of CHFR staining ranged from negative (1) to weak (2), moderate (3), and strong (4). The images on the top are at 10x magnification whereas the corresponding pictures on the bottom are 40x magnifications from sections of the above image.

Table 2.1: Correlation of CHFR expression with clinical and pathological variables from 160 patient samples.

Clinicopathologic variables	Patients with variable	P value*
Age		
<50	47	N/S
≥50	96	
Size		
< 2 cm	80	0.0179
≥ 2 cm	63	
Positive Lymph Nodes		
High (>4)	24	N/S
Low (1–3)	111	
ER expression		
Positive	87	0.0903
Negative	44	
PR expression		
Positive	71	N/S
Negative	61	
Her2/*neu*		
Positive	122	N/S
Negative	21	
Grade		
1	13	N/S **
2	63	
3	65	

* Wilcoxon rank test for significance ** Student's t-test

N/S: Not Significant

Discussion

Prior to this work, many studies focused on the expression profiles of *CHFR* mRNA, but results indicating possible correlations with clinical and pathological variables were contradictory. This may be because mRNA expression does not always reliably predict protein levels, due to processes such as post-transcriptional regulation. Therefore, in this report we analyzed CHFR protein expression then compared it to current and previous reports of mRNA expression levels to assess if mRNA detection could predict protein expression, and determined if protein expression correlated with clinical and pathological data in both cultured and primary breast cancers.

When the mRNA expression data from the quantitative RT-PCR was compared to the previously published Northern blot data (Figure 2.1), there were six breast cancer cell lines in which the mRNA expression levels were not consistent between the two methods. These lines were considered low by Northern blotting but were within the range of expression observed in IHMEC lines by quantitative RT-PCR. These cell lines were BT20, SUM52, SUM159, SUM149, MDA-MB-468, and MDA-MB-361. However, for three cell lines, the low expression level identified by Northern blotting matched that observed by Western blotting (BT20, SUM159, and MDA-MB-361) and, in agreement with CHFR's role in regulating mitotic entry, all three of these cell lines were previously determined to have a high mitotic index following nocodazole treatment. The other three cell lines (SUM52, SUM149, and MDA-MB-486) were found to have *CHFR* mRNA expression similar to the levels observed in IHMEC lines by quantitative RT-PCR, which was confirmed by Western blotting. Only one of these cell lines, MDA-MB-468, was previously determined to have the expected low mitotic index following nocodazole

treatment that has been associated with positive CHFR expression. The other two lines, SUM52 and SUM149, still had uncharacteristically high mitotic indices despite having CHFR expression levels similar to IHMECs, which may be due to a different impaired protein in the CHFR-mediated prophase checkpoint pathway.

The difference between Northern blot analysis and quantitative RT-PCR may be a result of the much higher sensitivity of quantitative RT-PCR to low amounts of sample or perhaps some transcripts were more easily detected by the quantitative RT-PCR probe in comparison to the probe used for Northern blotting. In addition, the arbitrary and non-quantitative identification of cell lines with "low" *CHFR* expression by Northern blot analysis, without the use of immortalized lines or mRNA from normal mammary tissue as a guide for what constitutes "normal" *CHFR* expression, lends itself to the mischaracterization of cell lines in terms of their expression levels. However, when the two mRNA detection methods are combined, the results resemble the relative expression observed by Western blotting. Cell lines with "normal or high" mRNA levels tended to have "normal or high" protein expression that resembled that seen in IHMECs, and vice versa. In conclusion, a single method of detecting mRNA expression was not sufficient to predict the amount of protein detected by Western blotting.

There were three cell lines, MDA-MB-231, SKBr3, and MCF10A, in which the *CHFR* mRNA levels agreed between the Northern blot and the quantitative RT-PCR, but the protein expression identified by Western blotting did not agree with the mRNA expression. Both MDA-MB-231 and SKBr3 were determined to have "high" *CHFR* mRNA expression but were found to have very low protein expression by Western blotting when compared to IHMECs. Interestingly, both of these cell lines had a high

mitotic index, which agrees with their classification as "low" expressing lines by Western blotting. The spontaneously immortalized IHMEC line, MCF10A, was found to have low *CHFR* mRNA expression using both methods, but Western blotting revealed that it actually expressed CHFR protein at levels similar to the other IHMEC lines, which agreed with the finding that it had a low mitotic index.

The lack of a direct correlation between mRNA levels and protein expression suggested that CHFR might be regulated by post-transcriptional or post-translational modifications. Previous studies have shown that CHFR auto-ubiquitinates and that it might be phosphorylated [5, 7, 16]. A recent publication also indicated that CHFR could be modified by poly(ADP-ribosyl)ation, which is the addition of long chains of ADP-ribose [9]. These modifications and perhaps others might begin to explain the differences between mRNA and protein expression levels due to changes in protein stability. In support of this, our lab and others have found that antibodies against CHFR occasionally, but not always, identify a second band; however, the identity of this band or the modification of CHFR that leads to the size differential has not been determined. The different band sizes may be due to the presence of alternative transcripts or protein modifications such as phosphorylation, ubiquitin conjugation, or poly(ADP-ribosyl)ation.

Attempts to identify when CHFR was expressed during the cell cycle using a double-thymidine block synchronization method indicated that CHFR was expressed during the S and G2/M phases of the cell cycle. Detection of CHFR during the G1 phase was difficult to interpret due to the inefficiency of the synchronization method. Further studies are required to identify how CHFR expression is regulated and when it is expressed during the cell cycle.

We noticed that the frequency of low or lost CHFR expression by Western blotting and immunohistochemistry (approximately 40%) was much greater than the incidence of CHFR over-expression or strong staining, which was 4.5% and 5.6%, respectively, in breast cancers. Of interest, during the course of this work we attempted to over-express CHFR in several mammary epithelial cell lines, both cancer and non-tumorigenic lines, using both transient and stable transfection and retroviral transduction methods, but nearly all attempts resulted in cellular toxicity. This suggested that the expression of CHFR must be tightly regulated such that too little may contribute to tumorigenesis but over-expression, which rarely occurs, may lead to cell death in many genetic backgrounds.

The frequency of low or lost expression in breast cancer cell lines (41%) was very comparable to the occurrence of lost expression in primary invasive breast cancers (36%). This suggests that the breast cancer cell lines are good models for studying the mechanisms and results of lost CHFR expression. It is interesting to note that had the category of "weak" CHFR expression by immunohistochemistry been included in the calculations, then nearly 61% of primary invasive breast cancers would have been considered to have "low or lost" CHFR expression. This is a staggeringly high number, which indicates that loss or down-regulation of CHFR protein expression may be a very common occurrence in breast cancers. The samples in this category obviously had less intense staining when compared to the intensity of CHFR staining in the three normal mammary tissue samples shown. However, because the threshold of the amount of CHFR necessary for proper cellular function has not been determined, we had to include this group along with the "moderate" and "strong" expression groups.

In regards to primary invasive breast carcinoma, the correlation between CHFR staining and small tumor size, a very important prognostic indicator, is remarkable and supports a role for CHFR as a tumor suppressor. In addition, the putative association of CHFR and ER expression may provide continued support of a role for CHFR as a biomarker for breast cancer treatment. This is particularly relevant given previous clinical trials that showed ER-positive, and therefore possibly CHFR-positive, breast cancers did not respond as well to paclitaxel treatment as ER-negative breast cancers [78-80]. This corresponds well with previously published work describing CHFR-negative cells as sensitive to microtubule poisons in culture, undergoing apoptosis sooner than their CHFR-positive counterparts. The weak association of expression between ER and CHFR also may help to elucidate another molecular pathway in which CHFR functions to mediate cell proliferation or a common means of gene expression regulation.

The frequency of decreased CHFR expression indicated that loss of expression was biologically relevant for tumorigenesis. It also was noted that low CHFR protein expression strongly correlated with a high mitotic index, indicating that CHFR may play an important role in regulating mitotic entry and/or proliferation. Of particular importance, the loss of CHFR expression strongly associated with the important pathological variable, and prognostic indicator, of large tumor size. When combined, these results suggest that CHFR may be a cancer-relevant protein with important tumor suppressive functions. In addition, the data indicate that a single method of detecting *CHFR* mRNA does not reliably predict protein expression, and that protein levels of CHFR can be used to identify correlations between expression and clinical and pathological variables.

Acknowledgements

This work was supported by a Department of Defense Breast Cancer Research Pre-doctoral Fellowship, #BC050310, and by the NIH National Research Service Award #5-T32-GM07544 from the National Institute of General Medicine Sciences to LMP and an NIH NCI grant RO1CA072877 to EMP. We would like to acknowledge A. Elif Erson for her guidance and data from the Northern blot and mitotic indices studies. We thank Esther Peterson for helpful suggestions and discussion, and Donita Sanders for technical assistance with IHC protocols. We thank Thomas Giordano, M.D., for primary normal breast tissue samples and Stephen Ethier, Ph.D., for the HPV and SUM breast cell lines.

Notes

Parts of this work were previously published as:

Privette, L.M., Gonzalez, M.E., Ding, L., Kleer, C.G., and Petty, E.M., "Altered expression of the early mitotic checkpoint protein, CHFR, in breast cancers: implications for tumor suppression," *Cancer Research*. 2007 Jul 1;67(13):6064-74. Published Online First June 27, 2007. doi: 10.1158/0008-5472.CAN-06-4109.

CHAPTER 3

ALTERED EXPRESSION OF CHFR IN MAMMARY EPITHELIAL CELLS: IMPLICATIONS FOR TUMOR SUPPRESSION

Summary

CHFR (Checkpoint with FHA and Ring Finger) is hypothesized to mediate a delay in cell cycle progression, early in mitosis, in response to microtubule stress, independent of the spindle assembly checkpoint. As a potential regulator of cell cycle progression, CHFR naturally becomes an interesting target for understanding cancer cells. In recent years, there has been increasing evidence supporting the role of CHFR as a tumor suppressor, most of which reports loss of expression, occasionally due to promoter hyper-methylation, in cancers compared to patient-matched normal tissues. To study the effects of low CHFR expression *in vitro*, we stably expressed a shRNA construct targeting CHFR in two lines of immortalized human mammary epithelial cells (IHMECs). Notably, decreased CHFR expression resulted in the acquisition of many phenotypes associated with malignant progression including accelerated growth rates, higher mitotic index, enhanced invasiveness, increased motility, greater aneuploidy, and amplified colony formation in soft agar. In complementary studies, over-expressing CHFR in the Hs578T breast cancer cell line abrogated several tumorigenic phenotypes in culture, further supporting the role of CHFR as a tumor suppressor in breast cancer.

Introduction

Breast cancer is caused by changes in gene expression or function that result in normal mammary epithelial cells growing uncontrollably and sometimes becoming able to metastasize to distant sites. Some of the characteristics that differentiate a cancer cell from a normal cell are that they become self-sufficient for growth signals, insensitive to anti-growth signals, they can evade apoptotic cell death, they have limitless replicative potential (i.e.: they are immortalized), they can promote angiogenesis, they can invade surrounding tissue to metastasize, and genomic instability often occurs [81]. The genes that affect these characteristics can be classified either as tumor suppressors or as oncogenes. Tumor suppressor genes are needed to decrease growth rates, maintain cell morphology and polarity, activate an apoptotic response, prevent genomic instability, and impede cellular invasion and motility to inhibit metastasis. On the contrary, oncogenes promote tumorigenesis by increasing growth rates, changing cellular morphology and polarity, deactivating the apoptotic response pathways, promoting genomic instability, and enhancing the invasive potential and motility of a cell to promote metastasis [81]. The expression of tumor suppressor genes is often down regulated in cancers or the protein becomes non-functional whereas oncogenes are typically over-expressed or functionally hyperactive in cancers compared to normal cells. However, for cancer to develop a combination of tumor suppressor loss and the gain of activated oncogenes is required [81].

Several methods can be used both in cell culture and by analyzing primary breast cancer tissue to determine if a gene has a role in regulating tumorigenesis. Though many assays themselves do not predict if a cell is tumorigenic, they can suggest that the cell has

phenotypically changed to resemble a cancer cell. As an example, the growth rate of the cell population can be measured by manually counting cells over the course of several days. However, changes in growth rates can be caused by either increased cellular proliferation ("self-sufficiency of growth signals") or decreased cell death by apoptosis [82]. Therefore, methods to monitor cellular metabolism or cell death are required to determine the causes of altered population growth rates. One method to test whether or not potentially cancerous cells have the ability to metastasize is through a chemo-invasion assay using a Matrigel collagen matrix to model the basement membrane of tissues, and by measuring cellular motility into surrounding empty spaces in a culture plate [83]. The chemo-invasion Matrigel assay tests if cells can migrate through the collagen matrix in order to reach a growth factor or chemoattractant. Cellular morphology and polarity changes can be noted by visual inspection of cell shape and by assessing protein marker expression that is characteristic of particular cell types. Likewise, genomic instability can be tested by manually counting the chromosomes on slides prepared from metaphase cells. The final cell culture method to assess tumorigenicity is to determine if cells have the ability to grow in colonies in a soft agar suspension, indicating they have lost cell-to-cell contact inhibition and have acquired anchorage-independent growth [84]. In addition to cell culture models, another means of determining if a cell has become tumorigenic is to inject the cells into immuno-compromised mice to determine if tumors are able to form *in vivo* [85].

Primary cancer tissue can be characterized by its visible difference from normal tissue when analyzed with a microscope. Primary malignant cancers will have lost tissue organization and will appear as a mass of unorganized cells, with possible evidence of

invasion into surrounding normal tissue and stroma. Diagnostic and prognostic information is gathered by looking for protein markers for proliferation, such as Ki67, and other defining characteristics such as the presence of estrogen and progesterone hormone receptors in breast cancer and aneuploidy [86]. Further characterization of cancer is done by staging the cancer according to tumor size and the presence or absence of metastasis; early stage cancers have small tumor sizes of less than two centimeters and no metastatic lesions [87].

To characterize the role of CHFR in breast cancer, we used both cultured breast cell lines and primary patient samples. Analysis of a tissue microarray composed of primary invasive breast cancer samples by immunohistochemistry indicated that CHFR staining was inversely correlated with tumor size. In view of this evidence that CHFR may have tumor suppressive properties, we mimicked cellular loss of expression via stable shRNA and transient siRNA targeting CHFR in two IHMEC lines. This decrease in expression led to the acquisition of many phenotypes associated with malignant progression.

Materials and Methods

Cell Culture

MCF10A and Hs578T cell lines were obtained from the American Type Culture Collection (AATC) and grown under recommended conditions. The human papilloma virus (HPV)-immortalized non-tumorigenic mammary cell line, HPV4-12, was developed and provided by S.P. Ethier (now available from Asterand) and cultured according to specified conditions [73]. A detailed description of relevant cell line information, including origins and hormone receptor status, has been compiled by Neve, R.M. *et al*

[74]. Table 3.1 briefly describes the three cell lines predominantly used in these experiments.

For retroviral transduction, PT67 packaging cells were transfected using FuGENE 6 with 10.0 μg of pRNA-H1.1/Hygro vector (GenScript Corp.) containing either a scrambled sequence or a CHFR shRNA construct targeting nucleotides 324-344, 1491-1511, or 2497-2517 (accession no. AF170724). We used the pLPCX retroviral vector for overexpression of full-length *CHFR* in Hs578T cells (Clontech Laboratories). Virus was collected after 48 hours and purified with a 0.45-micron filter. Equal parts of retrovirus-containing media and normal growth media were added to $1x10^6$ cells. Fresh media was added 24 hours later and selection with 20.0 μg/ml hygromycin (pRNAH1.1) or 1.5 μg/ml puromycin (pLPCX) began 48 hours post-infection. The resulting polyclonal cell population stably expressing the CHFR construct(s) was subsequently used for experimentation. MCF10A cells were transduced with all three shRNA constructs whereas HPV4-12 cells were transduced with the shRNA construct targeting nucleotides 324-344 to achieve maximum knockdown.

Transient transfection of siControl or a pool of four siRNAs targeting CHFR (si*GENOME*, Dharmacon RNA Technologies) was performed according to manufacturer's instructions. HPV4-12 cells were transfected using Dharmafect2 lipofection reagent and MCF10A cells with Dharmafect1. For both methods, stable shRNA and transient siRNA, knockdown of CHFR expression was confirmed using semi-quantitative duplex RT-PCR and Western blotting, followed by densitometry.

Table 3.1: A summary of important characteristics of the cell lines used in this work.

Cell Line	Origin	Ploidy	Method of Immortalization	Tumorigenic?
HPV4-12	Mammary gland epithelia	49, XXX (+7, +20)	Human Papilloma Virus (HPV) infection •Viral E6/E7 protein	No
MCF10A	Mammary gland epithelia	48, XX (+1, +7)	Spontaneous •Translocation interrupted p15/p16 locus •Additional rearrangements	No in nude mice Yes in semi-solid media
Hs578Tt	Mammary gland epithelia, carcinoma	Complex and variable chromosome number, 50-77	Carcinoma •Estrogen receptor (ER) negative •No endogenous viruses	No in nude mice Yes in semi-solid media

Western Blotting

To assess CHFR protein levels in asynchronous cells, 60.0 μg of total protein from 70-80% confluent cell cultures was separated on 10% SDS-PAGE gels using the Criterion or Ready gel systems (Bio-Rad Laboratories) and immunoblotted to Hybond-P PVDF membrane (Amersham Biosciences). Following one hour of incubation in a blocking solution of 2.5% non-fat dry milk and 0.1% TBS-Tween20, a monoclonal antibody against CHFR (Abnova Corp.) used at a 1:500 dilution in 2.5% non-fat dry milk and 0.05% TBS-Tween20 and incubated overnight at 4°C. CHFR was detected by hybridization with a goat anti-mouse:HRP secondary antibody (Cell Signaling Technology) at a 1:2000 dilution in 2.5% non-fat dry milk and 0.05% TBS-Tween20. For a loading control, blots were blocked in 5% non-fat dry milk and 0.1% TBS-Tween20 for one hour. The blots were then stripped and immunoblotted again with an antibody against GAPDH as a control. The anti-GAPDH antibody (Abcam) was used at a 1:10000 dilution and detected with a goat anti-mouse:HRP antibody at a 1:5,000 dilution, both in 5% non-fat dry milk and 0.05% TBS-Tween20. The Super Signal West Pico Chemiluminescent kit (Pierce) was used for detection and blots were exposed to Kodak Biomax XAR film. Relative CHFR expression was assessed by densitometry with the IS-1000 Digital Imaging System (Alpha Innotech Corp.). A ratio of CHFR:GAPDH was calculated and normalized to the control samples.

RT-PCR

For duplex RT-PCR, reaction conditions were optimized as previously described [75]. Primer concentrations were optimized to create equal band intensities between

CHFR and the internal *GAPDH* loading control, and the cycle number that resulted in the logarithmic phase of product generation was determined. Total RNA was isolated via the Qiagen RNeasy RNA isolation kit. cDNA was then generated from 1.0 μg of total RNA using the Qiagen Omniscipt Reverse Transcription kit and random hexamer primers. Primers to amplify CHFR cDNA were (forward/reverse, 5'-3'): CAGCAGTCCAGGATTACGTGTG/AGCAGTCAGGACGGGATGTTAC (500 bp) or TCCCCAGCAATAAACTGGTC/GTATGCCACGTTGTGTTCCG (205 bp) and primers for GAPDH cDNA amplification were (forward/reverse, 5'-3'): AGTCCATGCCATCACTGCCA/GGTGTCGCTGTTGAAGTCAG (340 bp). PCR products were separated on a 1.0% ethidium bromide-stained agarose gel. Densitometry was performed using the IS-1000 Digital Imaging System (Alpha Innotech Corp.)

For quantitative RT-PCR, cDNA samples from IHMECs and breast cancer cell lines were amplified in triplicate from the same total RNA sample following the manufacturer's instructions. Samples were amplified using TaqMan MGB FAM dye-labeled in an ABI7900HT model Real-Time PCR machine (Applied Biosystems). To amplify CHFR cDNA, probe set Hs00217191_m1 was utilized while the control, GAPDH, was amplified with probe set Hs99999905_m1 (Applied Biosystems).

Growth Curve Analysis

To determine the growth rate, $4x10^4$ cells were plated into each well in 6-well plates. Cells from three different wells were then manually counted with a hemacytometer. A new set of three wells were counted every two to three days for seven

or nine days, at which point at least one cell line began to reach confluence. Average cell numbers from the three wells were then plotted as a function of a time.

Immunofluorescence and Mitotic Index

Early mitotic chromosomes were identified via immunofluorescence using a Histone H3-phospho-Ser28 antibody (Upstate) at a 1:100 dilution and anti-rabbit Alexafluor488 secondary antibody at a 1:500 dilution both diluted in blocking solution. Cells were blocked in 5% non-fat dry milk, 1% BSA, and 0.025% TritonX-100 solution in PBS for one hour prior to incubation with primary antibody. Cells were counterstained with phalloidin conjugated to Alexafluor568 to detect the actin cytoskeleton and ProLong Gold anti-fade reagent with DAPI to detect all nuclei (both available from Molecular Probes/Invitrogen). Cells were visualized using a compound Leica DMRB miscroscope with a Leitz laser at 63x magnification (W. Nuhsbaum). The mitotic index was the percentage of H3-Ser28 stained nuclei from 1000 total (DAPI-stained) nuclei.

To assess for vimentin staining, cells were plated 24 hours prior to staining at a density of $3x10^4$ cells per chamber in two-chambered slides. MCF10A cells that were transiently transfected with a pool of four CHFR siRNAs were transfected 48 hours prior to seeding for immunofluorescence. Cells were blocked in 5% non-fat dry milk, 1% BSA, and 0.025% TritonX-100 solution in PBS for one hour prior to incubation with primary antibody. Staining was performed using an anti-vimentin antibody (1:40, Sigma Aldrich) which was hybridized in blocking buffer overnight at 4°C, and detected with an anti-mouse:Alexafluor 594 secondary antibody in blocking buffer for one hour at room temperature. Cells were counterstained with phalloidin:Alexafluor488, and preserved in

ProLong Gold antifade reagent with DAPI (all from Molecular Probes/Invitrogen, Carlsbad, CA). Cells were visualized using a compound Leica DMRB miscroscope with a Leitz laser at 63x magnification (W. Nuhsbaum, Inc.) and an Optronics camera system.

Apoptosis Assay/Annexin V Detection

Cells were seeded at $3x10^5$ cells per well in 6-well plates and transiently transfected with CHFR siRNA or the siControl negative control as described previously. Fifty-two hours post-transfection, cells were treated with either 0.67 μM nocodazole or 1.0 μM paclitaxel for 20 hours (both Sigma-Aldrich). Cells were then collected and labeled for Annexin V on the cell surface and DNA was stained with propidium iodide using the Vybrant Apoptosis Assay kit 2 according to manufacture's instructions (Molecular Probes/Invitrogen). Cells were then analyzed by flow cytometry and the apoptotic cells were those that stained for Annexin V on the cell surface but were negative for propidium iodide staining. The graphs presented indicate the percentage of apoptotic cells as assessed by flow cytometry.

Matrigel Invasion Assay

This invasion assay was performed according to manufacturer's instructions (BD Biosciences). In short, $2.5x10^4$ cells suspended in media without chemoattractant were plated in triplicate in Matrigel baskets in a 24-well plate. In the chamber below the baskets, either media without chemoattractant as a negative control or media containing chemoattractant was added. Chemoattractants for each cell line were: (1) HPV4-12 cells: 5% FBS, 1.0 μg/ml hydrocortisone, 10.0 μg/ml insulin, 100.0 ng/ml cholera toxin,

and 10.0 ng/ml epidermal growth factor, (2) MCF10A cells: 10% horse serum, 0.5 μg/ml hydrocortisone, 100.0 ng/ml cholera toxin, 10.0 μg/ml insulin, and 20.0 ng/ml epidermal growth factor, and (3) Hs578T cells: 10% FBS and 10.0 μg/ml insulin.

Cells were incubated for 22 hours at 37°C in 5% CO_2 for MCF10A and Hs578T cells or 10% CO_2 for HPV4-12 cells. The interior of the chambers were cleaned and the cells on the exterior were fixed and stained using the PROTOCOL Hema 3 staining kit (Fisher Scientific Co.). The number of stained cells on the exterior were counted using a Nikon TMS inverted microscope at 10x magnification.

Scrape Motility Assay

Cells were grown to confluency in 6-well plates and the cell monolayer was mechanically scarred using a plastic pipette tip. Cells were visualized for movement into the scratched surface with a Leica DMIRB inverted microscope with phase contrast optics and a 10x objective lens. Images were captured with a SPOT camera system (Diagnostic Instruments Inc.). The motility phenotype was quantified by using the ImageQuant v5.2 software package (GE Healthcare/Amersham Biosciences) to determine the area of the initial scrape and then the area of the same wound 24 hours later. Data are presented as the percentage of the scraped area that remains after the end-point.

Cellular Morphology

Cellular morphology was recorded when cultured cells reached 100% confluence. Images were gathered using a Leica DMIL inverted microscope (W. Nuhsbaum, Inc.) at

10x magnification and a SPOT RT Color camera with SPOT Advanced digital imaging software (Diagnostic Instruments Inc.).

Soft Agar Assay for Colony Formation

To perform the soft agar assay, an underlayer of a 1:1 mixture of 1.2% Noble agar and cell line-appropriate growth media with 40% serum was added to 6-well plates and allowed to solidify at room temperature for approximately 15 minutes. To create the overlayer for each well, we combined 2.0 ml of growth media with 40% serum, 1.0ml of 1.2% Noble agar, 0.6ml water, and $1.0x10^4$ cells and added it on top of the solidified underlayer. The solution solidified at room temperature for 15 minutes. Cells were maintained at 37°C in a humidified incubator with the appropriate levels of CO_2 and two to three drops of media were added to each well every three days. After 30 days, the number of colonies present in the overlayer was counted manually.

Ploidy Status and Nucleolar Changes

Cells were collected at 70% confluence by trypsinization and resuspended in 0.075 M KCl on ice for 30 minutes. Cells were fixed in a 3:1 mixture of methanol and glacial acetic acid with mild vortexing, dropped onto glass slides, and stained with 544 μg/ml Giemsa solution. To determine ploidy, the number of chromosomes was counted in at least 25 metaphases for each cell line and its derivatives.

To assess nucleolar changes, cells were prepared as described above and the number of nucleoli was counted in at least 50 cells, in triplicate, for each cell line. For

both methods listed here, images were recorded with a compound Leitz DMRB miscroscope (W. Nuhsbaum, Inc.) at 40x magnification and an Optronics camera.

Statistical Analysis

The ANOVA test was used to determine statistical significance when comparing quantitative phenotypic differences. Student's t-test was used to confirm a lack of statistical significance between parental and negative control cells for each experiment. For all tests, statistical significance was defined as $p \leq 0.05$. Error bars in the graphs presented here represent the standard error of the mean (SEM).

Results

Stable Loss of CHFR Results in Increased Growth Rates and Impairs the Checkpoint

CHFR expression was significantly decreased using a stably expressed shRNA construct, as determined by Western blotting and semi-quantitative duplex RT-PCR, in two IHMEC lines: HPV4-12 and MCF10A (Figure 3.1). Stable expression of shRNA reduced the amount of CHFR protein by at least 60% in HPV4-12 cells and by nearly 80% in MCF10A cells, and reduced the amount of mRNA by about 70% as determined by densitometry.

We first noticed that when CHFR expression was decreased by shRNA, the population growth rate dramatically increased for both IHMECs by at least three-fold over the course of 7-9 days ($p \leq 0.03$ for MCF10A and $p \leq 0.001$ for HPV4-12; Figure 3.2). The difference in growth rates is consistent over the time course but is most dramatic in

the last few days, possibly due to a cumulative effect, or because the cells grow slowly when seeded at a low density and grow better when the culture is denser.

In order to understand this increase in population growth, we assessed the percentage of mitotic cells by using immunofluorescence to stain cells for the mitotic marker phosphorylated histone H3-Ser28 – a residue that is phosphorylated during metaphase and is gradually dephosphorylated in anaphase and is associated with the initiation of chromosome condensation [88]. CHFR has been shown to delay chromosome condensation as part of the checkpoint response [17]. Therefore, phospho-H3-Ser28 as a marker of condensed chromosomes is a good method to determine if the cells have passed through the CHFR checkpoint and entered the later stages of mitosis. This method was also used to determine mitotic index, which was calculated as the percentage of phospho-H3-Ser28 positive cells in the population. There was a statistically significant five-to-six-fold increase in the number of H3-Ser28 stained (mitotic) cells in the population when CHFR expression was lowered by shRNA in both cell lines. This showed that more cells went through the CHFR checkpoint, entering the later stages of mitosis, with or without the stress of microtubule poisons such as nocodazole ($p<0.05$, Figure 3.3). In addition, the increase in phospho-H3-Ser28 positive cells following nocodazole treatment indicated that the checkpoint response to microtubule stress was bypassed when CHFR expression was decreased by shRNA (Figure 3.4). Though no difference was observed in MCF10A cells transiently transfected with CHFR siRNA, a similar increase in H3-Ser28 phosphorylation was observed when HPV4-12 cells were transiently transfected with a pool of four siRNAs

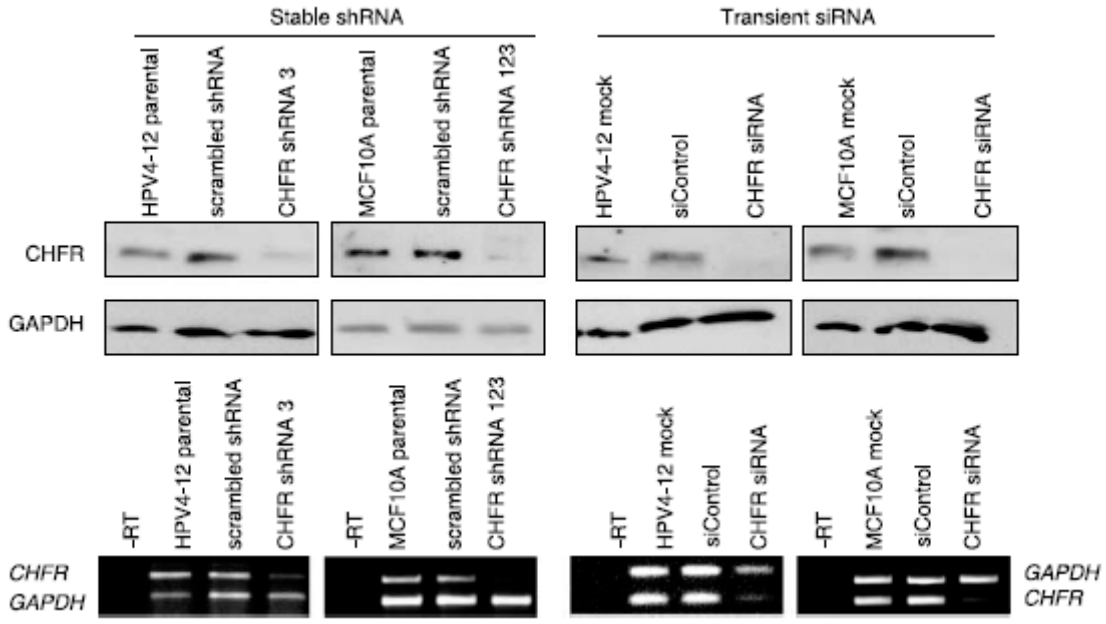

Figure 3.1: Targeting CHFR by RNAi dramatically decreases mRNA and protein expression.

Top: Western blotting shows a dramatic loss of CHFR protein following stable shRNA expression by retroviral transduction and transient siRNA transfection. HPV4-12 with CHFR shRNA3 had at least a 60% decrease while MCF10A with CHFRshRNA123 showed nearly an 80% stable knockdown of CHFR expression compared to parental and scrambled shRNA controls. Transient siRNA transfection resulted in a 95% decrease in HPV4-12 cells and an approximately 99% decrease in CHFR protein in MCF10A cells 72 hours after transfection. Bottom: Semi-quantitative duplex RT-PCR indicates a corresponding decrease in CHFR mRNA levels by about 70% for each cell line compared to controls.

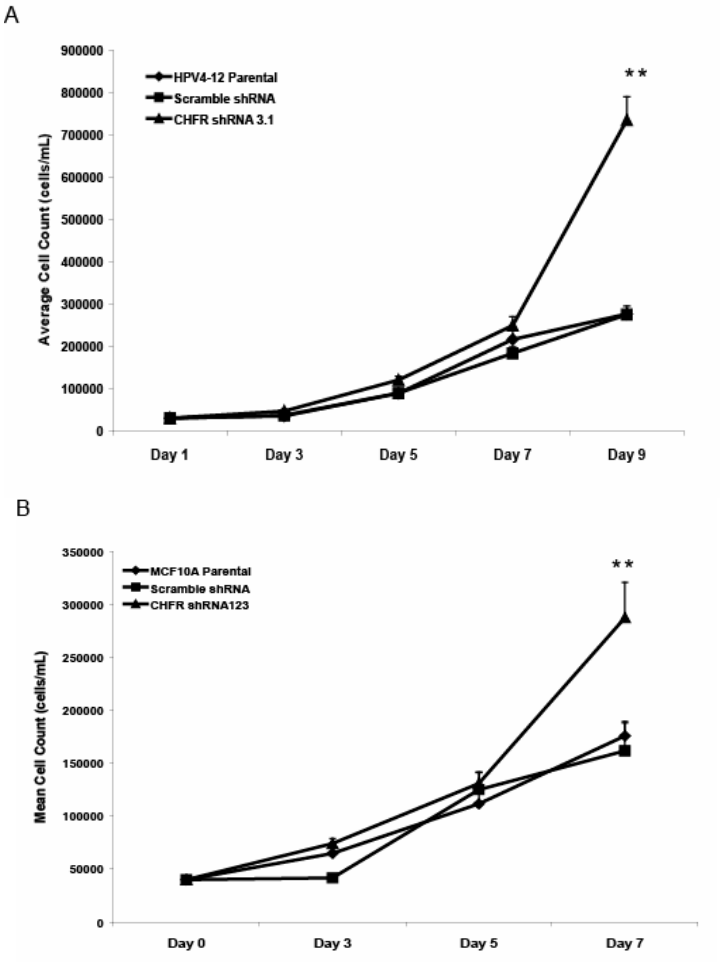

Figure 3.2: Stably decreased CHFR expression causes increased growth rates.

Growth curves for (A) HPV4-12 cells (top) and (B) MCF10A cells (bottom) following stable shRNA expression against CHFR (▲) compared to the parental cell lines (♦) and the scrambled shRNA (■) negative control cell lines. Cells were counted in triplicate every two days until at least one line reached confluency. The graph represents the average number of cells counted on each day per cell line. Cells with decreased CHFR expression by shRNA had a faster growth rate compared to the parental and scrambled shRNA controls. Two asterisks (**) indicates $p<0.001$.

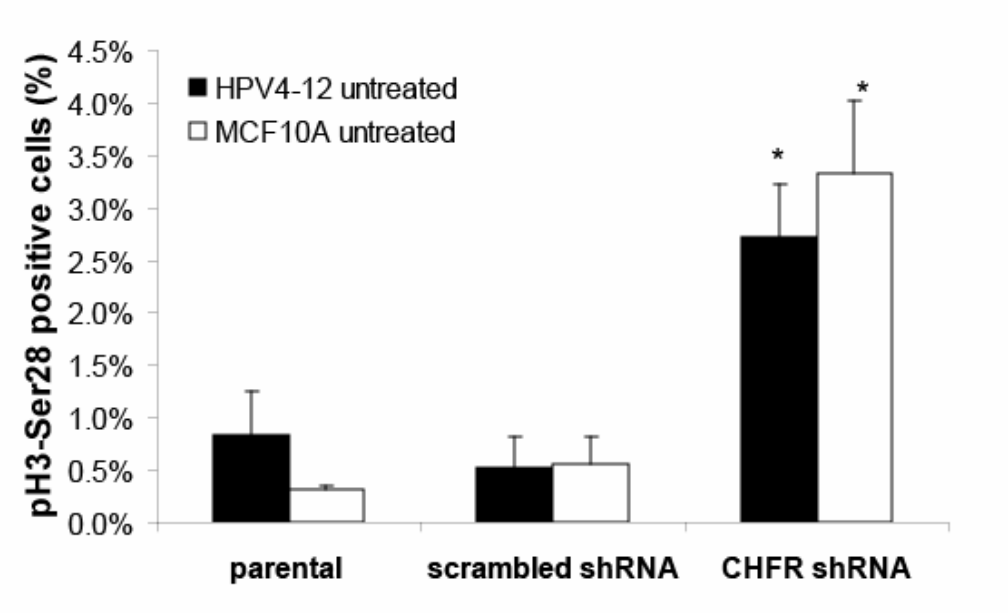

Figure 3.3: Decreased CHFR expression causes an increase in the mitotic index.

The mitotic index of cells with or without CHFR shRNA is represented as the average percentage of histone H3-Ser28 stained nuclei, which is a marker of early metaphase cells, out of ≥1000 total (DAPI-stained) nuclei from triplicate experiments for each cell line. Cells were either not treated with nocodazole in order to determine the basal percentage of mitotic cells in the population. Cells with decreased CHFR expression by shRNA showed approximately a six-fold increase in mitotic cells when compared to the parental and scrambled shRNA controls. One asterisk (*) indicates $p<0.05$

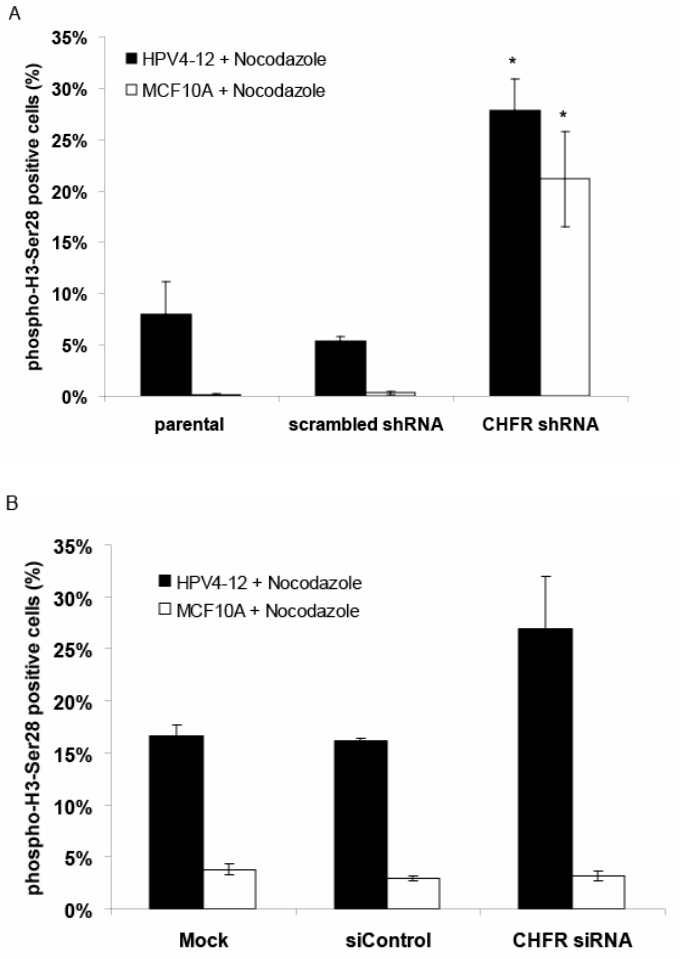

Figure 3.4: CHFR shRNA impaired the nocodazole-induced early mitotic checkpoint.

The mitotic index of cells is represented as the average percentage of histone H3-Ser28 stained nuclei out of ≥1000 total (DAPI-stained) nuclei from triplicate experiments for each cell line. Cells were treated with 200 ng/ml nocodazole to test for checkpoint response. (Top) Cells transduced with CHFR shRNA showed a four- or ten-fold increase in mitotic cells after nocodazole treatment when compared to the parental and scrambled shRNA controls. (Bottom) A similar trend was found in HPV4-12 cells transiently transfected with CHFR siRNA ($p<0.07$) but no change was observed in MCF10A cells transfected with siRNA.

for 72 hours prior to staining to decrease CHFR protein by approximately 95% ($p<0.07$, Figure 3.1 and 3.4).

To determine if decreasing CHFR expression would alter the apoptotic response of the cells, we tested untreated or nocodazole-treated cells for the presence of Annexin V on the cell surface by flow cytometry and used propidium iodide staining to differentiate between apoptotic and necrotic cells [89]. We found no difference between the cell lines with and without CHFR when they were untreated, which suggested that the increase in growth rates observed in the cells was not due to a decrease in cell death. In addition, there was no statistically significant difference in HPV4-12 cells transiently transfected with CHFR siRNA when compared to the mock transfected and siControl transfected cells following treatment with nocodazole. However, when CHFR expression was transiently decreased in MCF10A cells, there was a three-fold increase in apoptotic cells following nocodazole treatment ($p<0.05$, Figure 3.5).

The Stable Loss of CHFR Leads to Enhanced Invasive Potential and Increased Motility

To determine if decreasing CHFR expression would cause phenotypic changes reminiscent of cellular transformation, IHMECs with or without CHFR shRNA were subjected to the Matrigel invasion assay and the scrape (wound) motility assay. Surprisingly, there was a dramatic increase in the ability of the cells to invade through the Matrigel collagen matrix when CHFR expression was low: a 23-fold increase for MCF10A cells and a 5-fold increase for HPV4-12 cells ($p\leq0.001$ for both, Figure 3.6).

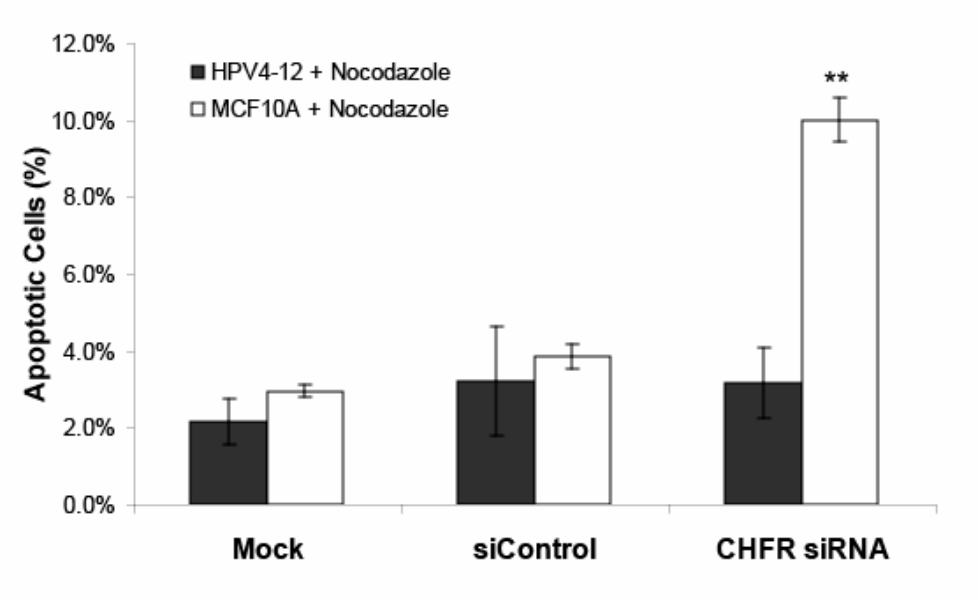

Figure 3.5: Transient knockdown of CHFR expression by siRNA increased the apoptotic response to nocodazole.

Transiently decreasing CHFR by siRNA in MCF10A cells, but not HPV4-12 cells, resulted in an increased apoptotic response to nocodazole. An Annexin V antibody was used to detect the presence of Annexin V on the cell surface. Cells were counterstained with propidium iodide and assessed by flow cytometry. The percent of Annexin V-positive and propidium iodide-negative (apoptotic) cells are presented in the graph. Two asterisks (**) indicates $p \leq 0.001$

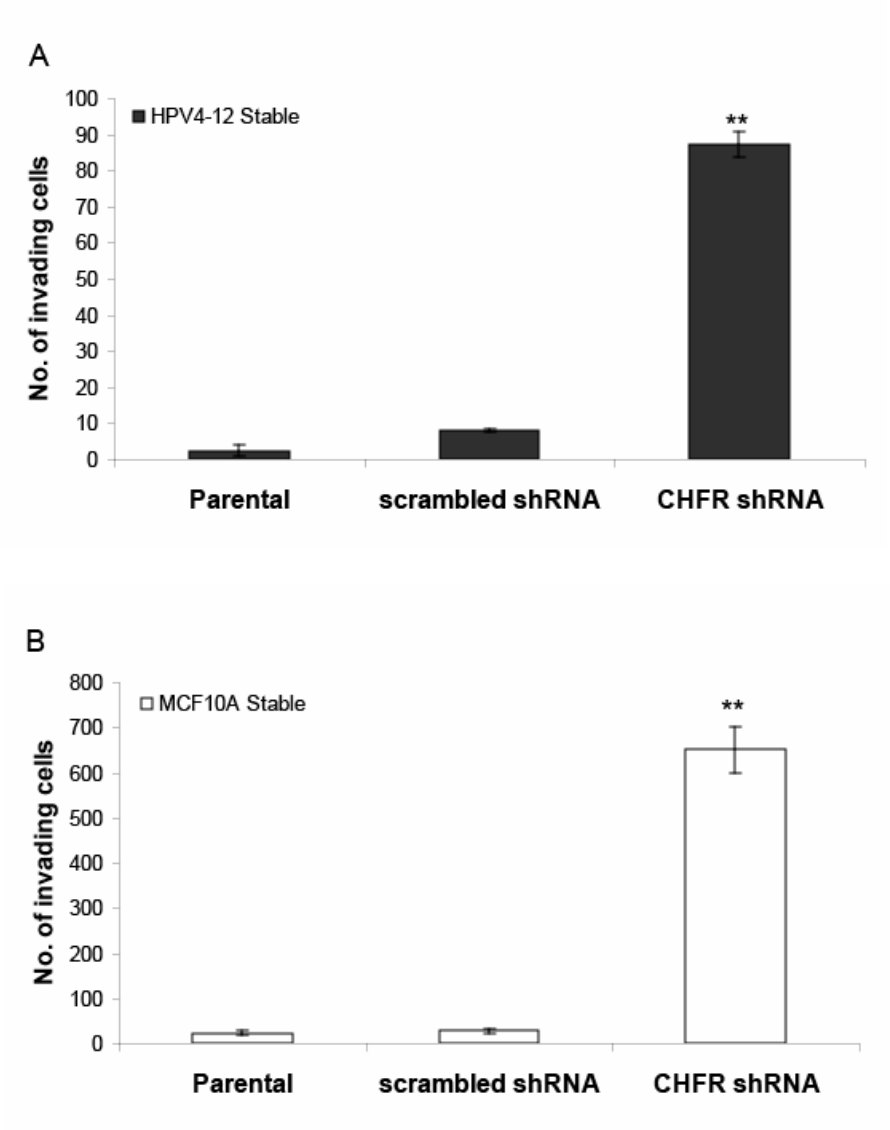

Figure 3.6: Stable loss of CHFR expression by shRNA caused enhanced invasion through Matrigel.

Stable knockdown of CHFR expression by shRNA resulted in greatly increased invasive potential through a Matrigel collagen matrix for both (A) HPV4-12 cells (top) and (B) MCF10A cells (bottom) compared to the control cell lines (parental and scrambled shRNA). Two asterisks (**) indicate that $p \leq 0.001$.

This dramatic change was also observed after transient transfection with a pool of four siRNAs, each targeting a different locus in *CHFR*, which indicated that this phenotype is directly caused by CHFR loss and is not a result of clonal selection during culture of the stable shRNA lines (Figures 3.1 and 3.7).

To assess changes in cellular motility, a wound was created in a confluent culture of IHMEC cells with or without CHFR shRNA. Motility was described as the percentage of the area of the initial wound that remained after a recovery period. IHMEC lines are not readily motile when their growth surface has been damaged and the remnants of the initial wound are clearly visible days later. However, when CHFR expression was decreased by stable shRNA, the cells became so motile that the wound was nearly entirely closed 24 (Figure 3.8). This was not a function of the increased population growth rates as cells with filipodia were clearly seen in the center of the wound less than 24 hours later. In addition, the assay was completed prior to the population doubling time as indicated in the growth curves presented in Figure 3.2.

Stably Decreased Levels of CHFR Causes Morphological Changes and Induces Colony Formation in Soft Agar

Normally, cells contain only one or two nucleoli in a nucleus and one frequently characterized change in cancer cells is increased number of nucleoli. In fact, changes in the number of nucleoli (>3) is strongly correlated with a negative prognosis for survival in breast cancer patients [90]. Interestingly, both IHMEC cell lines exhibited a marked increase in the number of nucleoli present in the nucleus, which was defined as three or more nucleoli, when CHFR expression was knocked down by shRNA. We found that

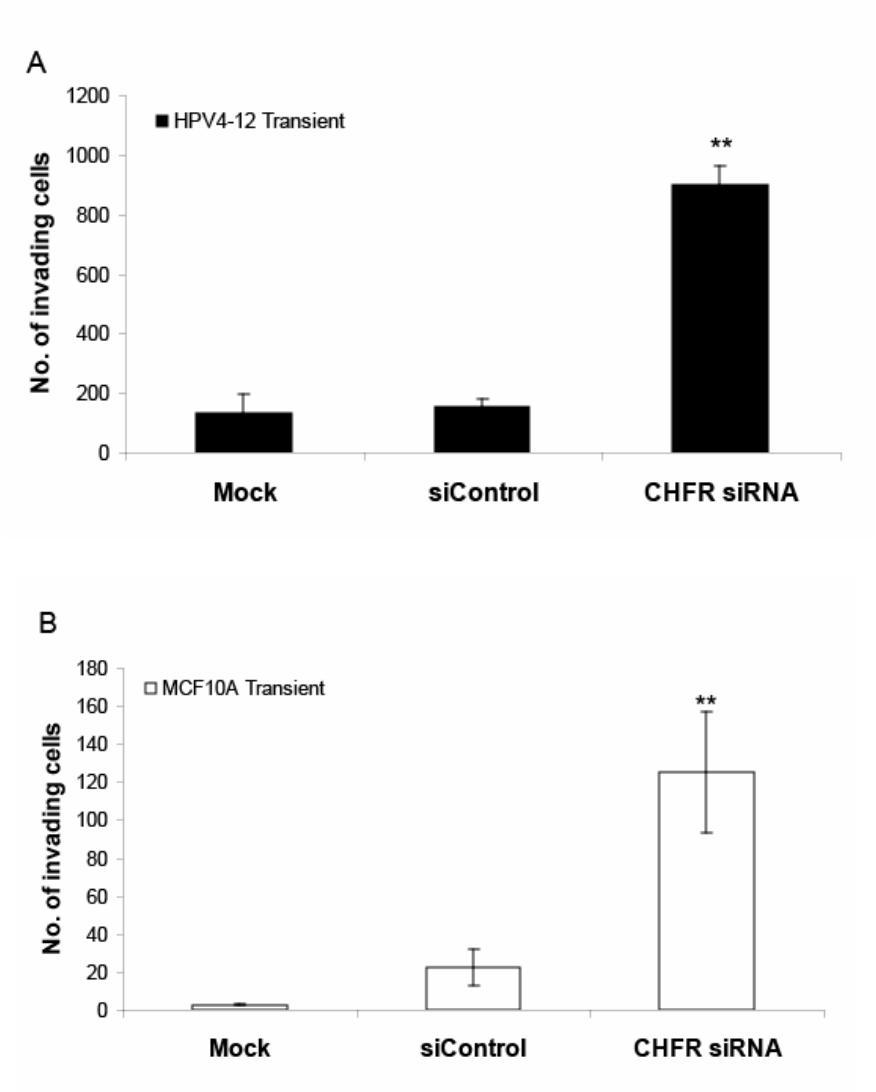

Figure 3.7: Transient loss of CHFR expression by siRNA caused enhanced cellular invasion through Matrigel.

Transient knockdown of CHFR expression results in greatly increased invasive potential through a Matrigel collagen matrix for both (A) HPV4-12 cells and (B) MCF10A cells compared to the control cell lines (mock transfected and siControl). Cells were transfected with siRNA and 48 hours later were seeded for the invasion assay, which was completed after 24 hours such that the assay was completed when CHFR expression was at its lowest. Two asterisks (**) indicate $p \leq 0.001$.

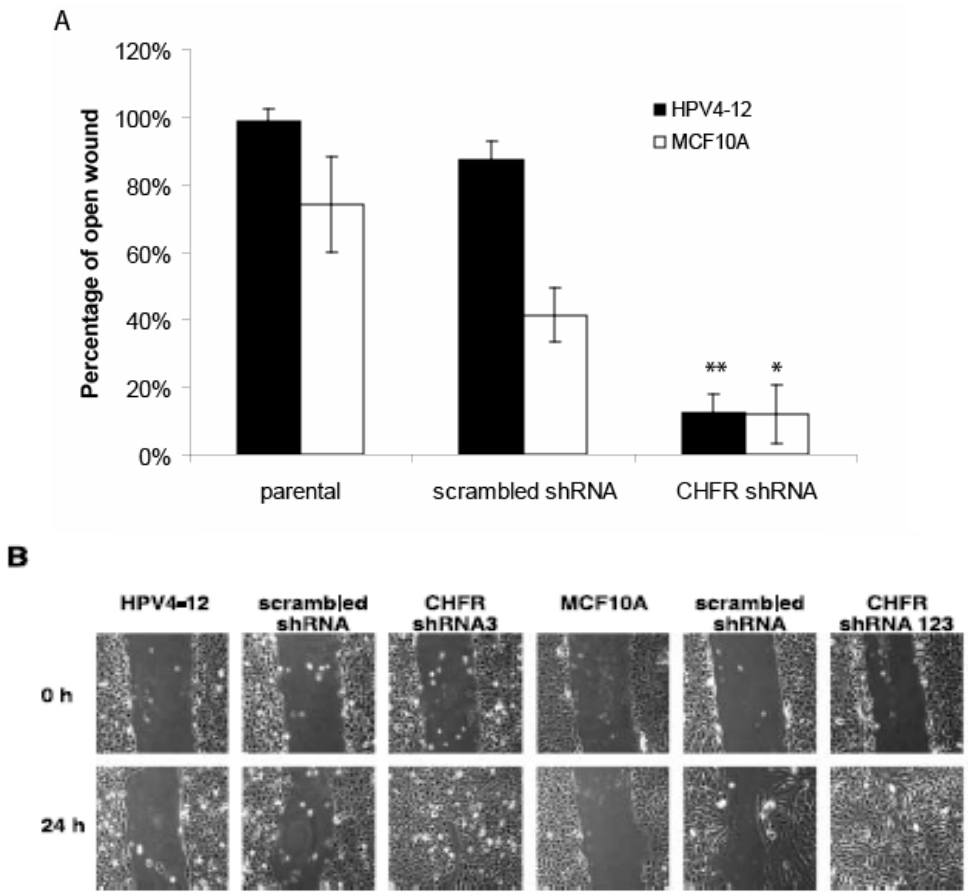

Figure 3.8: Loss of CHFR expression by stable shRNA increases cellular motility.

(A) Graphical representation of the degree of wound closure. Motility is described as the percentage of the original wounded area that remains vacant after incubation. The area of the vacant surface was calculated using ImageQuant v5.2 software. Two asterisks (**) indicates $p \leq 0.001$ and one asterisk (*) indicates $p \leq 0.05$ by ANOVA testing. (B) Digital phase contrast images at 10x magnification showing an increase in motility (closing a scraped wound in confluent culture) for HPV-12 (left) and MCF10A (right) cells following stable CHFR shRNA expression compared to controls. The "0 hrs" images depict the initial wound in the culture and the "24 hrs" images show wound closure.

29% of MCF10A:CHFRshRNA cells (compared to 9% for controls, $p \leq 0.001$) and 23% of HPV4-12:CHFRshRNA cells had greater than three nucleoli (compared to 13% for controls $p \leq 0.08$; Figure 3.9). This change in nucleolar organization and number may indicate alterations in cellular metabolism related to proliferation, genome organization, or gene expression.

Further evidence for the acquisition of tumorigenic phenotypes following knockdown of CHFR expression was noticed only in MCF10A cells. We observed that MCF10A cells with CHFR shRNA underwent a morphological change following approximately 10 passages in culture. These cells became elongated and showed more variability in cell size, which is suggestive of the epithelial-to-mesenchymal transition that is often observed during tumorigenesis (Figure 3.10). Further confirmation of this transition was indicated by increased expression of Vimentin, a marker of mesenchymal cells, as shown by immunofluorescence (Figure 3.11). To determine if the loss of CHFR altered the tumorigenicity of these cell lines, parental, scrambled shRNA, and CHFR shRNA-expressing cells were suspended in a mix of soft agar and growth media and assessed for their ability to form colonies. The MCF10A cell line has already been characterized as being tumorigenic in soft agar and the loss of CHFR did not enhance this phenotype. However, the HPV4-12 cell line does not form colonies in soft agar but when CHFR expression was decreased by shRNA, there was a modest but very significant increase in the number of colonies formed in soft agar ($p<0.001$, Figure 3.12), indicating that these cells potentially had become tumorigenic.

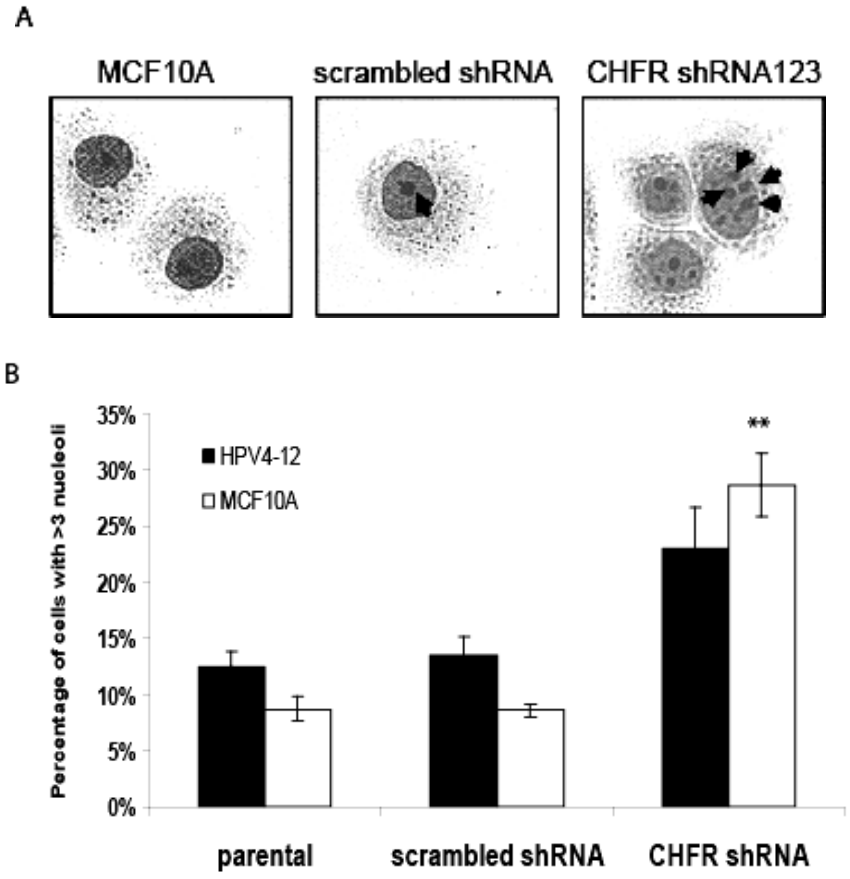

Figure 3.9: MCF10A cells with decreased CHFR expression by shRNA have amplified numbers of nucleoli.

(A) In Giemsa-stained cells, the nucleolus is depicted as a dark spot within the nucleus. Parental (far left) and scrambled shRNA controls (middle) normally contain one or two nucleoli whereas CHFR shRNA cells more frequently had greater than three nucleoli (arrows). (B) Graphical representation of the percentage of cells with greater than three nucleoli for each cell line; N=50 for each of three trials. Two asterisks (**) indicate $p \leq 0.001$.

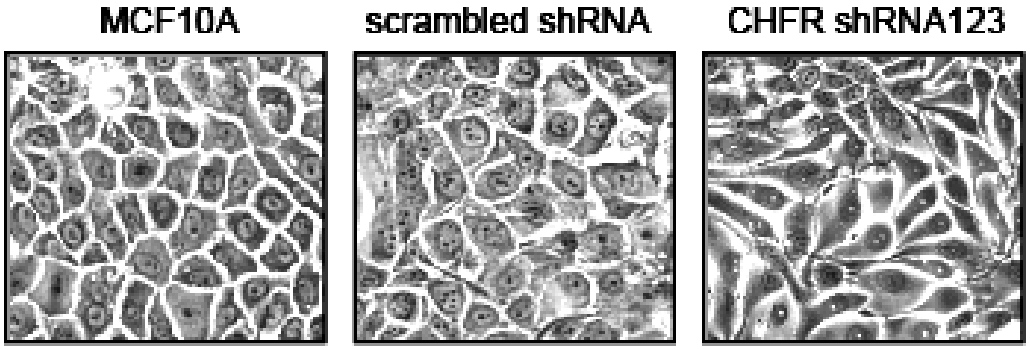

Figure 3.10: Stably decreased CHFR expression in MCF10A cells results in altered cellular morphology resembling an epithelial-to-mesenchymal transition.

MCF10A cells visualized by phase contrast light microscopy show a change in cellular shape from epithelial to an elongated morphology reminiscent of an epithelial to mesenchymal transition when CHFR expression is decreased by shRNA expression.

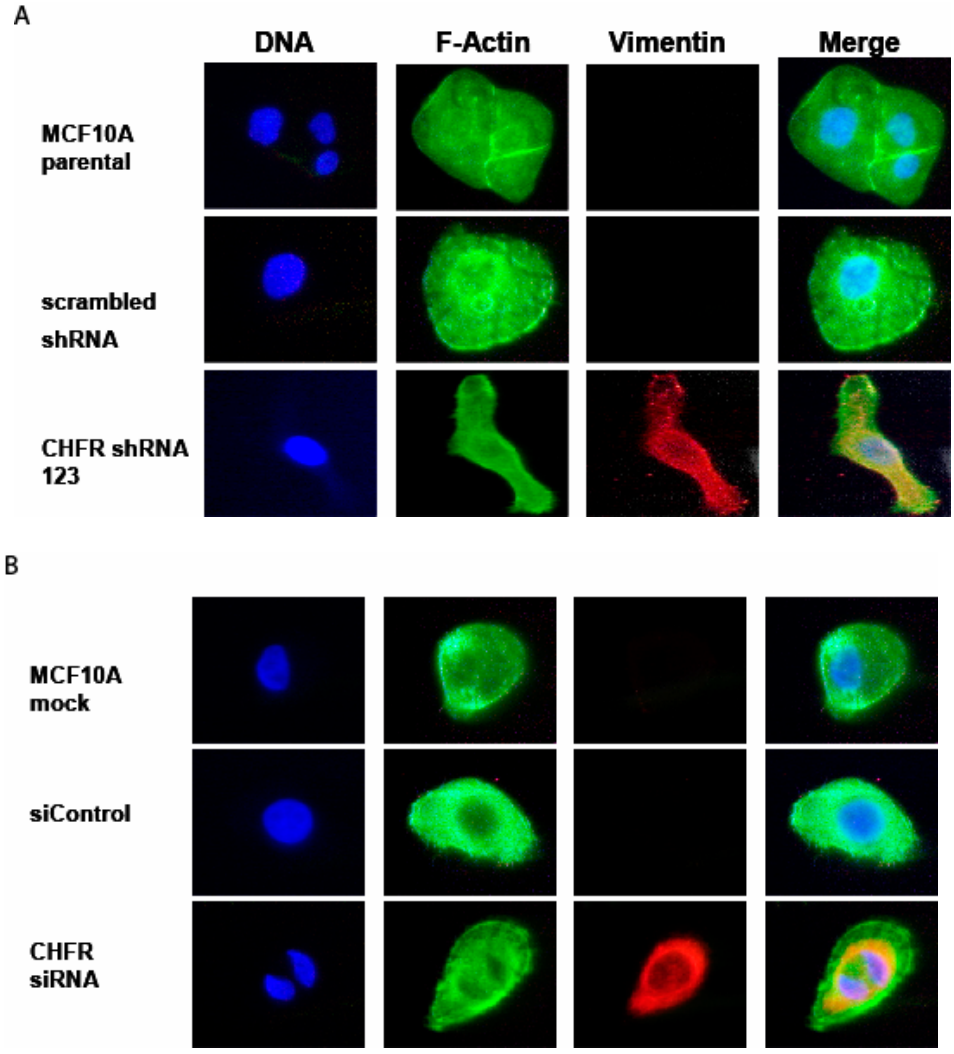

Figure 3.11: Increased Vimentin staining in cells with decreased CHFR expression by RNAi indicated an epithelial-to-mesenchymal transition.

(A) MCF10A cells stably transduced with CHFR shRNA123 or the non-targeting scrambled shRNA construct. (B) MCF10A mock transfected, siControl negative control transfected, and cells transiently transfected with a pool of CHFR siRNA. Cells were stained by immunofluorescence for DNA (DAPI, blue), F-actin (green), and Vimentin (red) and images were merged (far right panel). Increased Vimentin expression indicates an epithelial-to-mesenchymal morphology change.

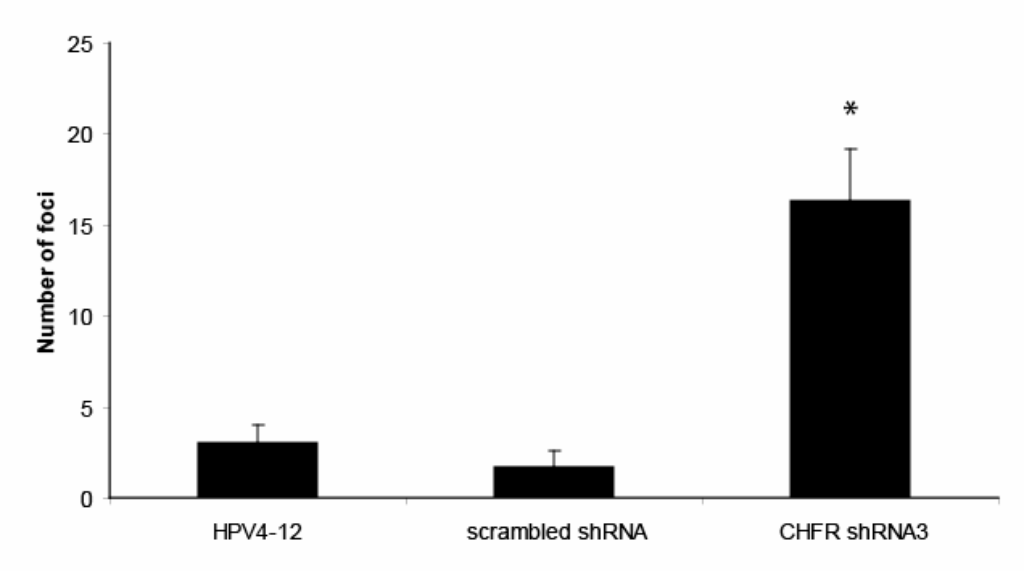

Figure 3.12: Stable loss of CHFR expression by shRNA in HPV4-12 cells causes amplified colony formation in soft agar, suggesting cellular transformation.

The graph depicts the three-fold increase in colonies formed by HPV4-12 cells when CHFR expression is decreased. Ten thousand cells were suspended in a mixture of noble agar and complete growth media and allowed to grow for 30 days. One asterisk (*) denotes $p<0.05$.

Over-expression of CHFR Reverses Tumorigenic Phenotypes in Breast Cancer Cells

We next determined if CHFR over-expression would affect a tumorigenic breast cancer cell line, Hs578T, which has no endogenous expression of CHFR protein. Hs578T cells over-expressed *CHFR* through a stably transduced retroviral construct containing the full-length cDNA (Figure 3.13). Over-expressing CHFR in Hs578T cells did not alter their apoptotic response to nocodazole or decrease colony formation in soft agar (data not shown). However, CHFR over-expression rescued other tumorigenic phenotypes, making the cells act less like cancer cells. Importantly, their ability to invade through a Matrigel collagen matrix dramatically decreased by 25-fold ($p \leq 0.001$; Figure 3.14) and there was nearly a six-fold decrease in motility using the scrape assay ($p \leq 0.001$; Figure 3.15, quantified in the right panel). Over-expression of CHFR resulted in a significant decrease in growth rates ($p < 0.05$, Figure 3.16 left panel) and fewer mitotic cells, as indicated by positive phospho-histone H3-Ser28 staining ($p < 0.05$, Figure 3.17). The prophase checkpoint also was partially restored in Hs578T cells over-expressing CHFR ($p < 0.05$, Figure 3.17).

Stable Knockdown of CHFR Expression Leads to Genomic Instability

Since genomic instability was previously reported for *Chfr* null mouse embryonic fibroblasts, we assessed the ploidy status of IHMECs after stable CHFR shRNA expression. Strikingly, 60-70% of these cells showed increased aneuploidy with anywhere from 49 to over 85 chromosomes, as opposed to less than 5% of cells in the normally hyper-diploid (48-49 chromosomes) parental lines (Figure 3.18).

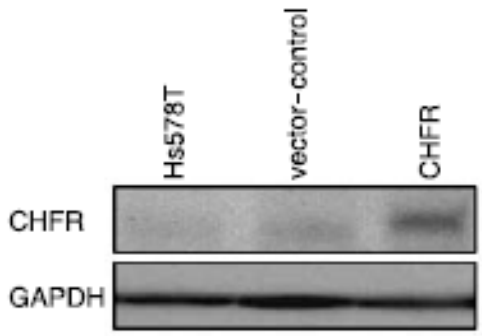

Figure 3.13: CHFR was stably over-expressed in the Hs578T breast cancer cell line by retroviral transduction.

Western blot showing increased CHFR expression (top) in cells retrovirally transduced with a Flag-tagged CHFR construct compared to the parental and empty vector negative controls. GAPDH is used as a loading control (bottom).

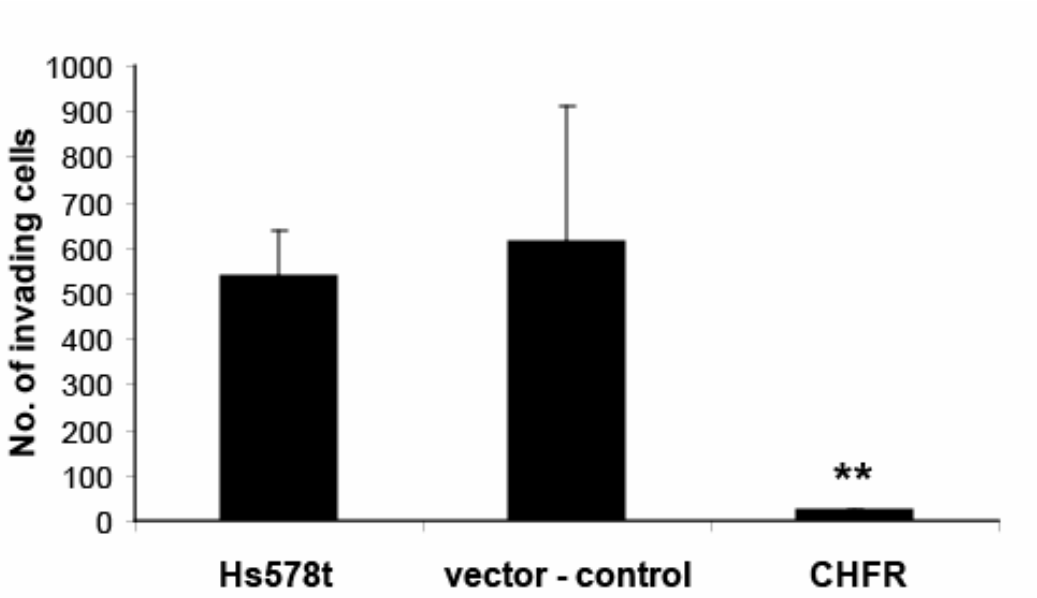

Figure 3.14: Over-expression of CHFR in the Hs578T breast cancer cell line dramatically decreased the cells' invasive potential through Matrigel.

Over-expression of CHFR in Hs578T cancer cells results in 25-fold loss of invasive potential through a Matrigel collagen matrix. Cells were seeded in the upper chamber of and assessed for invasion through the Matrigel 22 hours later. Two asterisks (**) indicate $p<0.001$.

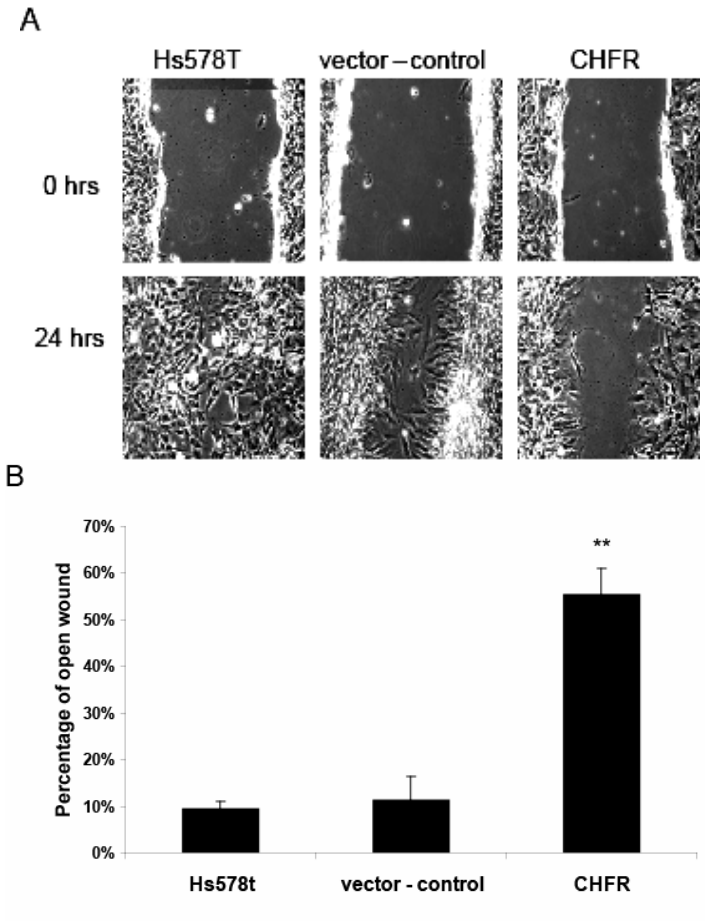

Figure 3.15: Over-expression of CHFR in Hs578T breast cancer cells decreased cellular motility.

(A) Phase contrast images at 10x magnification showing an increase in motility for Hs578T cells following stable CHFR over-expression. The "0 hrs" images depict the initial wound in the culture and the "24 hrs" images show wound closure after 24 hours. Hs578T cells over-expressing CHFR were less motile than their control counterparts were and could not sufficiently close the wound in less than 24 hours. (B) Graphical representation of the degree of wound closure depicted on the left; the graph describes the percentage of the original scraped area remaining after incubation for each cell line. Two asterisks (**) indicate $p \leq 0.001$.

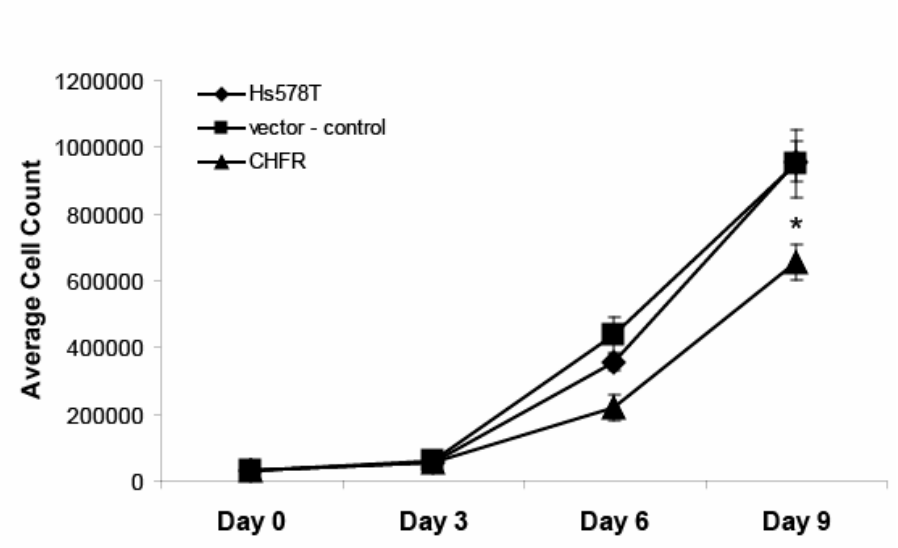

Figure 3.16: Stable over-expression of CHFR in Hs578T cells causes increased growth rates.

Growth curve analysis over the span of nine days showed that Hs578T breast cancer cells overexpressing CHFR (▲) had a slower growth rate, as indicated by a lower average cell count, than the parental (♦) or the vector negative control (■), despite being seeded at equal densities on day zero. One asterisk (*) indicates $p<0.05$.

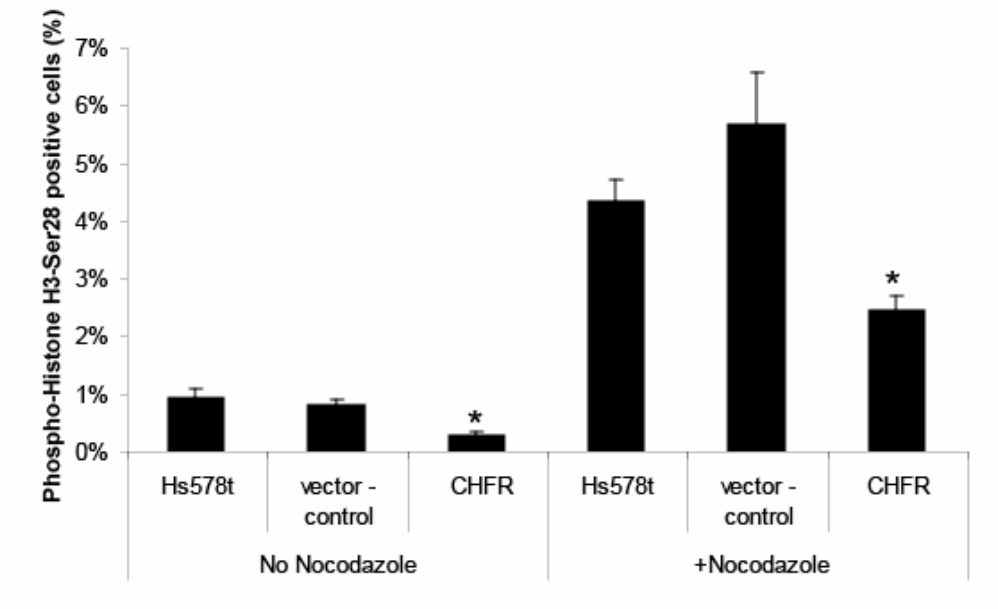

Figure 3.17: Hs578T cells over-expressing CHFR have a lower mitotic index and a partially restored early mitotic checkpoint.

Immunofluorescence staining for phospho-histone H3-Ser28 was used as a marker for mitotic cells. The percentage of cells positive for p-H3-Ser28 staining out of at least 1000 total nuclei (DAPI-stained) is presented for each cell line. Over-expression of CHFR led to approximately 50% fewer mitotic cells compared to parental and empty vector controls in both untreated and nocodazole (200 ng/ml) treated cells, indicating at least a partially restored checkpoint and a decrease in proliferation in untreated cells. One asterisk (*) indicates $p<0.05$.

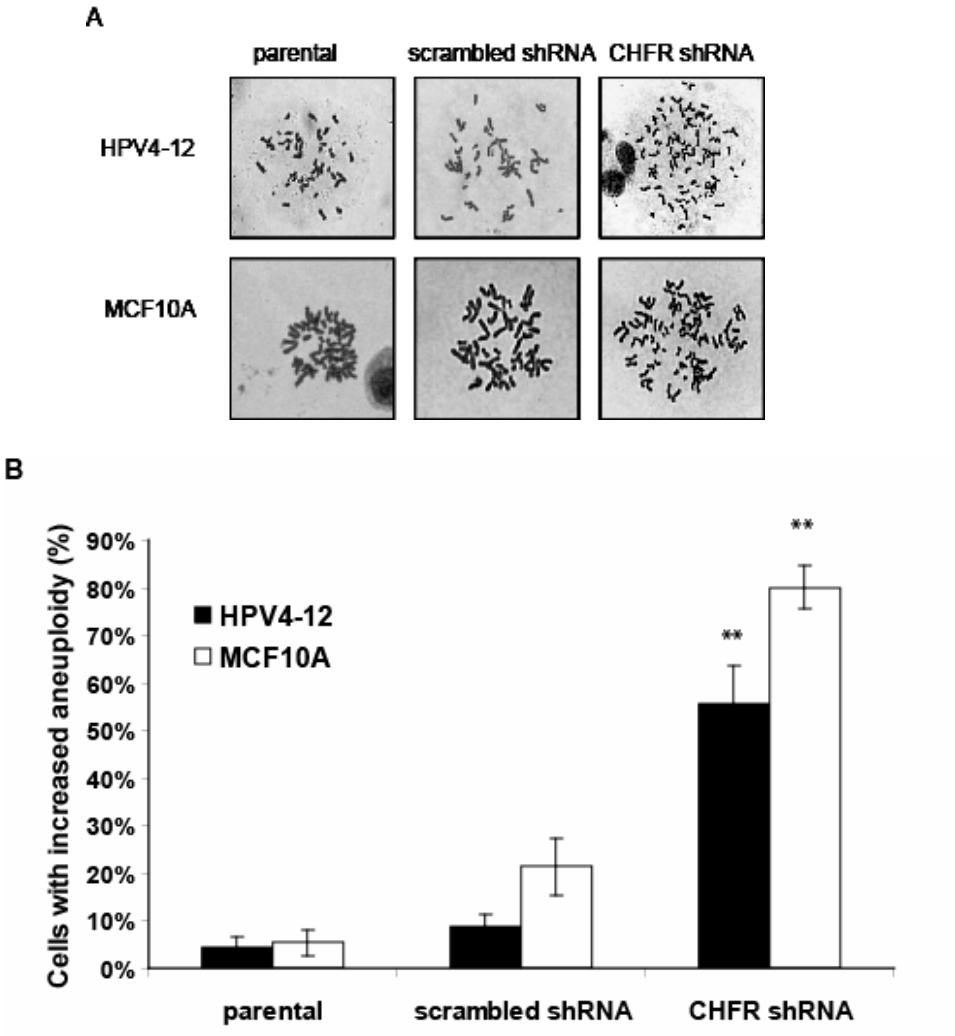

Figure 3.18: Stable loss of CHFR expression by shRNA in IHMECs leads to increased aneuploidy.

(A) Giemsa-stained metaphase spreads of parental, negative control, and CHFR shRNA cells. IHMECs with lowered CHFR expression showed a greatly increased incidence of aneuploidy. Both IHMEC cell lines are hyperdiploid and normally have either 48 chromosomes (MCF10A) or 49 chromosomes (HPV4-12). (B) Quantification of increased aneuploidy in CHFR shRNA cells showing that low CHFR expression results in 55-72% of the cells in the population becoming more aneuploid. The graph represents the percent of cells with increased aneuploidy above the normal hyperdiploid state, from 25 counted metaphases per trial, for each cell line. Two asterisks (**) denotes $p \leq 0.001$ as determined by the ANOVA test for significance.

Discussion

The findings presented here contribute significantly to the characterization of *CHFR* as a cancer-relevant gene with tumor suppressive properties. This work provided evidence that decreasing CHFR mRNA and protein using shRNA/siRNA resulted in two IHMEC cell lines acquiring phenotypes associated with malignant progression. These phenotypes included increased growth rates and mitotic indexes, the cells acquired the abilities of invasion and motility, and a striking percentage of cells became more aneuploid. In addition, the HPV4-12 cells without CHFR were able to form colonies in soft agar, an indication of cellular transformation, and the MCF10A cells without CHFR became sensitive to microtubule poisons and underwent an epithelial-to-mesenchymal morphology change. When CHFR was over-expressed in Hs578T breast cancer cells, the data suggested that higher CHFR levels did not have any adverse consequences and, in fact, reversed some tumorigenic phenotypes thereby further supporting the role of CHFR as a tumor suppressor. When the CHFR expression data is combined with the results of the phenotypic analysis *in vitro* and the correlation with tumor size *in vivo*, it appears that the loss of CHFR is relevant to tumorigenesis in mammary epithelial cells.

Importantly, decreased CHFR expression led to an increase in the number of mitotic (metaphase and anaphase) cells in the population. Previously, this phenotype had only been described to occur in the presence of nocodazole and was thought to be due to an impaired checkpoint. However, the fact that this phenomenon also occurs without microtubule poisons suggests that CHFR can possibly play a wider role in regulating the timing of mitotic entry. This may help explain why the growth rates were faster in cells

stably expressing CHFR shRNA and may be one contributing factor as to why CHFR-negative tumors tended to be larger.

Two of the most striking changes that resulted from altering CHFR expression were changes in invasion and motility of cells *in vitro*. This is the first time that CHFR has been implicated in a functional role other than cell-cycle regulation. Considering its proposed role of monitoring microtubule dynamics as indicated by its initiation of the checkpoint in response to microtubule stress, it is hypothesized that CHFR has an even larger part in cytoskeletal organization in which loss would more easily allow for the necessary reorganization of the cytoskeletal network required for motility. In addition, if the phenotypes observed in culture are found to mirror those seen in cancer patients (ie: patients with low CHFR tumors have a higher incidence of distant metastases), then CHFR expression may be an indicator for tumor stage and/or patient prognosis.

Our report that low CHFR expression leads to genomic instability corroborates previously published work in the mouse. These data are suggestive of a problem with the structure or function of the mitotic spindle that is not corrected due to an impaired CHFR checkpoint. However it could also indicate a defect in cytokinesis, which is plausible since work with the two yeast orthologs of CHFR show an interaction with the septin cytoskeletal network and the orthologs were shown to function in both the spindle checkpoint and in cytokinesis [10, 11]. Given the relatively frequent occurrence of low/lost CHFR in many types of tumors, this work may begin to explain the conundrum of the prevalence of aneuploidy in cancers but the lack of defective spindle checkpoint mediators such as the MAD and BUB proteins.

It is not surprising that the same phenotypes were not always observed in the two cell lines tested. This is likely due to the unique genetic defects that caused the immortalization of the cell lines, thereby providing a clue to the genetic and physical interactions that CHFR has within the cell. Specifically, the HPV4-12 cell line was immortalized with the HPV E6/E7 protein to inhibit p53 and pRb function while the MCF10A line was spontaneously immortalized following a t(3;9)(p14;p21) translocation that disrupted the p15/p16 gene in addition to other chromosomal rearrangements [91, 92]. The genetic differences may help to explain why MCF10A cells undergo a morphological change and an increase in apoptosis in response to microtubule poisons after CHFR shRNA, whereas HPV4-12 cells do not. Differences may also be attributed to the fact that these two IHMEC lines are grown in different media with different levels of CO_2, but it should be noted that the media are very similar and contain nearly identical supplements.

This work on the phenotypic changes that arise *in vitro* with CHFR expression variation provides a unique insight as to what may happen in cancer patients and presents many new avenues through which to study CHFR expression, function, and molecular interactions. We also comprehensively characterize the phenotypic changes that resemble cellular transformation in normal IHMEC cells when CHFR expression is substantially reduced. Through the combined findings of this work, we find the loss of CHFR to be an interesting dichotomy in breast cancer. This report shows that, on one hand, the loss of CHFR expression may indicate a larger and more aggressive tumor whereas in a surprising beneficial twist, it also makes the cancer cells sensitive to traditional chemotherapeutic agents that target the microtubules. It seems that as

evidence builds, CHFR will have potent tumor suppressive functions in breast cancer and may be a biomarker for tumor sensitivity to taxane treatment.

Acknowledgements

This work was supported by a Department of Defense Breast Cancer Research Pre-doctoral Fellowship, #BC050310, and by the NIH National Research Service Award #5-T32-GM07544 from the National Institute of General Medicine Sciences to LMP and an NIH NCI grant RO1CA072877 to EMP. Support was also provided to CGK via NIH NCI grants K08CA090876 and R01CA107469, and Department of Defense grant DAMD17-01-1-490. We thank Esther Peterson for helpful suggestions and discussion and Nancy McAnsh and Donita Sanders for technical assistance with IHC protocols. We also thank Stephen Ethier, Ph.D., for the HPV4-12 breast cell line.

Notes

Parts of this work were previously published as:

Privette, L.M., M.E. Gonzalez, L. Ding, C.G. Kleer, and E.M. Petty, "Altered expression of the early mitotic checkpoint protein, CHFR, in breast cancers: implications for tumor suppression," *Cancer Research*. 2007 Jul 1;67(13):6064-74.

Published Online First June 27, 2007. doi: 10.1158/0008-5472.CAN-06-4109.

CHAPTER 4

LOSS OF CHFR CAUSES GENOMIC INSTABILITY BY DISRUPTING MITOTIC SPINDLE PROTEINS

Summary

To investigate CHFR's role in breast cancer, we decreased CHFR expression by siRNA in MCF10A cells. This resulted in increased aneuploidy caused by mitotic defects including misaligned metaphase chromosomes, lagging anaphase chromosomes, multi-polar mitotic spindles, and multi-nucleated cells. CHFR siRNA also increased Aurora A expression and caused MAD2 and BUBR1 mislocalization during mitosis, suggesting that CHFR is involved in the mitotic spindle checkpoint and genomic instability. Furthermore, we found that CHFR interacted with both Aurora A and MAD2. These findings, along with CHFR's reported role in responding to microtubule poisons, suggested that CHFR might also interact with tubulins. We discovered that CHFR interacted with, and ubiquitinated, α-tubulin, and CHFR siRNA increased expression of both unmodified and acetylated α-tubulin. Importantly, our results suggest a novel role for CHFR regulating chromosome segregation where decreased expression, as seen in cancer cells, contributes to genomic instability.

Introduction

As previously noted, Checkpoint with FHA and RING Finger (CHFR) is recognized as a novel mitotic stress checkpoint pathway regulator and biomarker for treatment response to taxanes. It delays cells in prophase, prior to the mitotic spindle checkpoint, after microtubule poison exposure (i.e. nocodazole or paclitaxel) [3, 7, 18-20, 58, 63]. Subsequently, CHFR has been implicated in oncogenesis. *CHFR* expression is lost or decreased in tumors compared to normal tissues, sometimes due to promoter hyper-methylation [19, 21, 33, 44, 49, 55, 59, 63]. Importantly, CHFR has tumor suppressive activity in both a knockout mouse model [8] and in immortalized human mammary epithelial cells (IHMECs) [20]. Long-term loss of CHFR expression led to abnormal chromosome complements (i.e. increased aneuploidy) in both models.

Aneuploidy is a hallmark of many cancers. It may result from diverse mitotic defects including multi-polar spindles secondary to aberrant cytokinesis or centrosome amplification, sister chromatid cohesion defects, incorrect centromere attachment, or an impaired mitotic spindle assembly checkpoint ("spindle checkpoint") [93]. The spindle checkpoint prevents chromosome mis-segregation during cell division by delaying anaphase until the kinetochores of all sister chromatids are attached to the mitotic spindle. Spindle checkpoint gene mutations are rare, especially in breast cancers, but many cancer cells have an impaired or unregulated spindle checkpoint [93-95].

Aurora A kinase is crucial for centrosome amplification and maturation, mitotic entry, and spindle assembly [96-98]. Aurora A over-expression can override the spindle checkpoint, resulting in mitotic defects and mislocalization of the key spindle checkpoint proteins BUBR1 and MAD2, among others [99, 100]. Aurora A is amplified and/or

overexpressed in many cancers and correlates with improved patient survival following treatment with microtubule-targeting taxanes [101, 102]. Importantly, Aurora A may be a target for CHFR-mediated ubiquitination and subsequent proteasome degradation [8]. This suggests that CHFR expression may be important for genome stability and cellular responses to taxanes, potentially through its regulation of Aurora A expression.

It was hypothesized that the transient loss of CHFR causes genomic instability due to defects in mitotic spindle formation and function, potentially through Aurora A overexpression. To test this, CHFR expression was transiently decreased by siRNA in the genomically stable IHMEC cell line, MCF10A. Subsequent analysis of these cells revealed they became more aneuploid compared to the parental cells, had four major mitotic defects, showed mislocalization of the key spindle checkpoint proteins BUBR1 and MAD2, and had increased expression of mitotic proteins including Aurora A, α-tubulin, and acetylated α-tubulin.

Materials and Methods

Cell Culture

MCF10A and HEK293 cells were obtained from the American Type Culture Collection and cultured under recommended conditions. For CHFR knockdown, cells were untransfected ("mock") or transfected with 2.0 μM of either a non-targeting siControl siRNA or siRNAs targeting CHFR using Dharmafect1 according to manufacturer's instructions and analyzed 72 hours later (si*GENOME*, Dharmacon RNA Technologies). Cells were transfected with 6.0 μg of a Flag-tagged Aurora A construct (Xiaochun Yu, University of Michigan) or Flag-tagged CHFR using FuGENE 6 (Roche). Lysates were harvested 24 hours later. Cells were treated with 15 μM of MG132

(Calbiochem) for 10 hours and/or 200 ng/ml of nocodazole (Sigma-Aldrich) for 18 hours. To induce DNA damage, cells were treated with 0.3 μM aphidicolin for 24 hours.

Spectral Karyotyping (SKY) and Metaphase Spreads

MCF10A cells were treated with 50 ng/ml colcemid (Invitrogen) for 16h then collected and re-suspended in a hypotonic solution of 2.0% KCl and 2.0% $Na_3C_6H_5O_7$ for 7 minutes at 37°C. Metaphase spreads were then prepared and stained with Giemsa as previously described [20]. More than 25 metaphases were counted in triplicate.

SKY analysis was performed according to the manufacturer's protocol (Applied Spectral Imaging) and as previously described [103]. Briefly, cells and slides were prepared as described above and unstained slides were aged in 2x SSC, treated with pepsin (Amreso; 30.0 μg/ml in 0.01 N HCl), then rinsed with PBS. Slides were post-fixed in 1.0% paraformaldehyde in PBS/$MgCl_2$ and dehydrated in an ethanol series before and after denaturation in a 70% Formamide/2x SSC solution. The denatured SKY probes (Vial 1, SKY kit, Vista, CA) were hybridized to the slides and incubated at 37°C for two days. Following washings, antibodies (from vial 3 and 4, SKY kit) were added and incubated at 37°C for 1 hour each. The slides were counterstained with DAPI in anti-fade solution. All images were acquired using an SD200 SpectraCube spectral imaging system (ASI) attached to a Nikon E800 microscope consisting of an optical head (a Sagnac interferometer) coupled to a multi-line charge-coupled device camera (Hamamatsu, Bridgewater, NJ). Spectral Imaging (v. 2.6.1) and Sky View (v. 1.6.2) were used to acquire and analyze the images, respectively. The average of 10 metaphases was used to create the consensus karyotype.

Western Blotting

Whole cell lysates were collected from approximately 80% confluent cultures. For samples analyzed for ubiquitination, 2 mM of N-ethylmaleimide (NEM; Sigma) was added to the lysis buffer. Western blots were prepared as previously described [20]. Membranes were blocked for one hour at room temperature, and incubated overnight at 4°C in primary antibody. The following antibodies were used: a mouse CHFR monoclonal antibody (1:500 dilution, Abnova Corp.), a custom rabbit polyclonal antibody to the N-terminus of CHFR (1:1000), and a rabbit anti-Aurora A antibody (1.0 mg/ml, Xiaochun Yu). Mouse anti-α-tubulin, anti-γ-tubulin, anti-acetylated α-tubulin, and rabbit anti-Flag (all Sigma-Aldrich), anti-α-tubulin (Cell Signaling Technology), and anti-GST (Santa Cruz) antibodies were all used at a 1:1000 dilution. Anti-ubiquitin (1:100, Sigma) was also used and an anti-glyceraldehyde-3-phosphate dehydrogenase antibody (1:10,000, Abcam) was used for a loading control. Blots were incubated in secondary antibody, anti-mouse:HRP or anti-rabbit:HRP, diluted in the blocking solution. We used the SuperSignal West Pico chemiluminescent kit (Pierce) and exposed the blots to Kodak Biomax XAR film. Blots were stripped prior to re-probing. Where applicable, blots were analyzed from three experiments to verify expression changes. Densitometry was performed using the FluorChem 8900 imaging system (Alpha Innotech Corp.).

GST pull-down

A GST-CHFR fusion construct was created using the pGEX2T vector (Amersham) and expressed in the DH5α strain of *E. coli*. Logarithmic *E. coli* cultures

were collected in lysis buffer (2.5 mM PMSF in 1.0% Triton X-100 with a protease inhibitor cocktail from Roche), sonicated, and then cleared by centrifugation. One milligram of *E. coli* lysates was combined with 50.0 µl of washed Glutathione Sepharose 4B beads (Amersham) for 2 hours at 4°C. Then, 1.0 mg of whole cell lysates from MCF10A cells were added to the beads and incubated overnight at 4°C. Following washes with NTEN200 buffer (20.0 mM Tris-HCl, 1.0 mM EDTA, 0.5% NP-40, 25.0 µg/ml PMSF and 200.0 mM NaCl), bound proteins were eluted in 10.0 mM glutathione and collected by centrifugation. Isolated proteins were identified by Western blotting.

Immunoprecipitation

Immunoprecipitations were completed according to manufacturer's instructions using the Protein G immunoprecipitation kit (Sigma-Aldrich). Briefly, whole cell lysates were combined with 10.0 µl of the specified antibody (mouse IgG_1 isotype control from BD BioSciences, mouse anti-α-tubulin, or mouse anti-Flag M2 antibody) and diluted in the supplied 1x IP buffer and incubated for at least 2 hours at 4°C. Then, 50.0 µl of protein G beads were added to the lysate/antibody mix overnight at 4°C. Following washes, the immunoprecipitated lysates were boiled in the columns in 40.0 µl of 5x Laemmli's loading buffer then eluted by centrifugation and analyzed by Western blotting.

Immunofluorescence

MCF10A cells were plated in two-chambered slides then fixed in 4.0% paraformaldehyde and blocked in 5.0% milk, 1.0% BSA in 0.025% TBS-Triton X100. Staining was performed using an anti-α-tubulin antibody (1:100, Sigma-Aldrich), a rabbit

anti-Aurora A antibody (1:50, Cell Signaling Technology) or an anti-histone H3-phospho-Ser28 antibody (1:100, Upstate), which were hybridized in blocking buffer overnight at 4°C. Slides were hybridized with an anti-mouse:Alexafluor594 or an anti-rabbit:Alexafluor488 secondary antibody (Invitrogen) diluted to 1:200 in blocking buffer. Samples were preserved with ProLong Gold antifade reagent with DAPI (Invitrogen).

For BUBR1 and MAD2 localization, cells were prepared as above then permeabilized for 5 minutes in 0.5% TritonX-100 in 1x PBS after fixation. Samples were blocked in 5.0% milk in 0.1% TBST then hybridized with an anti-BUBR1 antibody (Sigma) or an anti-MAD2 antibody (BD BioSciences) at a 1:200 dilution in blocking buffer overnight at 4ºC. Slides were hybridized with an anti-mouse:Alexafluor594 secondary antibody (1:500, Invitrogen) in blocking buffer for 1 hour at room temperature then preserved with ProLong Gold Anti-fade reagent with DAPI (Invitrogen).

Microscopy

We used a Leica DMRB miscroscope (W. Nuhsbaum, Inc.) with an external Leica EL6000 light source and a 63x or a 100x objective lens. Images were recorded using a Retiga 2000R 12-bit digital camera and QCapture Pro v5.1 software (QImaging).

Data Analysis

Images were processed for resolution, magnification, and gamma settings using Adobe Photoshop CS2. We used the ANOVA test for statistical significance and $p<0.05$ was considered significant. Error bars depict the standard error from triplicate experiments. One asterisk (*) indicates $p\leq0.05$ and two asterisks (**) indicate $p\leq0.001$.

Results

Transient Loss of CHFR Expression Leads to Increased Aneuploidy

We previously reported that the stable loss of CHFR expression by shRNA in IHMECs led to increased aneuploidy after prolonged culture in the genomically stable, but hyper-diploid MCF10A cell line [20]. Spectral karyotyping (SKY) of these cells indicated two distinct cell populations - minimally greater aneuploid or near tetraploid (Figure 4.1). The parental karyotype of MCF10A cells, determined from eight metaphase spreads, was: 48,XX,1qhph,+del(1)(p?),t(3;9)(p14;p21),+del(7)(q?),i(8)(q10),t(3;5)(p?;?). The consensus karyotype of five metaphase cells from the minimally greater aneuploid population of MCF10A cells expressing CHFR shRNA was: 47~50,XX,+X,t(1;2)(q?;q?),t(3;9)(p14;p21),der(6)t(6;19)(p?;?),+del(7)(q?),t(3;5)(p?;?), der(11)t(8;11)(?;p?), t(15;18)(?;p?),+20. The consensus karyotype from five metaphase cells for the near tetraploid population was 81~95,XXXX,-1,t(1;2)(q?;q?),der(2)t(1;2)(q?;q?),-3,t(3;9)(p14;p21)x2,5,der(6)t(6;19)(p?;?)x2, +del(7)(q?),-9,t(3;5)(p?;?),-10,der(11)t(8;11)(?;p?)x2,-13,der(15)t(15;18)(?;p?)x2,-17,-18x2,+20x2,-22. In summary, MCF10A cells lacking CHFR gained chromosomes 20 and three metaphase cells indicated a gain of chromosome X. There were also four novel translocations t(1;2), t(6;19), t(8;11), and t(15;18) (Figure 4.1 B and C), suggesting that CHFR may regulate genomic stability via multiple mechanisms. The finding that novel translocations were present in the CHFR knockdown cells compared to the parental cell line indicates the absence of clonal selection of cells from the parental line. As an estimate of the frequency of tetraploidy, the incidence of bi-nucleated cells in the population was determined to be 12.45% in

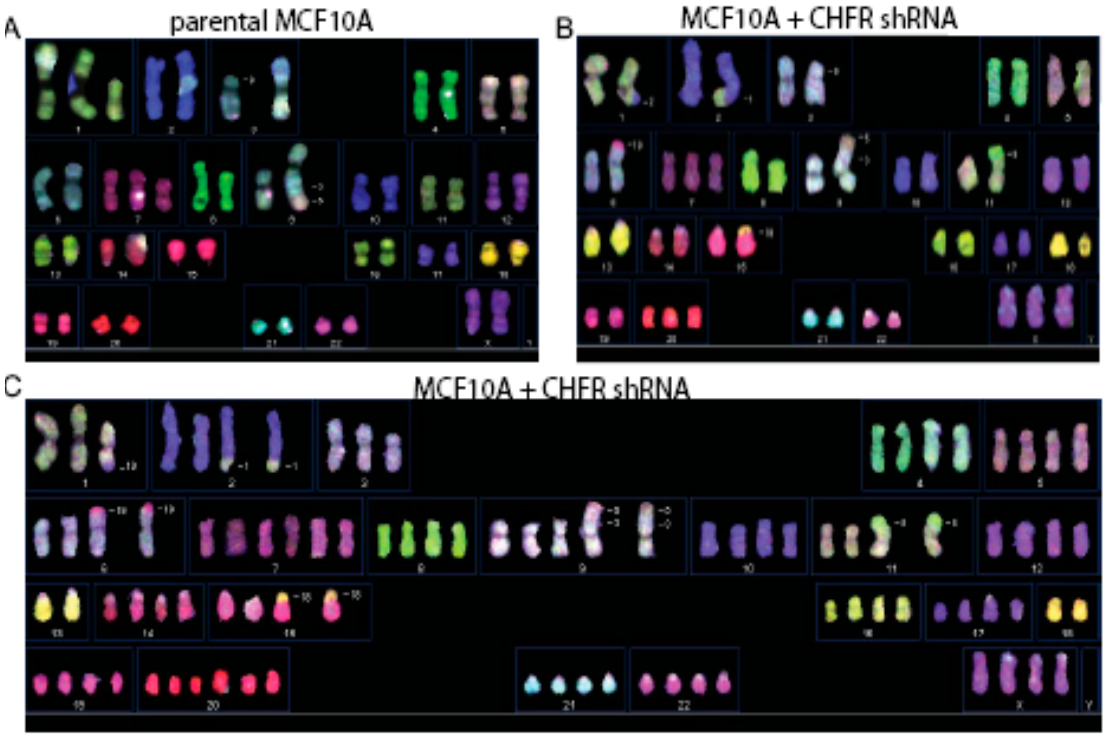

Figure 4.1: Stably decreased CHFR expression causes increased aneuploidy.

(A) SKY analysis of parental MCF10A cells shows the characteristic karyotype of this genomically stable hyper-diploid cell line. The karyotype of parental MCF10A cells was: 48,XX,1qhph,+del(1)(p?),t(3;9)(p14;p21),+del(7)(q?),i(8)(q10),t(3;5)(p?;?). (B and C) SKY analysis of MCF10A cells stably expressing shRNA against CHFR are either minimally more aneuploid (B) or nearly tetraploid (C) with novel chromosome translocations. The consensus karyotype for the minimally aneuploid population was 47~50,XX,+X,t(1;2)(q?;q?),t(3;9)(p14;p21),der(6)t(6;19)(p?;?),+del(7)(q?),t(3;5)(p?;?), der(11)t(8;11)(?;p?), t(15;18)(?;p?),+20. The consensus karyotype for the near tetraploid population was 81~95,XXXX,-1,t(1;2)(q?;q?),der(2)t(1;2)(q?;q?),-3, t(3;9)(p14;p21)x2,5,der(6)t(6;19)(p?;?)x2,+del(7)(q?),-9,t(3;5)(p?;?),-10,der(11)t(8;11)(?;p?)x2,-13,der(15) t(15;18)(?;p?)x2,-17,-18x2,+20x2,-22.

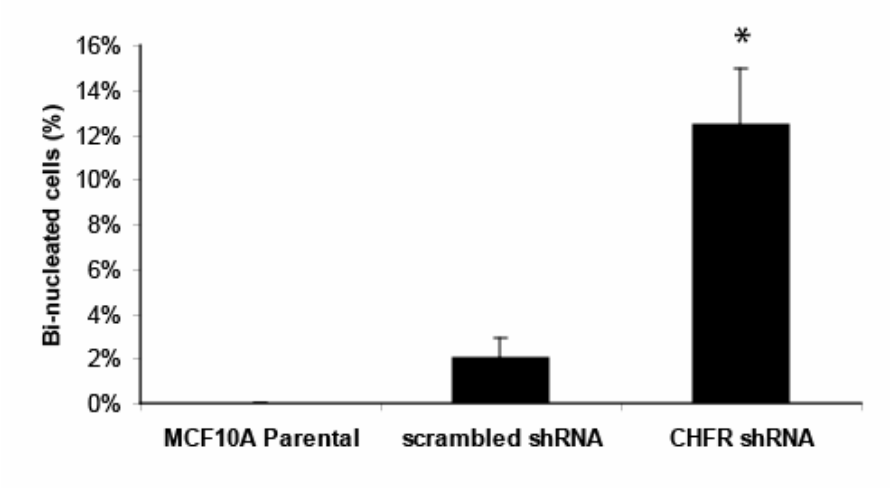

Figure 4.2: The stable decrease of CHFR expression by shRNA results in increased incidence of bi-nucleated cells.

A graphical representation of the frequency of bi-nucleated cells in parental MCF10A cells, those transduced with the scrambled shRNA control, and cells transduced to express stably shRNA against CHFR. Nearly 12.5% of CHFR shRNA cells were bi-nucleated, which is a possible indicator of the frequency of tetraploidy. One asterisk (*) indicates $p<0.05$.

CHFR shRNA cells compared to negative controls. However, additional cells may have been tetraploid but contained within one nucleus, which was not assessed in this assay.

To determine if the genomic instability arose due to prolonged culture following CHFR knockdown or clonal selection, MCF10A cells were transiently transfected with siRNAs targeting CHFR ("MCF10A:CHFR-siRNA cells") and analyzed for increased aneuploidy and chromosome breakage within three days post transfection. CHFR expression was decreased by at least 80% as detected by Western blotting at the 72 hours timepoint (Figure 4.3). We observed no chromosome breaks on metaphase spreads following treatment with aphidicolin to induce DNA damage (Figure 4.4 and data not shown). Of note, 32% of MCF10A:CHFR-siRNA cells were more aneuploid, typically having 49-59 chromosomes, compared to the mock transfected and non-targeting ("siControl") negative control counterparts 72 hours after transient transfection (Figure 4.5A and 4.5B, $p \leq 0.001$). This indicated that increased aneuploidy occurs within a few days after CHFR expression is decreased and that it is not simply a result of prolonged cell culture conditions. Given this, we wanted to elucidate the mechanism(s) by which amplified aneuploidy occurred in IHMECs that had lost CHFR expression.

CHFR Regulates Chromosome Attachment to the Mitotic Spindle

We performed immunofluorescence to visualize chromosomes during mitosis to examine the potential origins of increased aneuploidy in MCF10A:CHFR-siRNA cells. Nearly 25% of MCF10A:CHFR-siRNA cells had misaligned metaphase chromosomes when compared to the control cells (Figure 4.6A and 4.6B), and lagging chromosomes and chromosome bridges during anaphase (Figure 4.7). Together, these results suggested that the spindle checkpoint was disrupted in cells with decreased CHFR expression.

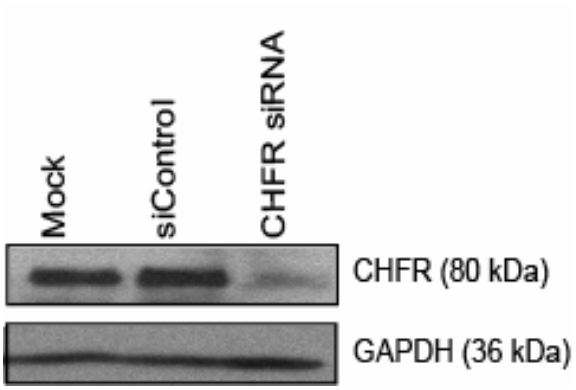

Figure 4.3: A pool of four siRNAs substantially decreases CHFR expression.

Western blotting shows >80% decrease in CHFR expression in MCF10A cells transiently transfected with siRNA against CHFR ("CHFR siRNA") compared to untransfected ("mock") and non-targeting siRNA ("siControl") transfected cells after 72h.

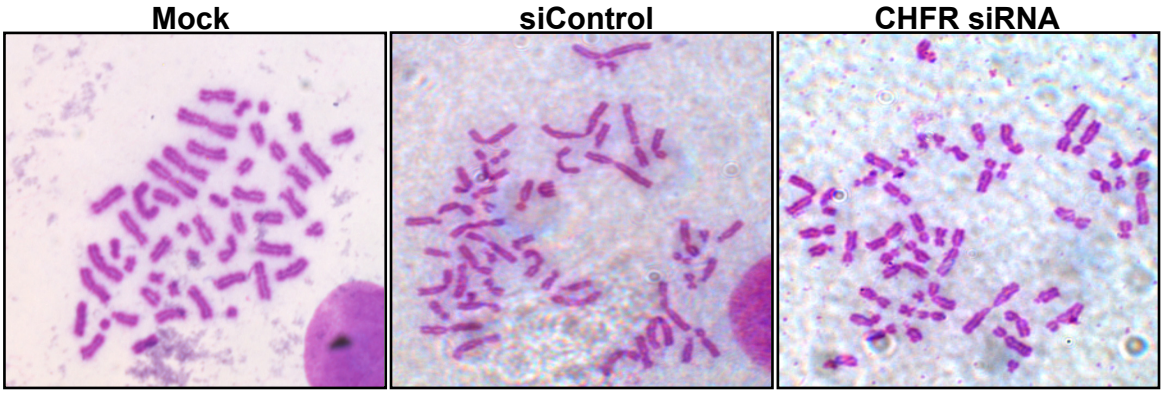

Figure 4.4: A transient decrease in CHFR expression by siRNA in MCF10A cells does not increase the incidence of chromosome breaks following treatment with 0.3 μM aphidicolin.

Untransfected ("Mock") MCF10A cells, non-targeting siRNA-transfected cells ("siControl"), and cells transfected with a pool of siRNAs against CHFR were treated with 0.3 μM aphidicolin for 24 hours and exposed to 50 ng/ml colcemid for 21 hours to enrich for metaphase cells. Metaphase spreads were created on glass slides and stained in Giemsa solution then visualized on a Leica DMRB microscope with a 100x objective lens to look for chromosome breaks. Chromosome breaks were not observed for any of the three samples.

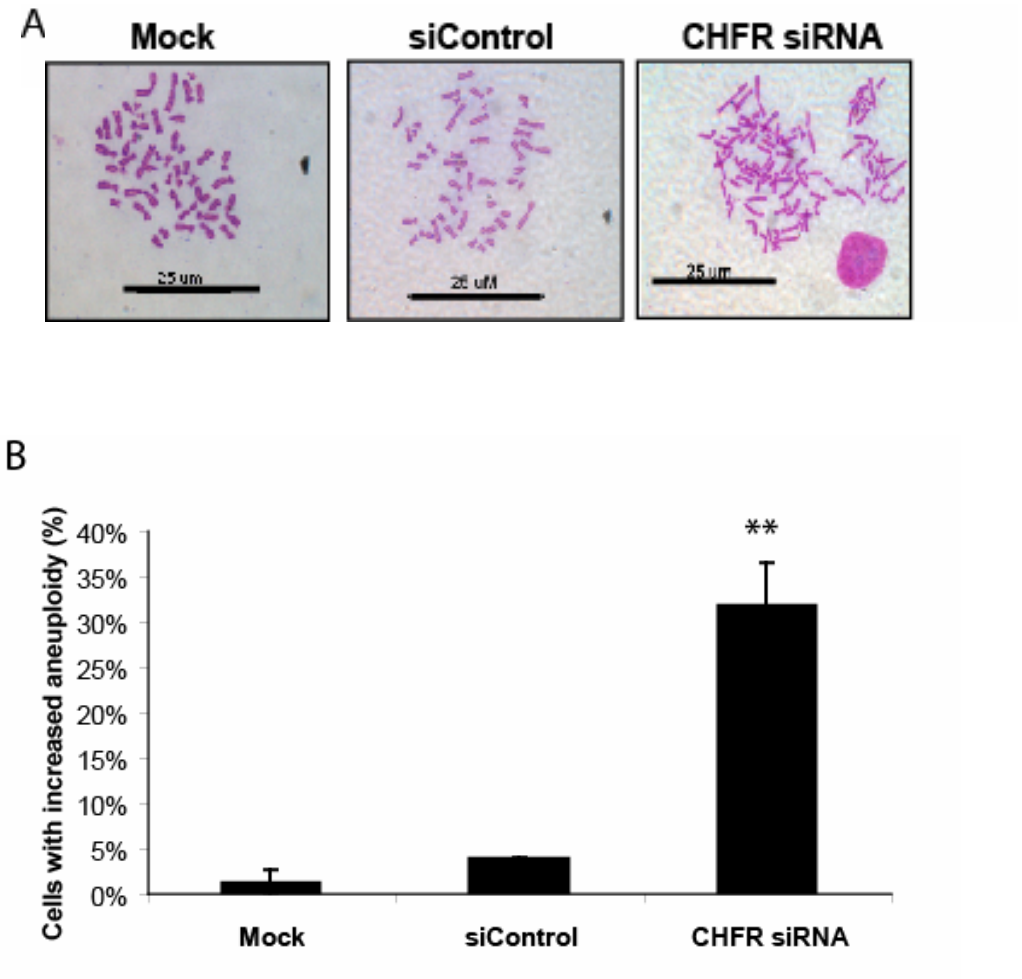

Figure 4.5: A transient loss of CHFR expression by siRNA in MCF10A cells results in increased aneuploidy within 72 hours.

(A) Metaphase spreads show that MCF10A cells transfected with siRNA against CHFR (right panel) are more aneuploid when compared to the mock transfected and non-targeting siControl negative control cells. Bar = 25 µm. (B) The graph shows the frequency of cells with increased aneuploidy in transiently transfected MCF10A cells. Cells with amplified aneuploidy had between 49-59 chromosomes, compared to 48 in the parental line.

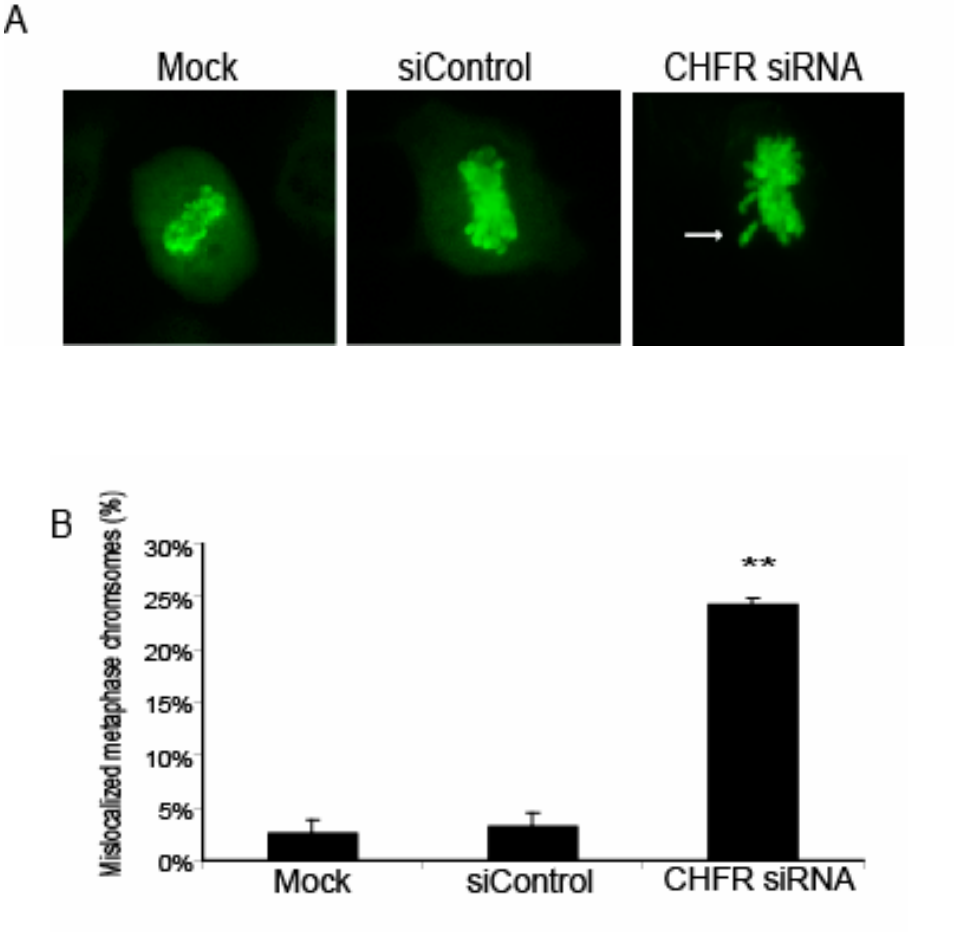

Figure 4.6: Lowered CHFR expression by siRNA causes misaligned chromosomes at the metaphase plate in MCF10A cells.

(A) Sister chromatids did not properly migrate to the metaphase plate in MCF10A:CHFR siRNA cells (arrow, right panel). Immunofluorescence (IF) detected phosphorylated histone H3-Ser28 (green) to identify metaphase chromosomes. (B) A graph of the data shown in (A); 24% of cells with CHFR siRNA have chromosomes improperly located during metaphase. Two asterisks (**) indicate $p<0.001$.

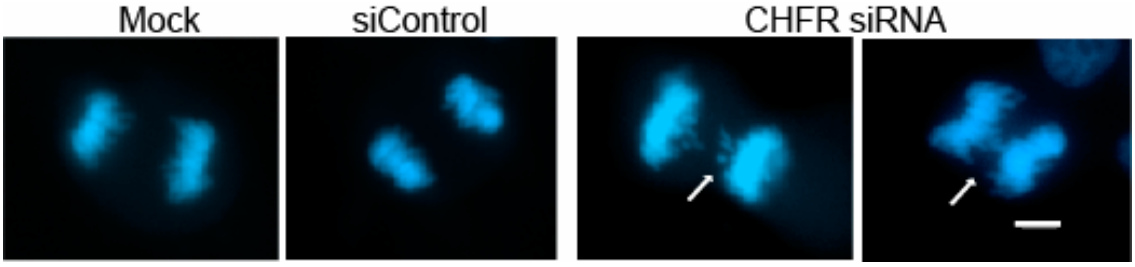

Figure 4.7: Targeting CHFR expression by siRNA causes lagging chromosomes during anaphase.

Immunofluorescence indicated that MCF10A:CHFR-siRNA cells have lagging chromosomes and chromosome bridges during anaphase (arrow, right panels). However, the negative control cells had a clear division between the two sets of separated sister chromatids that will be equally divided between the two daughter cells. DNA was stained blue with DAPI. White bar = 5 μm.

To test this hypothesis, we studied the localization of two critical spindle checkpoint proteins, BUBR1 and MAD2, during mitosis. Normally, both proteins have a punctate staining pattern early in mitosis, reflecting their localization to kinetochores prior to chromosome segregation at anaphase. Staining becomes diffuse later in mitosis after all chromosomes are attached to the mitotic spindle. Normal BUBR1 and MAD2L1 staining patterns were observed in negative control cells (Figure 4.8). In contrast, MCF10A:CHFR-siRNA cells demonstrated diffuse BUBR1 and MAD2 staining early in metaphase (Figure 4.8A and 4.8B, right panels). Although Western blotting showed that CHFR siRNA did not change MAD2 or BUBR1 expression, immunoprecipitation experiments revealed that CHFR could interact with MAD2, but not BUBR1 (Fig. 4.9, data not shown)

As noted above, some cells with stably decreased CHFR by shRNA were tetraploid (Figure 4.1). In fact, 6% of transiently transfected MCF10A:CHFR-siRNA cells were binucleated, suggesting tetraploidy, compared to only about 1% of negative control cells (Fig 4.10A and 4.10B, $p<0.05$). This was confirmed by the occasional tetraploid MCF10A:CHFR-siRNA metaphase spread when cells were assessed for changes in aneuploidy frequency.

CHFR Modulates Expression of Aurora A

The chromosome mis-segregation phenotypes in MCF10A:CHFR-siRNA cells were highly reminiscent of mouse embryonic fibroblasts (MEFs) that over-express Aurora A [99]. Previous studies also performed in MEFs from CHFR knockout mice showed similar mitotic defects and Aurora A over-expression [8]. To assess if Aurora A expression or localization was altered in our model, we performed Western blotting and

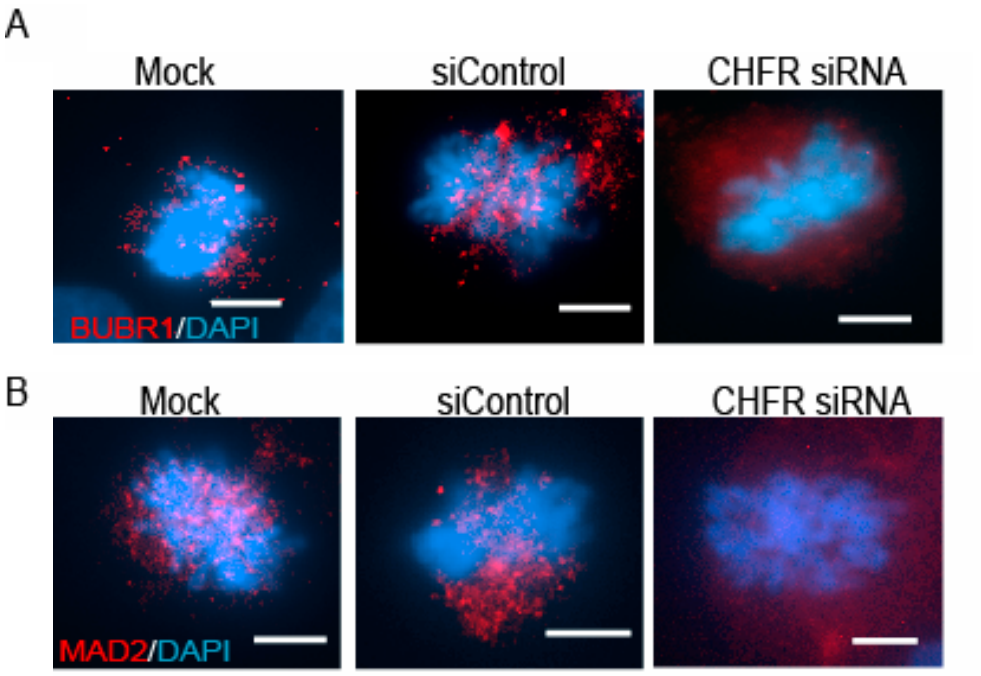

Figure 4.8: The mitotic spindle checkpoint proteins BUBR1 and MAD2 are mislocalized during metaphase following the loss of CHFR expression by siRNA.

Immunofluorescence to visualize BUBR1 and MAD2 revealed that cells with CHFR siRNA (right panels) had a diffuse BUBRI and MAD2 staining pattern (red, A and B respectively), indicating mislocalization. Control cells had the characteristic punctate staining patterns for BUBR1 and MAD2. DNA was stained blue with DAPI.

White bar = 5 μm.

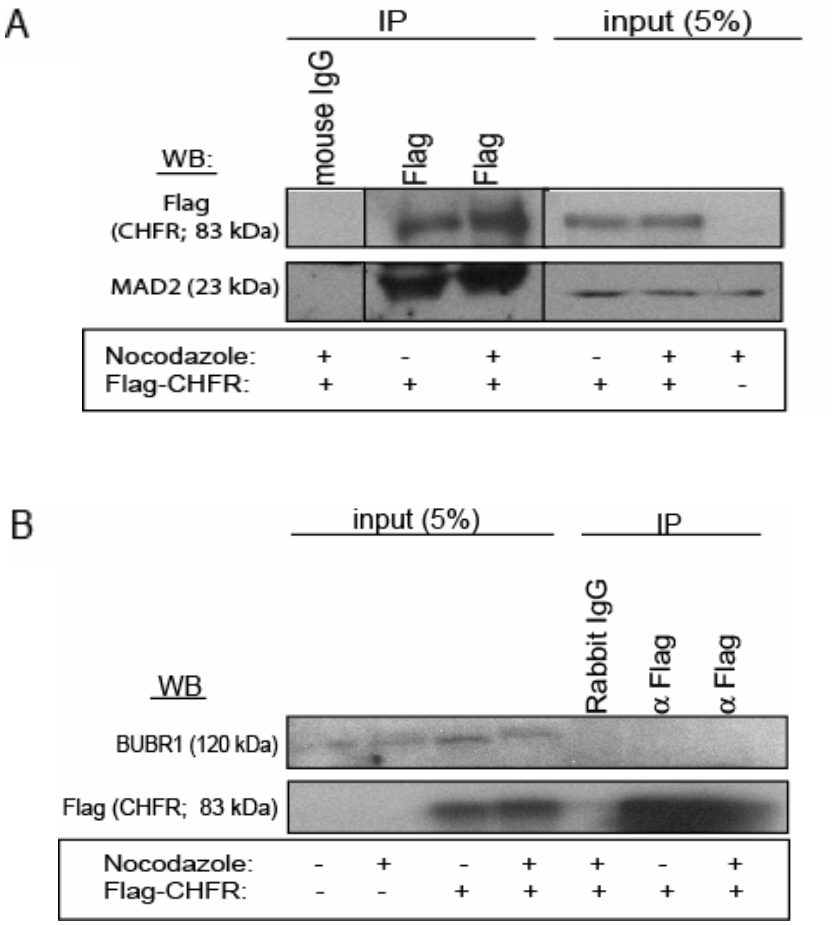

Figure 4.9: A Flag-tagged CHFR construct can interact with the mitotic spindle checkpoint protein MAD2, but not BUBR1.

(A) Endogenous MAD2 interacts with CHFR. HEK293 cells were transfected with a Flag-tagged CHFR construct, with or without nocodozaole treatment. Immunoprecipitation (IP) with an anti-Flag antibody was performed to isolate CHFR and subsequently analyzed by Western blotting (WB) for the Flag:CHFR fusion protein and endogenous MAD2. "Input" indicates 5% of the lysates used for the IP reaction. (B) The experiment was performed as above, but Western blotting was used to detect endogenous BUBR1. Flag:CHFR was not found to interact with BUBR1.

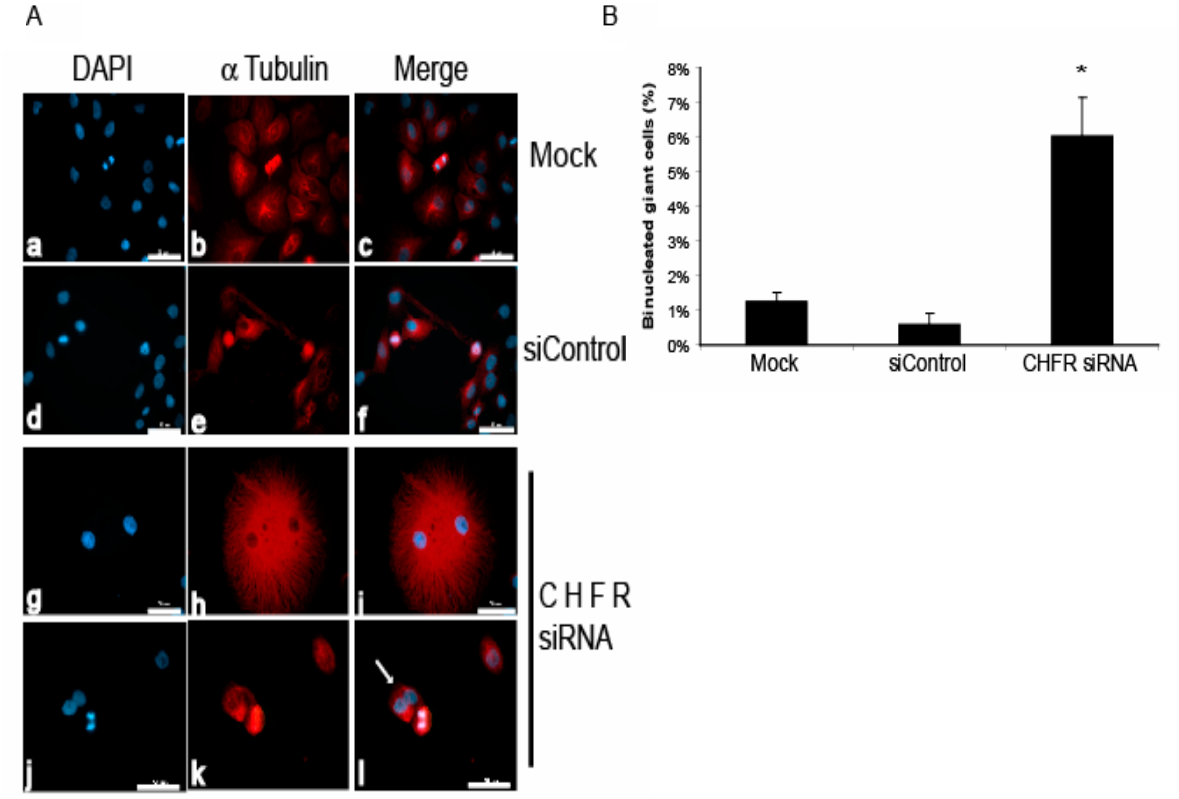

Figure 4.10: Decreased CHFR expression by siRNA causes an increase in the incidence of bi-nucleated giant cells.

(A) Immunofluorescence to detect cytoskeletal α-tubulin (red) during interphase shows that MCF10A:CHFR-siRNA cells become binucleated (subpanels i and l; arrow) compared to the negative control cells (subpanels c and f). DNA was stained blue with DAPI. White bar = 50 μm. (B) Quantification of the data shown in (A) in which 6% of cells lacking CHFR became bi-nucleated as opposed to about 1% incidence in control cells. One asterisk (*): $p<0.05$.

found that MCF10A:CHFR-siRNA cells had much greater Aurora A expression compared to the control cells (Figure 4.11A). It has been demonstrated that CHFR can interact with, and ubiquitinate, Aurora A by immunoprecipitation *in vitro* in non-mammary human cell lines [8]. We also found that Flag-tagged Aurora A could interact with endogenous CHFR in MCF10A cells by IP (Figure 4.11B). The physical interaction of these two proteins, combined with Aurora A over-expression in MCF10A:CHFR-siRNA cells, substantiates initial observations that Aurora A is a target for CHFR-mediated ubiquitination for degradation.

Early in mitosis, Aurora A localizes to centrosomes where it is involved in their maturation and separation and spindle formation [104]. We found that Aurora A localized strongly to the centrosomes during metaphase in control cells, as evidenced by the two distinct dots that colocalized to the spindle poles, as expected. However, in 16% of MCF10A:CHFR-siRNA cells, more than two Aurora A foci were detected, indicating increased Aurora A expression and centrosome amplification (Figure 4.12 $p<0.05$).

CHFR Regulates α-tubulin Expression

In MCF10A:CHFR-siRNA cells, the spindle was more condensed with poor polar microtubule formation (Figure 4.12A, bottom panel). It was hypothesized that CHFR may interact with tubulin proteins. A GST pull-down using a GST:CHFR fusion protein and lysates from MCF10A cells was performed. CHFR was found to interact with α-tubulin, but not β- or γ-tubulin when the MCF10A cells were treated with nocodazole (Figure 4.13 and data not shown). This was confirmed by immunoprecipitation, though the interaction was not dependent on nocodazole treatment (Figure 4.13).

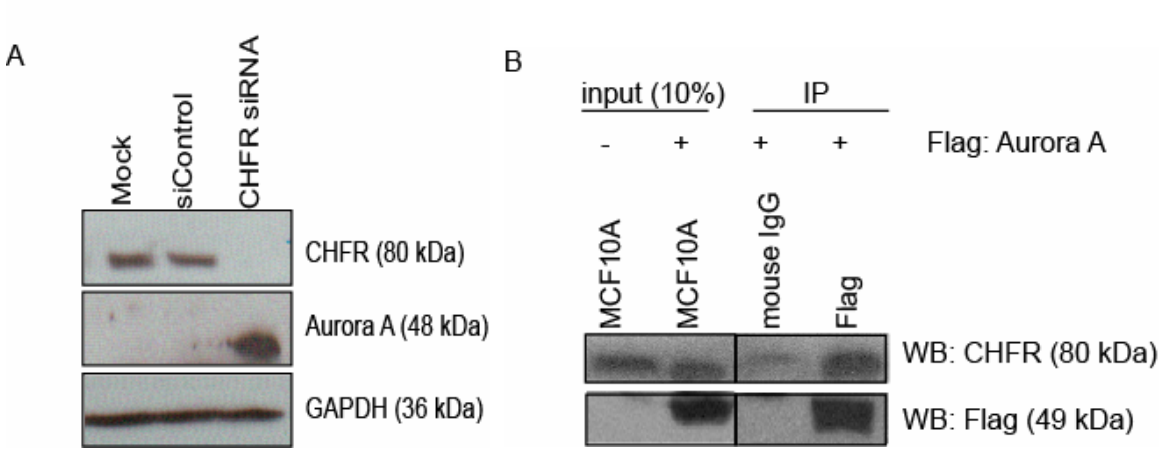

Figure 4.11: Endogenous CHFR interacts with Aurora A kinase and regulates its expression in MCF10A cells.

(A) MCF10A:CHFR-siRNA cells over-express Aurora A, as shown by Western blotting, compared to control cells. GAPDH was used as a loading control. (B) Flag:Aurora A interacts with endogenous CHFR by co-IP. Lysates from MCF10A cells transiently transfected with Flag-tagged Aurora A were subjected to IP with an anti-Flag (M2) antibody then probed for CHFR or Flag by Western blotting (WB) using rabbit antibodies. "Input" on the left indicates 10% of the lysates used for the IP reaction.

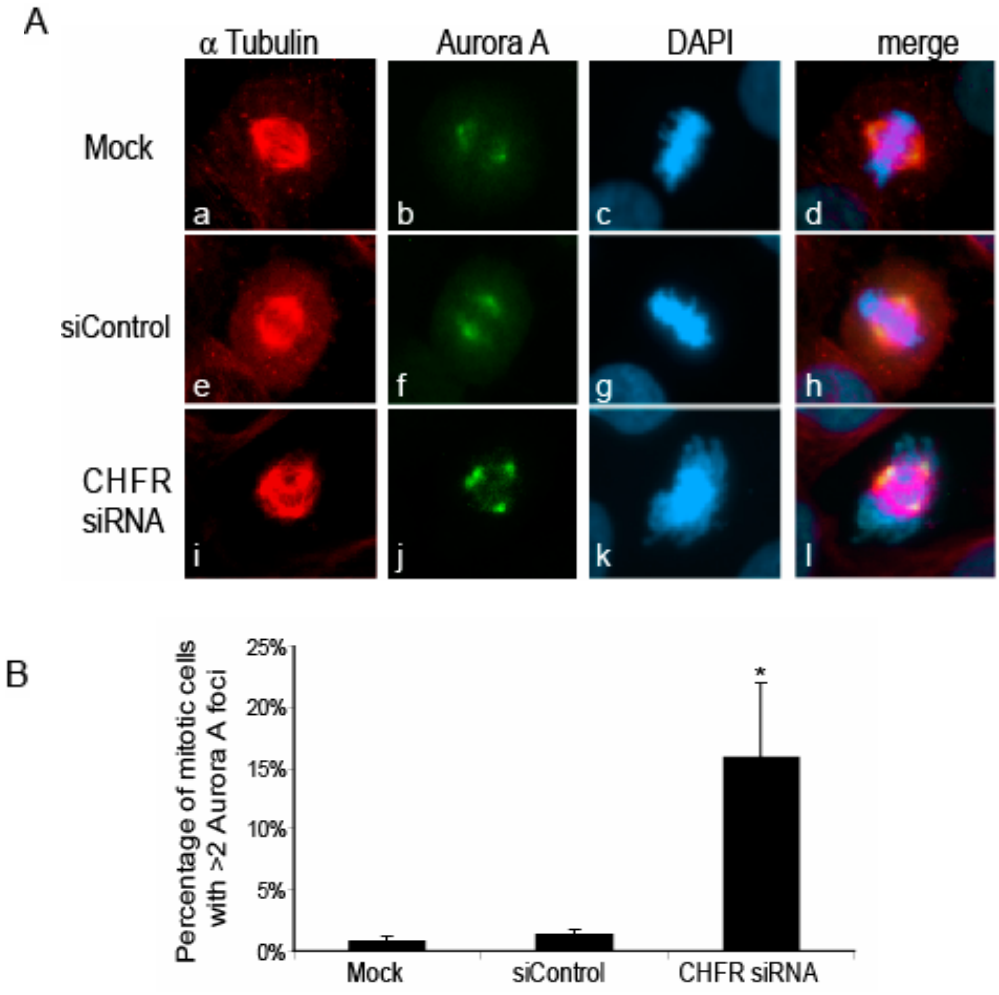

Figure 4.12: Lowered CHFR expression in MCF10A cells leads to increased numbers of Aurora A foci, suggesting centrosome amplification.

(A) Immunofluorescence for Aurora A (green) indicates that MCF10:CHFR-siRNA cells (bottom row) have greater than two Aurora A foci when compared to two foci in negative control cells during metaphase. Cells were stained with DAPI (blue) for DNA and for α-tubulin (red) to see the spindle. Note the compacted, disorganized mitotic spindle (red) in CHFR-siRNA cells (subpanel l versus subpanels d and h). (B) Quantification of the data in (A), in which 16% of cells without CHFR have greater than two Aurora A foci. One asterisk (*) indicates $p<0.05$.

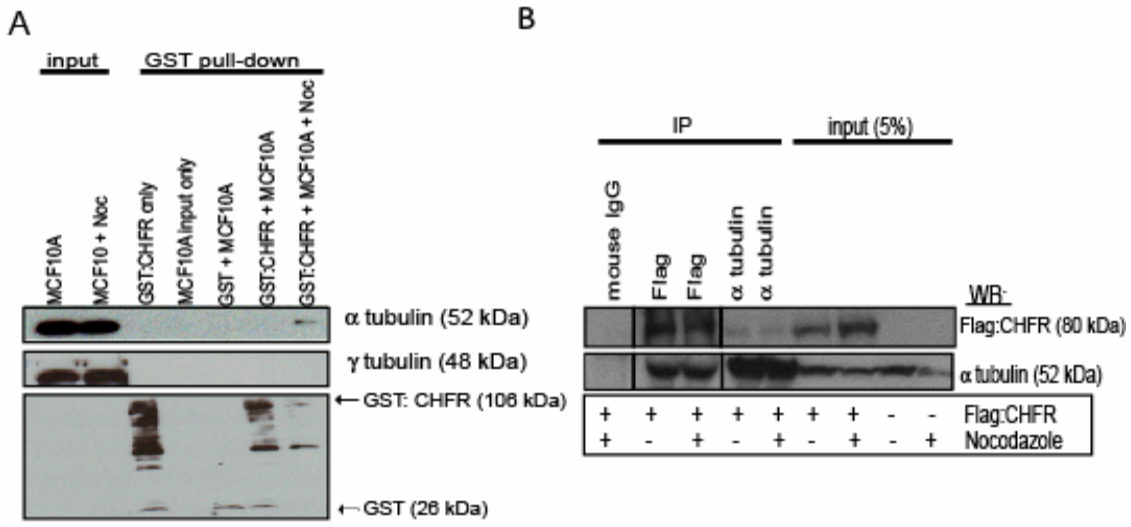

Figure 4.13: CHFR interacts with α-tubulin by GST pull-down and immunoprecipitation.

(A) A GST pull-down using a GST:CHFR fusion protein shows that CHFR can interact with α-tubulin, but not β- or γ-tubulin from MCF10A whole cell lysates as shown by Western blotting for tubulins. The "input" is 10% of the MCF10A whole cell lysates used for the GST pull-down. MCF10A cells were either untreated (-Noc) or treated with nocodazole (+Noc) prior to lysate collection. (B) CHFR interacts with α tubulin by IP. A Flag:CHFR construct was transfected into HEK293 cells and the lysates were used for IP with either anti-Flag or anti-α tubulin mouse antibodies then Western blotted (WB) with either anti-Flag or anti-α tubulin rabbit antibodies. Cells were either untreated or treated with nocodazole. The "input" indicates 5% of the lysates used for the IP reaction.

To determine if CHFR ubiquitinates α-tubulin, MCF10A cells transfected with control or CHFR siRNAs were treated with the proteasome inhibitor MG132 with or without nocodazole. Immunoprecipitation for α-tubulin then immunoblotting for ubiquitin indicated that CHFR can ubiquitinate α-tubulin during nocodazole exposure, as evidenced by the loss of ubiquitin signal in MCF10A:CHFR-siRNA cells (Figure 4.14, lane 3 vs. lane 6). Western blotting confirmed that CHFR can regulate α-tubulin as there was a reproducible increase in α-tubulin protein levels, but not in β-or γ-tubulin, in MCF10A:CHFR-siRNA cells (Figure 4.15 and data not shown, $p<0.05$). The amount of acetylated α-tubulin in MCF10A:CHFR-siRNA cells also was consistently double that of controls (Figure 4.15 $p<0.05$).

Discussion

The work presented here indicates that CHFR is important for the maintenance of genomic stability in mammary epithelial cells. Our results support and help explain the findings of aneuploidy in MEFs from *Chfr*$^{-/-}$ mice. The observed chromosome rearrangements that we noted by spectral karyotyping likely resulted from prolonged culture and the disruption of DNA damage response genes secondary to the increase in aneuploidy, which we have shown can develop within a few days after CHFR expression is decreased. To the contrary, the more frequent presence of additional chromosomes with a numeric change in chromosome number, or aneuploidy, in siRNA-treated cells provide powerful evidence that CHFR is required for genomic stability via proper chromosome segregation during mitosis. Furthermore, the lack of chromosome breaks in MCF10A cells transiently expressing siRNA against CHFR suggested that CHFR might not participate directly in the DNA damage response caused by

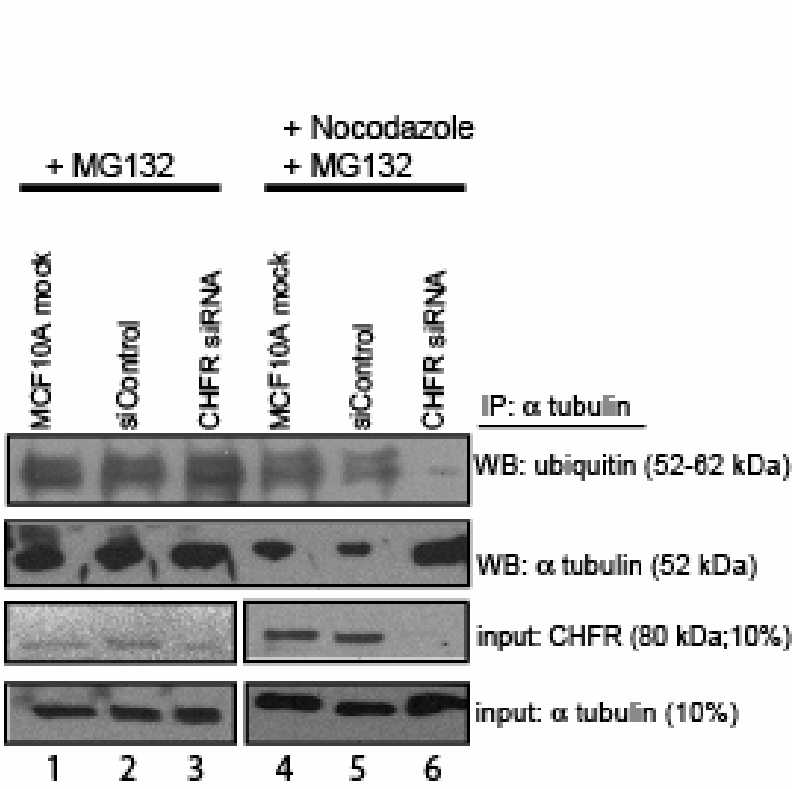

Figure 4.14: CHFR can ubiquitinate α-tubulin during nocodazole treatment.

MCF10A cells were cultured in 15 μM MG132 for 10 hours and either untreated or simultaneously treated with 200 ng/ml nocodazole for 18 hours. Western blotting of immunoprecipitated α-tubulin for ubiquitin shows that the amount of ubiquitinated α-tubulin is dramatically decreased in MCF10A:CHFR-siRNA cells treated with nocodazole. The "input" indicates 10% of the lysates used for the IP reaction.

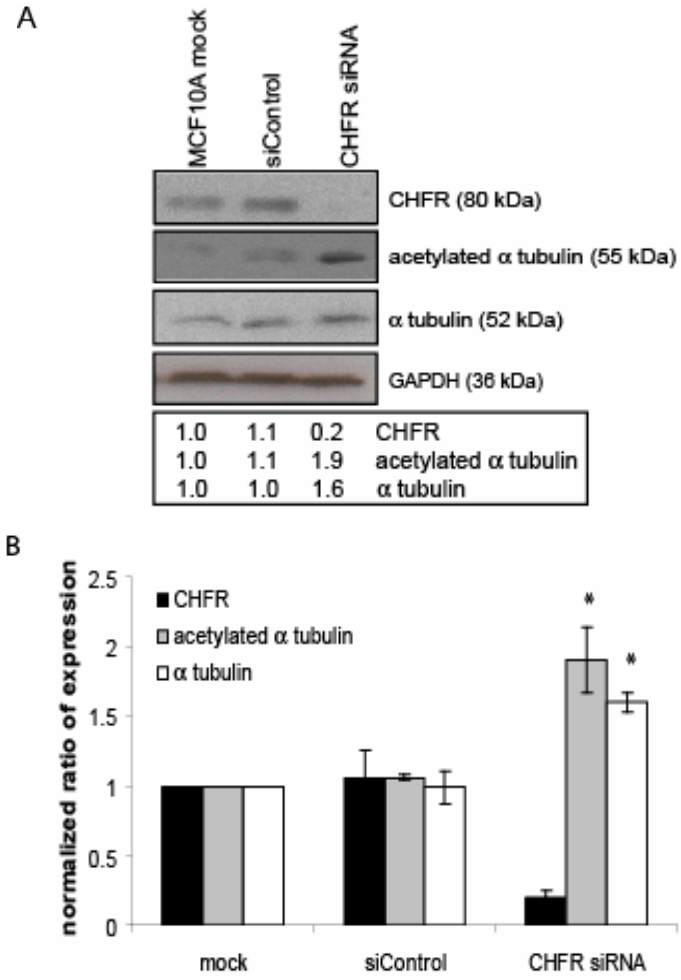

Figure 4.15: CHFR regulates α-tubulin expression and the amount of acetylated α-tubulin.

(A) Western blotting reveals that MCF10A:CHFR-siRNA cells have a modest increase in unmodified and acetylated α-tubulin protein levels compared to control cells. The box encompasses the normalized expression of each of the proteins, as determined by densitometry. (B) Quantification of the data presented in (A) from triplicate experiments, showing a reproducible 2-fold increase in acetylated α-tubulin protein levels and a modest increase in total α-tubulin expression. (*) denotes $p<0.05$.

aphidicolin. This conclusion is supported by previous studies in which CHFR expression did not alter the DNA damage response following treatment with other genotoxic reagents [7, 17].

The mis-localization of the key checkpoint proteins, BUBR1 and MAD2, following CHFR knockdown indicated an impaired spindle checkpoint, which would help to explain the observed increase in aneuploidy. With an impaired spindle checkpoint, cells with decreased CHFR expression could enter anaphase without all of their chromosomes localized to the metaphase plate, leading to the appearance of lagging chromosomes and unequal chromosome segregation amongst the two daughter cells. One potential outcome of improper chromosome segregation is that the cell can bypass cytokinesis, resulting in bi-nucleated cells and tetraploidy, which was also observed in this work [105]. Of interest, our work strongly agrees with previous findings that the yeast orthologs of CHFR, Dma1 and Dma2, also function in regulating the spindle checkpoint and cytokinesis [11, 12].

It is quite interesting to note that CHFR can interact with one spindle checkpoint protein, MAD2, but not another, BUBR1. This suggests that CHFR interacts with MAD2 when it is not in the spindle checkpoint complex at the kinetochore. Despite CHFR's E3 ubiquitin ligase activity, MAD2 (and BUBR1) expression was not altered in CHFR knockdown cells, indicating that the protein-protein interaction between CHFR and MAD2 is not for the purposes of regulating MAD2 protein levels. However, it has been shown that CHFR has the potential to regulate lysine-63 based ubiquitin chains on target proteins, which would likely alter the target protein's activity or function rather than target it for degradation by the proteasome [5]. Further work is suggested in order to

determine if CHFR can create Lys63-based ubiquitin chains or can mono-ubiquitinate MAD2 to alter its localization and/or function. Additional studies to determine if CHFR can interact with, or regulate, other mitotic spindle checkpoint proteins, such as Cdc20 or MAD1, will also be required to understand further the role of CHFR in the mitotic spindle checkpoint. It will also be interesting to find out if CHFR interacts with the open or closed conformation of MAD2, or both. Supporting our hypothesis that CHFR may participate in the spindle assembly checkpoint, recently published bioinformatics evidence indicated that CHFR might contain a KEN box motif. This indicates that CHFR may be targeted for proteasome-mediated degradation by the anaphase-promoting APC/C complex, which is a critical component of the mitotic spindle assembly checkpoint and the regulatory complex that controls mitotic exit [26]. A model of the mitotic spindle checkpoint, and where CHFR may participate, is shown in Figure 4.16.

We were able to confirm the previously published finding that CHFR can regulate Aurora A expression. Aurora A is amplified and over-expressed in many cancers, including breast, and over-expression in cultured cells leads to transformation [102, 104]. In addition, a transgenic mouse over-expressing Aurora A in the mammary epithelium leads to tumor formation and genomic instability [106]. CHFR was recently characterized as having tumor suppressor functions and, as shown here, many of its genomic instability phenotypes resemble Aurora A over-expression; therefore, we propose that one major mechanism by which CHFR inhibits oncogenesis may be through its negative regulation of Aurora A [8, 20]. Of interest, novel drugs are being generated that target the Aurora kinases [107]. Since decreased CHFR expression has been linked to sensitivity to microtubule-targeting drugs, future studies may find a synergistic effect

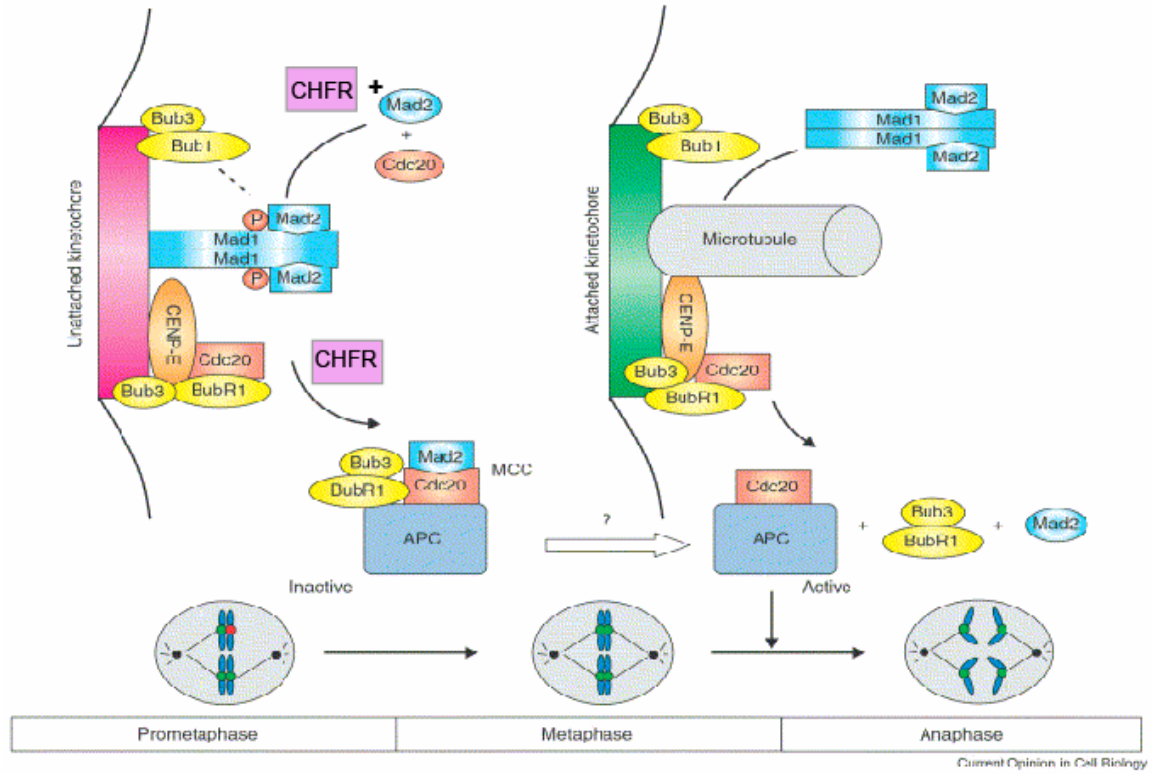

Figure 4.16: How CHFR may participate in the mitotic spindle assembly checkpoint to regulate MAD2 and BUBR1 localization.

The cytosolic open conformation of MAD2 is bound to Cdc20 until it is recruited to an unattached kinetochore in order to interact with MAD1. CHFR may interact with MAD2 here and be required for its localization to the kinetochore. BUBR1 is also bound to Cdc20, in addition to BUB3 and CENP-E at the kinetochore. CHFR may be indirectly or directly required for BUBR1 localization here at the kinetochore. MAD2, BUBR1, BUB3 and Cdc20 bind the anaphase-promoting complex (APC) to inhibit it from initiating anaphase. When the kinetochore becomes attached to a microtubule of the mitotic spindle, BUBR1, BUB3, and MAD2 are released from the kinetochore and detach from APC to activate it and allow the initiation of anaphase and the cleavage of separase. Adapted from an illustration by Hongtao Yu [108].

when taxanes and Aurora kinase inhibitors are both used for treatment.

These findings also indicate that CHFR may play a role in regulating α-tubulin turnover or stability, especially following microtubule stress. This is the first clue as to how the "CHFR checkpoint" responds to microtubule poisons, though an unidentified signaling cascade also is likely to be involved in this checkpoint. The ubiquitination and possible degradation of α-tubulin may be necessary to remove those α/β tubulin dimers that are targeted by microtubule poisons. In unstressed cells, CHFR may also be required for proper spindle formation, as indicated in Figure 4.12A. Aurora A kinase is also required for proper spindle formation, supposedly through its positive regulation of a protein called hepatoma up-regulated protein (HURP) [109]. HURP is required for both chromosome congression and alignment and for the polymerization and stabilization of microtubules during mitotic spindle formation. It will be interesting to determine in the future if CHFR's ability to control spindle formation is via its upstream regulation of Aurora A.

We also noted that one of the effects of decreasing CHFR expression is the up-regulation of the amount of acetylated α-tubulin protein. One of the characteristics of stabilized microtubules is the acetylation of α-tubulin on residue lysine 40. Acetylated α-tubulin is associated with decreased microtubule turnover and is localized to the mitotic spindle, centrosomes, and the mitotic midbody [110, 111]. An increase in acetylated α-tubulin, such as that observed here, would likely result in over-stabilized microtubules, which would hinder mitotic spindle movement or would prevent its proper formation. This may help to explain why CHFR negative cells are more sensitive to taxanes. The cellular stress of the over-stabilized acetylated microtubules, combined

with stress induced by microtubule poisons, may enable the cell to surpass a threshold of tolerable stress that would result in apoptosis. This hypothesis is supported by reports of a synergistic effect on both apoptotic response and microtubule stabilization, as indicated by acetylated α-tubulin, when endometrial cancer cells are treated with both the histone deacetylase inhibitor (HDI) trichostatin A and paclitaxel [112]. Interestingly, some of the targets of HDIs are also tubulin deacetylase proteins, such as HDAC6 and SIRT2 [113, 114]. Recent studies also show that treating cells with HDIs down-regulates Aurora A expression [115]. Therefore, it will be interesting to determine in future studies if the synergistic effect between HDIs and taxanes is different in CHFR-positive versus CHFR-negative cancer cells.

The finding that CHFR knockdown results in increased amounts of acetylated α-tubulin is particularly interesting because another protein found to initiate a "CHFR checkpoint-like" response is SIRT2, a tubulin and histone deacetylase [24]. SIRT2 over-expression is a phenocopy of CHFR over-expression in regards to the regulation of mitotic entry and response to mitotic stress. Therefore, hypothetically, decreased SIRT2 expression should resemble decreased CHFR expression in both response to mitotic stress and the amount of acetylated α-tubulin in the cell. Future studies should determine if the increase in acetylated α-tubulin after decreased CHFR expression is due to SIRT2 or through the activation of Aurora A-regulated HURP.

I have also found that CHFR over-expression is toxic to many breast cell lines independent of the method of transfection or retroviral transduction (both transient and stable; data not shown). This suggests that CHFR expression must be tightly regulated – too much is toxic whereas too little causes genomic instability and tumorigenesis. This is

reminiscent of other mitotic checkpoint proteins, such as MAD2, in that both too little and too much of the protein are deleterious [116]. In support of this finding, over-expression of the yeast orthologs of CHFR in *S. cerevisiae* dramatically increase the cells' doubling time due to delays in both the G1 and the G2/M phases of the cell cycle [28]. Future work on the mechanism of CHFR over-expression toxicity likely will answer many of the questions that remain about the function of CHFR. However, I speculate that CHFR target proteins are not being properly modified or targeted for degradation when CHFR is over-expressed, resulting in either impaired cell cycle progression or an up-regulated apoptotic response.

These findings have led me to suggest a model for how CHFR may regulate genomic instability and/or tumorigenesis (Figure 4.17). We propose that decreased or lost CHFR expression causes over-expression of Aurora A and both unmodified and acetylated α-tubulin, and mis-localization of MAD2. Aurora A over-expression could lead to centrosome amplification, an impaired spindle checkpoint, and possibly defective mitotic spindle formation, leading to aneuploidy and impaired cytokinesis. The MAD2 mis-localization also causes an impaired spindle checkpoint response. The increase in acetylated α-tubulin could cause stress on the mitotic spindle. Both pathways would lead to genomic instability, contributing to tumorigenesis. As indicated by the generality of this model, much research remains in order to elucidate the role of CHFR in regulating mitosis and genomic instability. Cancer often develops in concert with the loss of cell cycle regulation and genomic instability; CHFR may function in both processes.

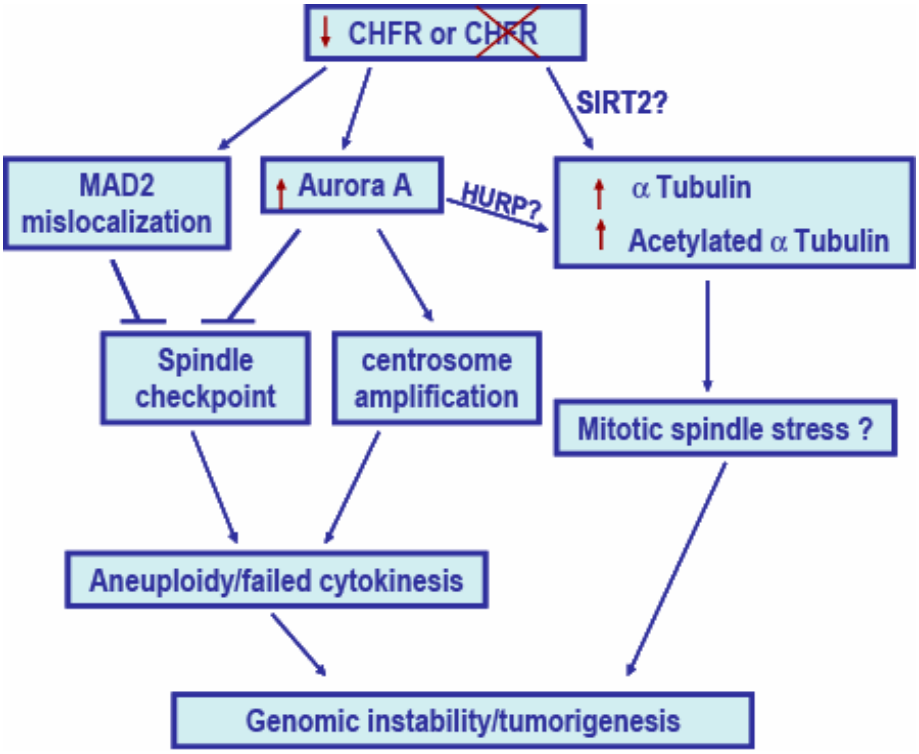

Figure 4.17: A proposed model of how CHFR regulates genomic instability, which could lead to tumorigenesis.

Decreased or lost CHFR expression causes Aurora A, α-tubulin, and acetylated α-tubulin over-expression and MAD2 mis-localization. The increase in acetylated α-tubulin occurs by an unknown mechanism, possibly through HURP or SIRT2 and may stress the mitotic spindle. Aurora A over-expression causes centrosome amplification. Both Aurora A over-expression and MAD2 mis-localization result in an impaired spindle checkpoint, contributing to aneuploidy and/or failed cytokinesis. Both processes lead to mitotic defects causing genomic instability, and possibly tumorigenesis.

Acknowledgements

This work was supported by a Department of Defense BCRP Fellowship, #BC050310, and by the NIH National Research Service Award #5-T32-GM07544 from the National Institute of General Medicine Sciences to LMP and an NIH NCI grant RO1CA072877 to EMP. We thank Esther Peterson for helpful suggestions, Xiaochun Yu for reagents and insightful discussions, and Sally Camper for sharing her Leica DMRB microscope.

CHAPTER 5

CONCLUSIONS

CHFR Has Tumor Suppressive Functions and Alters Cellular Response to Microtubule-Targeting Chemotherapeutic Drugs

CHFR was first characterized as a cell cycle checkpoint protein that delayed mitosis, in prophase, in response to microtubule-targeting drugs such as paclitaxel and nocodazole [3]. Following its initial discovery, subsequent work has shown that *CHFR* mRNA expression was low or lost in cancers compared to controls and that this loss, often due to promoter hyper-methylation, correlated with an increased sensitivity to microtubule-targeting drugs [40, 53]. These data suggested that CHFR might be a tumor suppressor that could function as a biomarker for chemotherapeutic response to taxane treatment.

To begin testing the hypothesis that CHFR may have tumor suppressive capabilities in breast cancer, the mRNA and protein expression levels of CHFR were analyzed. It was determined that *CHFR* mRNA expression was low or lost in 18% of cultured breast cancers by quantitative RT-PCR; however, 41% of cultured breast cancer cell lines had low or lost CHFR protein expression. This finding indicated a single method of analyzing *CHFR* mRNA levels did not predict protein expression, which is particularly important when trying to associate CHFR expression with clinical and pathological variables. Some of the discrepancy between mRNA and protein expression,

particularly in the MCF10A, SKBr3, and MDA-MB-231 cell lines, suggested that CHFR expression might be regulated post-transcriptionally or post-translationally. Some of the potential mechanisms of post-translational regulation include the ability of CHFR to auto-ubiquitinate, poly(ADP-ribosyl)ation, and phosphorylation [5, 7, 9, 16]. Of interest, immunohistochemistry from 142 primary invasive breast cancer patient samples revealed that 36% of the samples did not stain for CHFR expression, a relatively high frequency of occurrence. The finding that more breast cancers had low or lost CHFR expression compared to the very infrequent occurrence of over-expression (about 5% of samples), hinted that CHFR may have tumor suppressive qualities.

To mimic the loss of CHFR expression, two IHMEC lines, HPV4-12 and MCF10A, were engineered to lower CHFR expression by RNAi with a stably expressed short hairpin RNA (shRNA) or a transient transfected pool of short interfering RNAs (siRNAs). The cells that had lost CHFR expression exhibited several phenotypic changes relevant for tumorigenesis. These cells had a faster population growth rate, increased mitotic indices both with and without nocodazole exposure, enhanced invasiveness and motility, amplified colony formation in soft agar only for HPV4-12 cells, and an epithelial-to-mesenchymal transition in morphology for MCF10A cells. Both cell lines also became more aneuploid after CHFR knockdown when compared to the hyper-diploid state of the parental cell lines. In complementary experiments, over-expressing CHFR in the low-expressing breast cancer cell line Hs578T caused the reversal of many tumorigenic phenotypes, making these cells more closely resemble non-tumorigenic immortalized cells or normal mammary epithelial cells. In particular, CHFR over-expressing cells had a slower growth rate, a decreased mitotic index with and without

nocodazole treatment, and a nearly abolished invasive potential and motile ability. The dramatic results of altering CHFR expression in cultured breast cells support the hypothesis that CHFR has tumor suppressive functions in breast cancer.

One of the most striking findings from these experiments was the dramatic influence of CHFR expression on cellular invasion through Matrigel and motility. This work is the first report of this association and is highly important, as it was not a predicted outcome of altering CHFR expression. The ability for cells to move and invade the surrounding tissues and extracellular matrix is required for cancer metastasis. CHFR's strong influence on invasion and motility in cell culture models warrants further testing in mouse models and from annotated primary breast cancer samples to determine if its expression can indicate the potential for tumor metastasis. Of note, the epithelial-to-mesenchymal transition in cellular morphology that was observed in MCF10A cells with decreased CHFR expression is also associated with increased invasive potential, likely due to altered cell-cell contacts and enhanced cell motility [117]. Additionally, since CHFR monitors microtubule stability and acetylation, it is possible that this ability to regulate the cytoskeleton would have an impact on cellular motility and invasion, both of which require a dynamic rearrangement of the cytoskeleton in order to occur. In fact, previous reports have shown that acetylated alpha tubulin is present at the tail processes of motile fibroblasts [118]. The increase in acetylated alpha tubulin that results from loss of CHFR expression by RNAi likely contributes to the increased motility and invasion of these cells.

Another interesting result after the knockdown of CHFR expression were the cells' increased apoptotic response to both nocodazole and paclitaxel exposure.

However, this change was only observed in MCF10A cells, not HPV4-12 cells. A potential explanation for this difference is the method in which these two cells were immortalized. MCF10A cells arose spontaneously and were later found to have been immortalized after a chromosome translocation t(3;9)(p14;p21) that disrupted the p15/p16 gene in addition to other chromosomal rearrangements [91, 92]. The HPV4-12 cells were immortalized with the human papilloma virus E6 and E7 proteins, which impair the critical p53 and pRb tumor suppressor proteins [91]. This suggested that perhaps the p53 or pRb tumor suppressors might be critical for the apoptotic response to taxanes in CHFR-null cells. Though the altered apoptotic response to taxanes provided further evidence that CHFR may be a biomarker for chemotherapeutic response, this was the first report to indicate that other genetic and molecular factors might also need to be considered in addition to CHFR expression.

Finally, immunohistochemistry for CHFR expression on an annotated breast cancer microarray found that positive CHFR expression correlated with a small (less than 2 cm) tumor size. This supported the finding in cell culture models that over-expression of CHFR expression decreased growth rates, which could be thought of as creating a smaller tumor *in vivo.* Of interest, a small tumor size is one of the criteria used to label a cancer as an early stage tumor. In addition, there was a trend of positive CHFR expression being associated with estrogen receptor positive breast cancers. This is particularly relevant given previous clinical trials have shown that ER-positive, and therefore possibly CHFR-positive, breast cancers did not respond as well to paclitaxel treatment as ER-negative breast cancers [78-80]. This corresponds well with the fact that CHFR-positive cells are more resistant to apoptosis following taxane exposure when

compared to their CHFR-negative counterparts. This trend between CHFR and ER status might also be a clue to identifying the molecular pathway through which CHFR regulates cellular proliferation. Taken together, the results from altering CHFR expression in cultured mammary epithelial cells and the findings in primary invasive breast cancers indicate that CHFR has potent tumor suppressive qualities.

CHFR Contributes to the Maintenance of Genomic Stability

Both the work presented here and previous studies using mouse embryonic fibroblasts from *Chfr* knockout mice described the occurrence of aneuploidy after prolonged loss or decreased CHFR expression [8]. To determine the mechanism of increased aneuploidy, CHFR expression was transiently decreased by siRNAs and chromosome segregation was analyzed using immunofluorescence. MCF10A cells treated with siRNA against CHFR became more aneuploid within 72 hours and four key mitotic defects were observed that could explain the origins of the increased aneuploidy: (1) misaligned chromosomes at the metaphase plate, (2) lagging chromosomes during anaphase, (3) multi-polar mitotic spindles, and (4) multi-nucleated giant cells. Aside from the poorly formed multi-polar mitotic spindles, the other mitotic defects indicated an impaired mitotic spindle assembly checkpoint. Therefore, the localization of the key spindle checkpoint proteins MAD2 and BUBR1 were analyzed. Indeed, both MAD2 and BUBR1 were not properly localized to the kinetochores in MCF10A cells with decreased CHFR expression by siRNA; rather, they were diffusely distributed throughout the cytoplasm indicating an impaired spindle checkpoint.

This is the first report that CHFR may participate in a checkpoint other than the initially described prophase checkpoint that responds to microtubule stress. Though the

results are preliminary, the fact that CHFR may help to regulate the spindle assembly checkpoint is an exciting new finding. However, there is debate that these two checkpoints may actually be the same checkpoint, as earlier studies have shown that the spindle checkpoint also delays mitosis in response to microtubule stress [119, 120]. It is apparent that further work is required to determine if the CHFR-mediated prophase checkpoint is independent of the spindle assembly checkpoint and how CHFR functions in the checkpoint(s). I hypothesize that the two checkpoints are intimately linked for the proper regulation of mitotic events and that CHFR plays a major role in controlling both checkpoints, either directly or as an upstream regulator of signaling proteins and their degradation.

Novel CHFR Interacting Proteins

Three proteins required for proper chromosome segregation were identified that could interact with CHFR: MAD2, Aurora A kinase, and α-tubulin. The preliminary data indicating an interaction between CHFR and MAD2 is a novel finding that links CHFR with the spindle checkpoint. Although CHFR can interact with MAD2, there was no evidence that CHFR can regulate the amount of MAD2 protein, as the amount of MAD2 does not change when CHFR expression is altered. Therefore, CHFR likely does not control the degradation of MAD2, but may change its function, localization, or conformation via lysine-63 polyubiquitin chains or by mono-ubiquitination.

Previously published work indicated that CHFR could interact with, and ubiquitinate, Aurora A kinase in order to regulate its expression [8]. This protein interaction was confirmed in this work in MCF10A mammary epithelial cells and it was noted that decreased CHFR expression resulted in Aurora A over-expression, presumably

due to a lack of CHFR-mediated degradation. This interaction has many implications as Aurora A kinase is an important regulator of many mitotic processes including centrosome duplication and maturation, mitotic spindle formation, and spindle checkpoint function [96-98]. Therefore, CHFR may be a key mitotic checkpoint protein, as it appears to be upstream of proteins such as Aurora A and PLK-1 kinases that are crucial to the regulation and progression of mitotic events.

Finally, this work identified a novel interaction between CHFR and α-tubulin by both GST pull-down and immunoprecipitation experiments. Of interest, CHFR was found to ubiquitinate α-tubulin when cells were treated with nocodazole, which was the first clue as to how CHFR is involved in the cellular response to microtubule stress. In support of this, Western blotting indicated that there was a slight, but reproducible, increase of α-tubulin protein when CHFR expression was decreased by siRNA. This would cause a change in the carefully regulated 1:1 stoichiometry of α- and β-tubulin dimers, which may alter the kinetics of microtubule assembly. Finally, when CHFR expression was decreased there was also an increase in acetylated α-tubulin, which is a key component of the mitotic spindle. This may be due to either the deregulation of the Aurora A-controlled protein HURP or the down-regulation of another potential protein in the CHFR checkpoint, the tubulin deacetylase SIRT2 [24, 98, 109, 113]. This increase in stabilized, acetylated α-tubulin would likely cause increased stress on the mitotic spindle and may impair proper spindle dynamics for chromosome segregation.

In summary, CHFR appears to interact with several key mitotic proteins including Aurora A, MAD2, α-tubulin, and potentially PLK-1. The number of prospective CHFR interacting proteins could be large, but CHFR may also have only a limited number of

interacting proteins. Unfortunately, there is currently no information as to how CHFR recognizes its target proteins. However, CHFR's primary function seems to be regulating protein function and turnover via different methods of target protein ubiquitination (ie: Lys48 vs. Lys63 polyubiquitin chains) as a means to control cell cycle progression and checkpoints. The protein interactions described above and those described in other reports, and their potential downstream effects, are summarized in Figure 5.1.

Future Directions

Stemming from the results presented here, I believe there are two major directions in which future work on CHFR should continue. First, several aspects of the potential tumor suppressive functions of CHFR remain to be tested. Several of the findings presented here could be pursued further, such as the mechanism(s) through which CHFR regulates cellular motility and invasion and how CHFR expression may be related to estrogen receptor (ER) expression and function. In addition, cells with altered CHFR expression (i.e.: decreased expression by RNAi in IHMECs or over-expression in breast cancer cell lines) should be injected into immuno-compromised mice to determine if changes in CHFR expression lead to altered tumorigenicity. Using additional information from breast cancer patients, CHFR expression should also be tested for correlation with other clinical and pathological variables such as tumor stage, the presence of distant (non-lymph node) metastasis, and patient response to chemotherapy treatment with taxanes.

A second direction for future research on CHFR is to define further its function in mitotic checkpoints. In particular, the novel finding of an interaction with MAD2

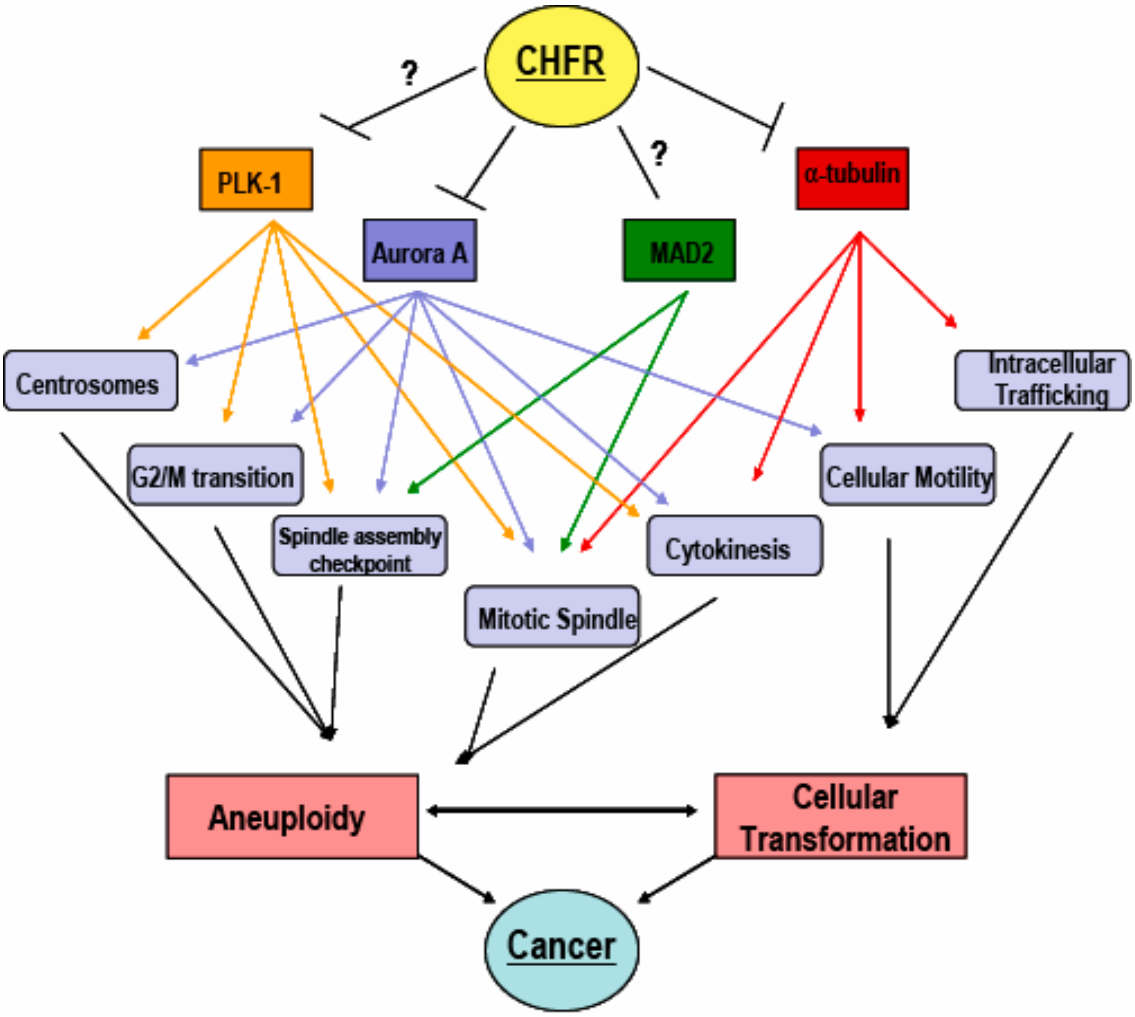

Figure 5.1: CHFR may be an upstream regulator of many proteins involved in mitotic events in order to prevent cellular transformation and aneuploidy.

There is evidence that CHFR can negatively regulate α-tubulin, Aurora A, PLK-1 in addition to interacting with MAD2 for unknown reasons. These four potential target proteins control intracellular trafficking, cellular motility, and many aspects of mitotic progression and mitotic spindle assembly. Cellular transformation and/or aneuploidy can occur when any of these processes go awry.

warrants further experimentation to determine: (1) which domains of CHFR and MAD2 interact, (2) if CHFR can ubiquitinate MAD2, (3) if there a direct interaction between the two proteins, or do they function in a complex, and (4) whether CHFR interacts with the open or closed conformation of MAD2. Elucidating the subcellular localization of CHFR during the course of the cell cycle, particularly with live cell imaging, will also clarify how CHFR may function to regulate the cell cycle. Further, complementation tests to determine if CHFR directly influences the mitotic spindle assembly checkpoint or if it regulates the checkpoint via its regulation of target proteins such as Aurora A are required. Finally, finding the reason why the over-expression of CHFR can be toxic will greatly expand our knowledge of how CHFR functions to regulate the cell cycle and mediate the cellular response to microtubule stress.

Since there is relatively little known about CHFR, there are numerous paths in which future research should be directed. However, the work presented here has provided several new leads as to which directions will be fruitful in order to answer the many questions that remain regarding the functional role of CHFR in cell cycle regulation, genomic instability, and cancer.

REFERENCES

[1] (2007-2008). American Cancer Society. Breast Cancer Facts and Figures. Atlanta: American Cancer Society Inc.

[2] Harris, L, Fritsche, H, Mennel, R, Norton, L, Ravdin, P, Taube, S, Somerfield, MR, Hayes, DF, and Bast, RC, Jr. (2007). American Society of Clinical Oncology 2007 update of recommendations for the use of tumor markers in breast cancer. J Clin Oncol. 25, 5287-5312.

[3] Scolnick, DM, and Halazonetis, TD. (2000). Chfr defines a mitotic stress checkpoint that delays entry into metaphase. Nature. 406, 430-435.

[4] Daniels, MJ, Marson, A, and Venkitaraman, AR. (2004). PML bodies control the nuclear dynamics and function of the CHFR mitotic checkpoint protein. Nat Struct Mol Biol. 11, 1114-1121.

[5] Bothos, J, Summers, MK, Venere, M, Scolnick, DM, and Halazonetis, TD. (2003). The Chfr mitotic checkpoint protein functions with Ubc13-Mms2 to form Lys63-linked polyubiquitin chains. Oncogene. 22, 7101-7107.

[6] Kang, D, Chen, J, Wong, J, and Fang, G. (2002). The checkpoint protein Chfr is a ligase that ubiquitinates Plk1 and inhibits Cdc2 at the G2 to M transition. J Cell Biol. 156, 249-259.

[7] Chaturvedi, P, Sudakin, V, Bobiak, ML, Fisher, PW, Mattern, MR, Jablonski, SA, Hurle, MR, Zhu, Y, Yen, TJ, and Zhou, BB. (2002). Chfr regulates a mitotic stress pathway through its RING-finger domain with ubiquitin ligase activity. Cancer Res. 62, 1797-1801.

[8] Yu, X, Minter-Dykhouse, K, Malureanu, L, Zhao, WM, Zhang, D, Merkle, CJ, Ward, IM, Saya, H, Fang, G, van Deursen, J, and Chen, J. (2005). Chfr is required for tumor suppression and Aurora A regulation. Nat Genet. 37, 401-406.

[9] Ahel, I, Ahel, D, Matsusaka, T, Clark, AJ, Pines, J, Boulton, SJ, and West, SC. (2008). Poly(ADP-ribose)-binding zinc finger motifs in DNA repair/checkpoint proteins. Nature. 451, 81-85.

[10] Fraschini, R, Bilotta, D, Lucchini, G, and Piatti, S. (2004). Functional characterization of Dma1 and Dma2, the budding yeast homologues of

Schizosaccharomyces pombe Dma1 and human Chfr. Mol Biol Cell. 15, 3796-3810.

[11] Guertin, DA, Venkatram, S, Gould, KL, and McCollum, D. (2002). Dma1 prevents mitotic exit and cytokinesis by inhibiting the septation initiation network (SIN). Dev Cell. 3, 779-790.

[12] Murone, M, and Simanis, V. (1996). The fission yeast dma1 gene is a component of the spindle assembly checkpoint, required to prevent septum formation and premature exit from mitosis if spindle function is compromised. Embo J. 15, 6605-6616.

[13] Plans, V, Guerra-Rebollo, M, and Thomson, TM. (2007). Regulation of mitotic exit by the RNF8 ubiquitin ligase. Oncogene.

[14] Huen, MS, Grant, R, Manke, I, Minn, K, Yu, X, Yaffe, MB, and Chen, J. (2007). RNF8 Transduces the DNA-Damage Signal via Histone Ubiquitylation and Checkpoint Protein Assembly. Cell.

[15] Mailand, N, Bekker-Jensen, S, Faustrup, H, Melander, F, Bartek, J, Lukas, C, and Lukas, J. (2007). RNF8 Ubiquitylates Histones at DNA Double-Strand Breaks and Promotes Assembly of Repair Proteins. Cell.

[16] Shtivelman, E. (2003). Promotion of mitosis by activated protein kinase B after DNA damage involves polo-like kinase 1 and checkpoint protein CHFR. Mol Cancer Res. 1, 959-969.

[17] Summers, MK, Bothos, J, and Halazonetis, TD. (2005). The CHFR mitotic checkpoint protein delays cell cycle progression by excluding Cyclin B1 from the nucleus. Oncogene. 24, 2589-2598.

[18] Ogi, K, Toyota, M, Mita, H, Satoh, A, Kashima, L, Sasaki, Y, Suzuki, H, Akino, K, Nishikawa, N, Noguchi, M, Shinomura, Y, Imai, K, Hiratsuka, H, and Tokino, T. (2005). Small interfering RNA-induced CHFR silencing sensitizes oral squamous cell cancer cells to microtubule inhibitors. Cancer Biol Ther. 4, 773-780.

[19] Satoh, A, Toyota, M, Itoh, F, Sasaki, Y, Suzuki, H, Ogi, K, Kikuchi, T, Mita, H, Yamashita, T, Kojima, T, Kusano, M, Fujita, M, Hosokawa, M, Endo, T, Tokino, T, and Imai, K. (2003). Epigenetic inactivation of CHFR and sensitivity to microtubule inhibitors in gastric cancer. Cancer Res. 63, 8606-8613.

[20] Privette, LM, Gonzalez, ME, Ding, L, Kleer, CG, and Petty, EM. (2007). Altered expression of the early mitotic checkpoint protein, CHFR, in breast cancers: implications for tumor suppression. Cancer Res. 67, 6064-6074.

[21] Erson, AE, and Petty, EM. (2004). CHFR-associated early G2/M checkpoint defects in breast cancer cells. Mol Carcinog. 39, 26-33.

[22] Inoue, T, Hiratsuka, M, Osaki, M, and Oshimura, M. (2007). The molecular biology of mammalian SIRT proteins: SIRT2 in cell cycle regulation. Cell Cycle. 6, 1011-1018.

[23] Matsusaka, T, and Pines, J. (2004). Chfr acts with the p38 stress kinases to block entry to mitosis in mammalian cells. J Cell Biol. 166, 507-516.

[24] Inoue, T, Hiratsuka, M, Osaki, M, Yamada, H, Kishimoto, I, Yamaguchi, S, Nakano, S, Katoh, M, Ito, H, and Oshimura, M. (2007). SIRT2, a tubulin deacetylase, acts to block the entry to chromosome condensation in response to mitotic stress. Oncogene. 26, 945-957.

[25] Akhter, S, Richie, CT, Deng, JM, Brey, E, Zhang, X, Patrick, C, Jr., Behringer, RR, and Legerski, RJ. (2004). Deficiency in SNM1 abolishes an early mitotic checkpoint induced by spindle stress. Mol Cell Biol. 24, 10448-10455.

[26] Michael, S, Trave, G, Ramu, C, Chica, C, and Gibson, TJ. (2008). Discovery of candidate KEN box motifs using Cell Cycle keyword enrichment combined with native disorder prediction and motif conservation. Bioinformatics.

[27] Hirota, T, Kunitoku, N, Sasayama, T, Marumoto, T, Zhang, D, Nitta, M, Hatakeyama, K, and Saya, H. (2003). Aurora-A and an interacting activator, the LIM protein Ajuba, are required for mitotic commitment in human cells. Cell. 114, 585-598.

[28] Loring, GL, Christensen, KC, Gerber, SA, and Brenner, C. (2008). Yeast Chfr homologs retard cell cycle at G(1) and G(2)/M via Ubc4 and Ubc13/Mms2-dependent ubiquitination. Cell Cycle. 7, 96-105.

[29] Oh, YM, Yoo, SJ, and Seol, JH. (2007). Deubiquitination of Chfr, a checkpoint protein, by USP7/HAUSP regulates its stability and activity. Biochem Biophys Res Commun. 357, 615-619.

[30] Bertholon, J, Wang, Q, Falette, N, Verny, C, Auclair, J, Chassot, C, Navarro, C, Saurin, JC, and Puisieux, A. (2003). Chfr inactivation is not associated to chromosomal instability in colon cancers. Oncogene. 22, 8956-8960.

[31] Mariatos, G, Bothos, J, Zacharatos, P, Summers, MK, Scolnick, DM, Kittas, C, Halazonetis, TD, and Gorgoulis, VG. (2003). Inactivating mutations targeting the chfr mitotic checkpoint gene in human lung cancer. Cancer Res. 63, 7185-7189.

[32] Kang, HC, Kim, IJ, Jang, SG, Hong, SH, Hwang, JA, Shin, HR, and Park, JG. (2008). Coding region polymorphisms in the CHFR mitotic stress checkpoint gene are associated with colorectal cancer risk. Cancer Lett. 260, 170-179.

[33] Toyota, M, Sasaki, Y, Satoh, A, Ogi, K, Kikuchi, T, Suzuki, H, Mita, H, Tanaka, N, Itoh, F, Issa, JP, Jair, KW, Schuebel, KE, Imai, K, and Tokino, T. (2003). Epigenetic inactivation of CHFR in human tumors. Proc Natl Acad Sci U S A. 100, 7818-7823.

[34] Natrajan, R, Williams, RD, Hing, SN, Mackay, A, Reis-Filho, JS, Fenwick, K, Iravani, M, Valgeirsson, H, Grigoriadis, A, Langford, CF, Dovey, O, Gregory, SG, Weber, BL, Ashworth, A, Grundy, PE, Pritchard-Jones, K, and Jones, C. (2006). Array CGH profiling of favourable histology Wilms tumours reveals novel gains and losses associated with relapse. J Pathol. 210, 49-58.

[35] Rickert, CH, Dockhorn-Dworniczak, B, Busch, G, Moskopp, D, Albert, FK, Rama, B, and Paulus, W. (2001). Increased chromosomal imbalances in recurrent pituitary adenomas. Acta Neuropathol. 102, 615-620.

[36] Rutherford, S, Hampton, GM, Frierson, HF, and Moskaluk, CA. (2005). Mapping of candidate tumor suppressor genes on chromosome 12 in adenoid cystic carcinoma. Lab Invest. 85, 1076-1085.

[37] Aubele, M, Auer, G, Braselmann, H, Nahrig, J, Zitzelsberger, H, Quintanilla-Martinez, L, Smida, J, Walch, A, Hofler, H, and Werner, M. (2002). Chromosomal imbalances are associated with metastasis-free survival in breast cancer patients. Anal Cell Pathol. 24, 77-87.

[38] Ichikawa, T, Hosoki, S, Suzuki, H, Akakura, K, Igarashi, T, Furuya, Y, Oshimura, M, Rinker-Schaeffer, CW, Nihei, N, Barrett, JC, Isaacs, JT, and Ito, H. (2000). Mapping of metastasis suppressor genes for prostate cancer by microcell-mediated chromosome transfer. Asian J Androl. 2, 167-171.

[39] Jaeger, EB, Chekmareva, MA, Tennant, TR, Luu, HH, Hickson, JA, Chen, SL, Samant, RS, Sokoloff, MH, and Rinker-Schaeffer, CW. (2004). Inhibition of prostate cancer metastatic colonization by approximately 4.2 Mb of human chromosome 12. Int J Cancer. 108, 15-22.

[40] Banno, K, Yanokura, M, Kawaguchi, M, Kuwabara, Y, Akiyoshi, J, Kobayashi, Y, Iwata, T, Hirasawa, A, Fujii, T, Susumu, N, Tsukazaki, K, and Aoki, D. (2007). Epigenetic inactivation of the CHFR gene in cervical cancer contributes to sensitivity to taxanes. Int J Oncol. 31, 713-720.

[41] Brandes, JC, van Engeland, M, Wouters, KA, Weijenberg, MP, and Herman, JG. (2005). CHFR promoter hypermethylation in colon cancer correlates with the microsatellite instability phenotype. Carcinogenesis. 26, 1152-1156.

[42] Chen, K, Sawhney, R, Khan, M, Benninger, MS, Hou, Z, Sethi, S, Stephen, JK, and Worsham, MJ. (2007). Methylation of multiple genes as diagnostic and therapeutic markers in primary head and neck squamous cell carcinoma. Arch Otolaryngol Head Neck Surg. 133, 1131-1138.

[43] Cheung, HW, Ching, YP, Nicholls, JM, Ling, MT, Wong, YC, Hui, N, Cheung, A, Tsao, SW, Wang, Q, Yeun, PW, Lo, KW, Jin, DY, and Wang, X. (2005). Epigenetic inactivation of CHFR in nasopharyngeal carcinoma through promoter methylation. Mol Carcinog. 43, 237-245.

[44] Corn, PG, Summers, MK, Fogt, F, Virmani, AK, Gazdar, AF, Halazonetis, TD, and El-Deiry, WS. (2003). Frequent hypermethylation of the 5' CpG island of the mitotic stress checkpoint gene Chfr in colorectal and non-small cell lung cancer. Carcinogenesis. 24, 47-51.

[45] Derks, S, Postma, C, Carvalho, B, van den Bosch, SM, Moerkerk, PT, Herman, JG, Weijenberg, MP, de Bruine, AP, Meijer, GA, and van Engeland, M. (2007). Integrated analysis of chromosomal, microsatellite and epigenetic instability in colorectal cancer identifies specific associations between promoter methylation of pivotal tumour suppressor and DNA repair genes and specific chromosomal alterations. Carcinogenesis.

[46] Gong, H, Liu, W, Zhou, J, and Xu, H. (2005). Methylation of gene CHFR promoter in acute leukemia cells. J Huazhong Univ Sci Technolog Med Sci. 25, 240-242.

[47] Henken, FE, Wilting, SM, Overmeer, RM, van Rietschoten, JG, Nygren, AO, Errami, A, Schouten, JP, Meijer, CJ, Snijders, PJ, and Steenbergen, RD. (2007). Sequential gene promoter methylation during HPV-induced cervical carcinogenesis. Br J Cancer. 97, 1457-1464.

[48] Homma, N, Tamura, G, Honda, T, Jin, Z, Ohmura, K, Kawata, S, and Motoyama, T. (2005). Hypermethylation of Chfr and hMLH1 in gastric noninvasive and early invasive neoplasias. Virchows Arch. 446, 120-126.

[49] Honda, T, Tamura, G, Waki, T, Kawata, S, Nishizuka, S, and Motoyama, T. (2004). Promoter hypermethylation of the Chfr gene in neoplastic and non-neoplastic gastric epithelia. Br J Cancer. 90, 2013-2016.

[50] Kang, GH, Lee, S, Cho, NY, Gandamihardja, T, Long, TI, Weisenberger, DJ, Campan, M, and Laird, PW. (2007). DNA methylation profiles of gastric carcinoma characterized by quantitative DNA methylation analysis. Lab Invest.

[51] Kang, HC, Kim, IJ, Park, JH, Shin, Y, Park, HW, Ku, JL, Yang, HK, Lee, KU, Choe, KJ, and Park, JG. (2004). Promoter hypermethylation and silencing of

CHFR mitotic stress checkpoint gene in human gastric cancers. Oncol Rep. 12, 129-133.

[52] Kawasaki, T, Ohnishi, M, Nosho, K, Suemoto, Y, Kirkner, GJ, Meyerhardt, JA, Fuchs, CS, and Ogino, S. (2008). CpG island methylator phenotype-low (CIMP-low) colorectal cancer shows not only few methylated CIMP-high-specific CpG islands, but also low-level methylation at individual loci. Mod Pathol.

[53] Koga, Y, Kitajima, Y, Miyoshi, A, Sato, K, Sato, S, and Miyazaki, K. (2006). The significance of aberrant CHFR methylation for clinical response to microtubule inhibitors in gastric cancer. J Gastroenterol. 41, 133-139.

[54] Ludwig, AH, Bujko, M, Bidzinski, M, and Kupryjanczyk, J. (2007). CHFR gene is neither mutated nor hypermethylated in ovarian cancer. Cancer Detect Prev. 31, 257-261.

[55] Mizuno, K, Osada, H, Konishi, H, Tatematsu, Y, Yatabe, Y, Mitsudomi, T, Fujii, Y, and Takahashi, T. (2002). Aberrant hypermethylation of the CHFR prophase checkpoint gene in human lung cancers. Oncogene. 21, 2328-2333.

[56] Morioka, Y, Hibi, K, Sakai, M, Koike, M, Fujiwara, M, Kodera, Y, Ito, K, and Nakao, A. (2006). Aberrant methylation of the CHFR gene is frequently detected in non-invasive colorectal cancer. Anticancer Res. 26, 4267-4270.

[57] Morioka, Y, Hibi, K, Sakai, M, Koike, M, Fujiwara, M, Kodera, Y, Ito, K, and Nakao, A. (2006). Aberrant methylation of the CHFR gene in digestive tract cancer. Anticancer Res. 26, 1791-1795.

[58] Sakai, M, Hibi, K, Kanazumi, N, Nomoto, S, Inoue, S, Takeda, S, and Nakao, A. (2005). Aberrant methylation of the CHFR gene in advanced hepatocellular carcinoma. Hepatogastroenterology. 52, 1854-1857.

[59] Shibata, Y, Haruki, N, Kuwabara, Y, Ishiguro, H, Shinoda, N, Sato, A, Kimura, M, Koyama, H, Toyama, T, Nishiwaki, T, Kudo, J, Terashita, Y, Konishi, S, Sugiura, H, and Fujii, Y. (2002). Chfr expression is downregulated by CpG island hypermethylation in esophageal cancer. Carcinogenesis. 23, 1695-1699.

[60] Tokunaga, E, Oki, E, Nishida, K, Koga, T, Yoshida, R, Ikeda, K, Kojima, A, Egashira, A, Morita, M, Kakeji, Y, and Maehara, Y. (2006). Aberrant hypermethylation of the promoter region of the CHFR gene is rare in primary breast cancer. Breast Cancer Res Treat. 97, 199-203.

[61] Tozawa, T, Tamura, G, Honda, T, Nawata, S, Kimura, W, Makino, N, Kawata, S, Sugai, T, Suto, T, and Motoyama, T. (2004). Promoter hypermethylation of DAP-kinase is associated with poor survival in primary biliary tract carcinoma patients. Cancer Sci. 95, 736-740.

[62] van Doorn, R, Zoutman, WH, Dijkman, R, de Menezes, RX, Commandeur, S, Mulder, AA, van der Velden, PA, Vermeer, MH, Willemze, R, Yan, PS, Huang, TH, and Tensen, CP. (2005). Epigenetic profiling of cutaneous T-cell lymphoma: promoter hypermethylation of multiple tumor suppressor genes including BCL7a, PTPRG, and p73. J Clin Oncol. 23, 3886-3896.

[63] Yanokura, M, Banno, K, Kawaguchi, M, Hirao, N, Hirasawa, A, Susumu, N, Tsukazaki, K, and Aoki, D. (2007). Relationship of aberrant DNA hypermethylation of CHFR with sensitivity to taxanes in endometrial cancer. Oncol Rep. 17, 41-48.

[64] Yoshida, K, Hamai, Y, Suzuki, T, Sanada, Y, Oue, N, and Yasui, W. (2006). DNA methylation of CHFR is not a predictor of the response to docetaxel and paclitaxel in advanced and recurrent gastric cancer. Anticancer Res. 26, 49-54.

[65] Milne, AN, Sitarz, R, Carvalho, R, Polak, MM, Ligtenberg, M, Pauwels, P, Offerhaus, GJ, and Weterman, MA. (2007). Molecular analysis of primary gastric cancer, corresponding xenografts, and 2 novel gastric carcinoma cell lines reveals novel alterations in gastric carcinogenesis. Hum Pathol. 38, 903-913.

[66] Kobayashi, C, Oda, Y, Takahira, T, Izumi, T, Kawaguchi, K, Yamamoto, H, Tamiya, S, Yamada, T, Iwamoto, Y, and Tsuneyoshi, M. (2006). Aberrant expression of CHFR in malignant peripheral nerve sheath tumors. Mod Pathol. 19, 524-532.

[67] Mata, J, Marguerat, S, and Bahler, J. (2005). Post-transcriptional control of gene expression: a genome-wide perspective. Trends Biochem Sci. 30, 506-514.

[68] Holcik, M, and Sonenberg, N. (2005). Translational control in stress and apoptosis. Nat Rev Mol Cell Biol. 6, 318-327.

[69] Rosenwald, IB. (2004). The role of translation in neoplastic transformation from a pathologist's point of view. Oncogene. 23, 3230-3247.

[70] Bartel, DP. (2004). MicroRNAs: genomics, biogenesis, mechanism, and function. Cell. 116, 281-297.

[71] Calin, GA, and Croce, CM. (2006). MicroRNA signatures in human cancers. Nat Rev Cancer. 6, 857-866.

[72] He, L, He, X, Lowe, SW, and Hannon, GJ. (2007). microRNAs join the p53 network--another piece in the tumour-suppression puzzle. Nat Rev Cancer. 7, 819-822.

[73] Ethier, SP, Mahacek, ML, Gullick, WJ, Frank, TS, and Weber, BL. (1993). Differential isolation of normal luminal mammary epithelial cells and breast cancer cells from primary and metastatic sites using selective media. Cancer Res. 53, 627-635.

[74] Neve, RM, Chin, K, Fridlyand, J, Yeh, J, Baehner, FL, Fevr, T, Clark, L, Bayani, N, Coppe, JP, Tong, F, Speed, T, Spellman, PT, DeVries, S, Lapuk, A, Wang, NJ, Kuo, WL, Stilwell, JL, Pinkel, D, Albertson, DG, Waldman, FM, McCormick, F, Dickson, RB, Johnson, MD, Lippman, M, Ethier, S, Gazdar, A, and Gray, JW. (2006). A collection of breast cancer cell lines for the study of functionally distinct cancer subtypes. Cancer Cell. 10, 515-527.

[75] Erson, AE, Niell, BL, DeMers, SK, Rouillard, JM, Hanash, SM, and Petty, EM. (2001). Overexpressed genes/ESTs and characterization of distinct amplicons on 17q23 in breast cancer cells. Neoplasia. 3, 521-526.

[76] Van den Eynden, GG, Van der Auwera, I, Van Laere, S, Colpaert, CG, van Dam, P, Merajver, S, Kleer, CG, Harris, AL, Van Marck, EA, Dirix, LY, and Vermeulen, PB. (2004). Validation of a tissue microarray to study differential protein expression in inflammatory and non-inflammatory breast cancer. Breast Cancer Res Treat. 85, 13-22.

[77] Kleer, CG, Cao, Q, Varambally, S, Shen, R, Ota, I, Tomlins, SA, Ghosh, D, Sewalt, RG, Otte, AP, Hayes, DF, Sabel, MS, Livant, D, Weiss, SJ, Rubin, MA, and Chinnaiyan, AM. (2003). EZH2 is a marker of aggressive breast cancer and promotes neoplastic transformation of breast epithelial cells. Proc Natl Acad Sci U S A. 100, 11606-11611.

[78] Berry, DA, Cirrincione, C, Henderson, IC, Citron, ML, Budman, DR, Goldstein, LJ, Martino, S, Perez, EA, Muss, HB, Norton, L, Hudis, C, and Winer, EP. (2006). Estrogen-receptor status and outcomes of modern chemotherapy for patients with node-positive breast cancer. Jama. 295, 1658-1667.

[79] Poole, C. (2004). Adjuvant chemotherapy for early-stage breast cancer: the tAnGo trial. Oncology (Williston Park). 18, 23-26.

[80] Sezgin, C, Karabulut, B, Uslu, R, Sanli, UA, Goksel, G, Zekioglu, O, Ozdemir, N, and Goker, E. (2005). Potential predictive factors for response to weekly paclitaxel treatment in patients with metastatic breast cancer. J Chemother. 17, 96-103.

[81] Hanahan, D, and Weinberg, RA. (2000). The hallmarks of cancer. Cell. 100, 57-70.

[82] Kastan, MB, Canman, CE, and Leonard, CJ. (1995). P53, cell cycle control and apoptosis: implications for cancer. Cancer Metastasis Rev. 14, 3-15.

[83] Albini, A, Benelli, R, Noonan, DM, and Brigati, C. (2004). The "chemoinvasion assay": a tool to study tumor and endothelial cell invasion of basement membranes. Int J Dev Biol. 48, 563-571.

[84] Hamburger, AW. (1987). The human tumor clonogenic assay as a model system in cell biology. Int J Cell Cloning. 5, 89-107.

[85] Eagle, H, Foley, GE, Koprowski, H, Lazarus, H, Levine, EM, and Adams, RA. (1970). Growth characteristics of virus-transformed cells. Maximum population density, inhibition by normal cells, serum requirement, growth in soft agar, and xenogeneic transplantability. J Exp Med. 131, 863-879.

[86] Wong, WW, Vijayakumar, S, and Weichselbaum, RR. (1992). Prognostic indicators in node-negative early stage breast cancer. Am J Med. 92, 539-548.

[87] Singletary, SE, and Greene, FL. (2003). Revision of breast cancer staging: the 6th edition of the TNM Classification. Semin Surg Oncol. 21, 53-59.

[88] Goto, H, Tomono, Y, Ajiro, K, Kosako, H, Fujita, M, Sakurai, M, Okawa, K, Iwamatsu, A, Okigaki, T, Takahashi, T, and Inagaki, M. (1999). Identification of a novel phosphorylation site on histone H3 coupled with mitotic chromosome condensation. J Biol Chem. 274, 25543-25549.

[89] Vermes, I, Haanen, C, Steffens-Nakken, H, and Reutelingsperger, C. (1995). A novel assay for apoptosis. Flow cytometric detection of phosphatidylserine expression on early apoptotic cells using fluorescein labelled Annexin V. J Immunol Methods. 184, 39-51.

[90] van Diest, PJ, Mouriquand, J, Schipper, NW, and Baak, JP. (1990). Prognostic value of nucleolar morphometric variables in cytological breast cancer specimens. J Clin Pathol. 43, 157-159.

[91] Band, V, Zajchowski, D, Kulesa, V, and Sager, R. (1990). Human papilloma virus DNAs immortalize normal human mammary epithelial cells and reduce their growth factor requirements. Proc Natl Acad Sci U S A. 87, 463-467.

[92] Cowell, JK, LaDuca, J, Rossi, MR, Burkhardt, T, Nowak, NJ, and Matsui, S. (2005). Molecular characterization of the t(3;9) associated with immortalization in the MCF10A cell line. Cancer Genet Cytogenet. 163, 23-29.

[93] Kops, GJ, Weaver, BA, and Cleveland, DW. (2005). On the road to cancer: aneuploidy and the mitotic checkpoint. Nat Rev Cancer. 5, 773-785.

[94] Myrie, KA, Percy, MJ, Azim, JN, Neeley, CK, and Petty, EM. (2000). Mutation and expression analysis of human BUB1 and BUB1B in aneuploid breast cancer cell lines. Cancer Lett. 152, 193-199.

[95] Percy, MJ, Myrie, KA, Neeley, CK, Azim, JN, Ethier, SP, and Petty, EM. (2000). Expression and mutational analyses of the human MAD2L1 gene in breast cancer cells. Genes Chromosomes Cancer. 29, 356-362.

[96] Fu, J, Bian, M, Jiang, Q, and Zhang, C. (2007). Roles of Aurora kinases in mitosis and tumorigenesis. Mol Cancer Res. 5, 1-10.

[97] Mori, D, Yano, Y, Toyo-oka, K, Yoshida, N, Yamada, M, Muramatsu, M, Zhang, D, Saya, H, Toyoshima, YY, Kinoshita, K, Wynshaw-Boris, A, and Hirotsune, S. (2007). NDEL1 phosphorylation by Aurora-A kinase is essential for centrosomal maturation, separation, and TACC3 recruitment. Mol Cell Biol. 27, 352-367.

[98] Koffa, MD, Casanova, CM, Santarella, R, Kocher, T, Wilm, M, and Mattaj, IW. (2006). HURP is part of a Ran-dependent complex involved in spindle formation. Curr Biol. 16, 743-754.

[99] Anand, S, Penrhyn-Lowe, S, and Venkitaraman, AR. (2003). AURORA-A amplification overrides the mitotic spindle assembly checkpoint, inducing resistance to Taxol. Cancer Cell. 3, 51-62.

[100] Jiang, Y, Zhang, Y, Lees, E, and Seghezzi, W. (2003). AuroraA overexpression overrides the mitotic spindle checkpoint triggered by nocodazole, a microtubule destabilizer. Oncogene. 22, 8293-8301.

[101] Lassmann, S, Shen, Y, Jutting, U, Wiehle, P, Walch, A, Gitsch, G, Hasenburg, A, and Werner, M. (2007). Predictive value of Aurora-A/STK15 expression for late stage epithelial ovarian cancer patients treated by adjuvant chemotherapy. Clin Cancer Res. 13, 4083-4091.

[102] Zhou, H, Kuang, J, Zhong, L, Kuo, WL, Gray, JW, Sahin, A, Brinkley, BR, and Sen, S. (1998). Tumour amplified kinase STK15/BTAK induces centrosome amplification, aneuploidy and transformation. Nat Genet. 20, 189-193.

[103] McGhee, EM, Cotter, PD, Weier, JF, Berline, JW, Turner, MA, Gormley, M, and Palefsky, JM. (2006). Molecular cytogenetic characterization of human papillomavirus16-transformed foreskin keratinocyte cell line 16-MT. Cancer Genet Cytogenet. 168, 36-43.

[104] Marumoto, T, Zhang, D, and Saya, H. (2005). Aurora-A - a guardian of poles. Nat Rev Cancer. 5, 42-50.

[105] Shi, Q, and King, RW. (2005). Chromosome nondisjunction yields tetraploid rather than aneuploid cells in human cell lines. Nature. 437, 1038-1042.

[106] Wang, X, Zhou, YX, Qiao, W, Tominaga, Y, Ouchi, M, Ouchi, T, and Deng, CX. (2006). Overexpression of aurora kinase A in mouse mammary epithelium induces genetic instability preceding mammary tumor formation. Oncogene. 25, 7148-7158.

[107] Manfredi, MG, Ecsedy, JA, Meetze, KA, Balani, SK, Burenkova, O, Chen, W, Galvin, KM, Hoar, KM, Huck, JJ, LeRoy, PJ, Ray, ET, Sells, TB, Stringer, B, Stroud, SG, Vos, TJ, Weatherhead, GS, Wysong, DR, Zhang, M, Bolen, JB, and Claiborne, CF. (2007). Antitumor activity of MLN8054, an orally active small-molecule inhibitor of Aurora A kinase. Proc Natl Acad Sci U S A. 104, 4106-4111.

[108] Yu, H. (2002). Regulation of APC-Cdc20 by the spindle checkpoint. Curr Opin Cell Biol. 14, 706-714.

[109] Yu, CT, Hsu, JM, Lee, YC, Tsou, AP, Chou, CK, and Huang, CY. (2005). Phosphorylation and stabilization of HURP by Aurora-A: implication of HURP as a transforming target of Aurora-A. Mol Cell Biol. 25, 5789-5800.

[110] Piperno, G, LeDizet, M, and Chang, XJ. (1987). Microtubules containing acetylated alpha-tubulin in mammalian cells in culture. J Cell Biol. 104, 289-302.

[111] Webster, DR, and Borisy, GG. (1989). Microtubules are acetylated in domains that turn over slowly. J Cell Sci. 92 (Pt 1), 57-65.

[112] Dowdy, SC, Jiang, S, Zhou, XC, Hou, X, Jin, F, Podratz, KC, and Jiang, SW. (2006). Histone deacetylase inhibitors and paclitaxel cause synergistic effects on apoptosis and microtubule stabilization in papillary serous endometrial cancer cells. Mol Cancer Ther. 5, 2767-2776.

[113] North, BJ, Marshall, BL, Borra, MT, Denu, JM, and Verdin, E. (2003). The human Sir2 ortholog, SIRT2, is an NAD+-dependent tubulin deacetylase. Mol Cell. 11, 437-444.

[114] Zhang, Y, Li, N, Caron, C, Matthias, G, Hess, D, Khochbin, S, and Matthias, P. (2003). HDAC-6 interacts with and deacetylates tubulin and microtubules in vivo. Embo J. 22, 1168-1179.

[115] Park, JH, Jong, HS, Kim, SG, Jung, Y, Lee, KW, Lee, JH, Kim, DK, Bang, YJ, and Kim, TY. (2007). Inhibitors of histone deacetylases induce tumor-selective cytotoxicity through modulating Aurora-A kinase. J Mol Med.

[116] Perez de Castro, I, de Carcer, G, and Malumbres, M. (2007). A census of mitotic cancer genes: new insights into tumor cell biology and cancer therapy. Carcinogenesis. 28, 899-912.

[117] Guarino, M, Rubino, B, and Ballabio, G. (2007). The role of epithelial-mesenchymal transition in cancer pathology. Pathology. 39, 305-318.

[118] Prescott, AR, Vestberg, M, and Warn, RM. (1989). Microtubules rich in modified alpha-tubulin characterize the tail processes of motile fibroblasts. J Cell Sci. 94 (Pt 2), 227-236.

[119] Rieder, CL, and Maiato, H. (2004). Stuck in division or passing through: what happens when cells cannot satisfy the spindle assembly checkpoint. Dev Cell. 7, 637-651.

[120] Wang, Y, and Burke, DJ. (1995). Checkpoint genes required to delay cell division in response to nocodazole respond to impaired kinetochore function in the yeast Saccharomyces cerevisiae. Mol Cell Biol. 15, 6838-6844.